Project No. 609687

FP7-ENERGY-2013-IRP

ELECTRA

European Liaison on Electricity Committed Towards long-term Research Activities for Smart Grids

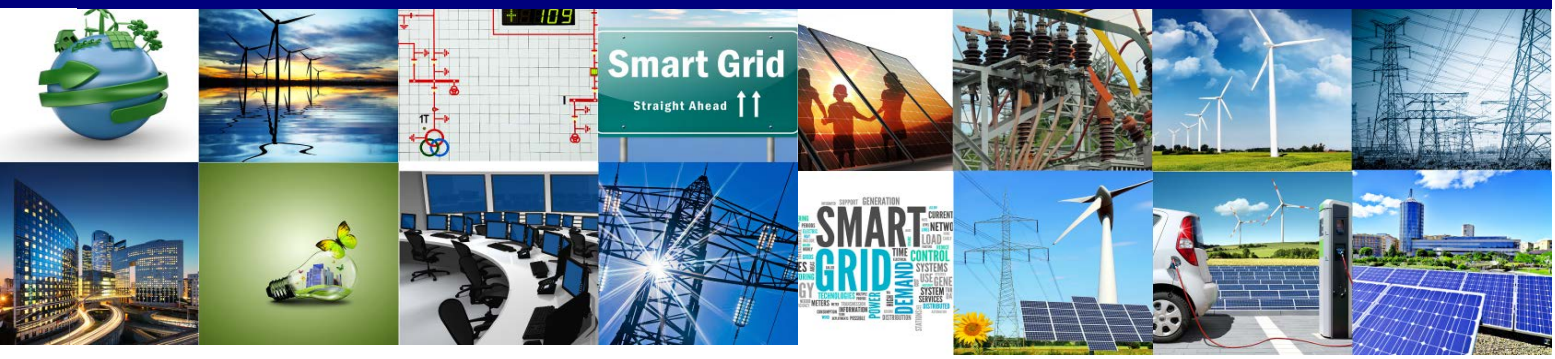

WP 7

Integration and Lab Testing for Proof of Concept

Deliverable 7.1

Report on the evaluation and validation of the ELECTRA WoC control concept

08/04/2018

ID&Title	**D7.1** Report on the evaluation and validation of the ELECTRA WoC control concept	**Number of pages:**	106

Short description (Max. 50 words):

This report summarizes the evaluation and validation of the ELECTRA Web-of-Cells concept which has been implemented for the proof of concept in selected validation environments provided by the project partners. The performed experiments have been realized in simulations and in laboratory environments and showed the feasibility of the Web-of-Cells concept and integrated functions for balancing and voltage control. Future work is necessary to further refine the concept and functions and to focus the controller implementations on higher technology readiness levels.

Version	Date	Modification's nature
V0.1	04/12/2017	Draft structure of document
V0.2	31/01/2018	First draft version
V0.3	21/03/2018	Final draft ready for review
V1.00	22/03/2018	Under review
V2.00	08/04/2018	Released

Accessibility

☒ PU, Public
☐ PP, Restricted to other program participants (including the Commission Services)
☐ RE, Restricted to other a group specified by the consortium (including the Commission Services)
☐ CO, Confidential, only for members of the consortium (including the Commission Services)

If restricted, please specify here the group:	

Owner / Main responsible:		
Task 7.3 Leader:	Thomas Strasser (AIT)	
Reviewed by:		
WP 7 Leader:	Thomas Strasser (AIT)	21/03/2018
Final Approval by:		
ELECTRA Technical Committee TOQA appointed Reviewer:	Chris Caerts (VITO) Mihai Calin (DERlab)	27/03/2018 06/04/2018

Authors

Name	Last Name	Organization	Country
Thomas	Strasser	AIT	Austria
Aadil	Latif	AIT	Austria
Fabian	Leimgruber	AIT	Austria
Mazheruddin	Syed	USTRATH	UK
Efren	Guillo	USTRATH	UK
Graeme	Burt	USTRATH	UK
Mattia	Marinelli	DTU	Denmark
Alexander	Prostejovsky	DTU	Denmark
Michel	Rezkalla	DTU	Denmark
Julia	Merino Fernández	TECNALIA	Spain
Evangelos	Rikos	CRES	Greece
Roberto	Ciavarella	ENEA	Italy
Maria	Nuschke	IEE	Germany
Antonio	Coelho	INESC P	Portugal
Antonio	Guagliardi	RSE	Italy
Mattia	Cabiati	RSE	Italy
Andrei	Morch	SINTEF	Norway
Merkebu	Degefa	SINTEF	Norway
Seppo	Hänninen	VTT	Finland
Riku	Pasonen	VTT	Finland
Mihai	Calin	DERlab	Germany
Ozgur	Kahraman	TUBITAK	Turkey

Copyright

Consisting of:

Coordinator	
Ricerca Sul Sistema Energetico – (RSE)	Italy
Participants	
Austrian Institute of Technology GmbH - (AIT)	Austria
Vlaamse Instelling Voor Technologisch Onderzoek N.V. - (VITO)	Belgium
Belgisch Laboratorium Van De Elektriciteitsindustrie - (LABORELEC)	Belgium
Danmarks Tekniske Universitet - (DTU)	Denmark
Teknologian Tutkimuskeskus - (VTT)	Finland
Commissariat A L'Energie Atomique Et Aux Energies Alternatives - (CEA)	France
Fraunhofer-Gesellschaft Zur Förderung Der Angewandten Forschung E.V – (IEE)	Germany
Centre For Renewable Energy Sources And Saving - (CRES)	Greece
Agenzia Nazionale per Le Nuove Tecnologie, L´Energia E Lo Sviluppo Economico Sostenibile - (ENEA)	Italy
Fizikalas Energetikas Instituts - (IPE)	Latvia
SINTEF Energi AS - (SINTEF)	Norway
Instytut Energetyki - (IEN)	Poland
Instituto De Engenharia De Sistemas E Computadores Do Porto - (INESC P)	Portugal
Fundacion Tecnalia Research & Innovation - (TECNALIA)	Spain
Joint Research Centre European Commission - (JRC)	Belgium
Nederlandse Organisatie Voor Toegepast Natuurwetenschappelijk Onderzoek – (TNO)	Netherlands
Turkiiye Bilimsel Ve Teknolojik Arastirma Kurumu - (TUBITAK)	Turkey
University Of Strathclyde - (USTRATH)	UK
European Distributed Energy Resources Laboratories (DERlab)	Germany
Institute for Information Technology at University of Oldenburg (OFFIS)	Germany

Executive Summary

An important activity within ELECTRA IRP was to prototypically evaluate the proposed Web-of-Cells real-time control approach and its corresponding control schemes related to voltage and balancing control. Outcomes of various simulation studies of the individual control functions have been used as basis for this evaluation work. This report documents and summarizes the implementation and integration work which has been carried out in several research facilities provided by the consortium.

The main validation goal was to experimentally implement the Web-of-Cells control schemes in selected testing scenarios in order to proof that local problems can be solved locally within an ELECTRA cell. This includes the demonstration of the effectiveness of distributed controls in relation to a number of selected grid scenarios taking available laboratory evaluation capabilities of involved ELECTRA partners into account.

In order to compare the performance of the implemented control schemes and corresponding functions across multiple laboratories, a Key Performance Indicator based validation approach has been developed and realized. With this tool in hand an effective evaluation of the ELECTRA results in comparison with traditional control approaches (i.e., business as usual case) was possible.

At the end, 15 different simulation and laboratory-based experiments with corresponding testing criteria have been derived and implemented. As planned, the Technology Readiness Level of ELECTRA IRP outcomes reaches 3 to 4 (i.e., “Prototype or component validation under laboratory conditions”) where higher levels are clearly beyond the scope of the project. ELECTRA took developments of the Web-of-Cells concept up to laboratory-scale validation, encompassing the flexible (aggregate) resource level, cell level, and inter-cell level. The physical, single device level was not in scope for the research but was involved when setting up the test cases and performing the individual lab-scale experiments.

Results from the experiments principally showed the feasibility of the distributed WoC real-time control approach and its corresponding control schemes. However, the validation work conducted has been focussed primarily on the containment and restoration from discrete incidents in scenarios of a few cells but the handling of continuous streams of forecast deviations should be also possible. The focus of the laboratory work has therefore been to validate the ability of the control functions to mitigate such discrete, local incidents. Validation of scalability – involving larger numbers of cells responding in real-time – remains a future research challenge to be addressed.

For increasing the TRL of the Web-of-Cells concept and enabling the implementation and application in real networks, further effort at the device level as well as on the actual communication interfaces and protocols is required, in order to ensure the provision of the required flexibility. Before applying the Web-of-Cells approach in real networks, it is needed to further detail and refine the concepts as well as to analyse and verify them taking into consideration the implementation of the functionalities at device level in particular. Since corresponding proof of concept tests have been carried out with some limitations, further research and development on higher Technology Readiness Levels is necessary. This includes the further development of rules for defining cells, the provision of extended power system models and networks and corresponding benchmark criteria.

Terminologies

ACE	Area Control Error
aFCC	Adaptive FCC
AGC	Automatic Generation Control
AMI	Advanced Metering Infrastructure
BAU	Business as Usual
BCL	Balance Control Loop
BRC	Balance Restoration Control
BSC	Balance Steering Control
CIGRE	International Council on Large Electric Systems
CHIL	Controller Hardware-in-the-Loop
CHP	Combined Heat Power
CPFC	Cell Power-Frequency Characteristic
CSA	Cell Set-point Adjuster
DER	Distributed Energy Resource
DBRC	Direct Balance Restoration Control
DPSL	Dynamic Power System Laboratory
DSM	Demand Side Management
EV	Electric Vehicle
ELFC	Enhanced Load Frequency Control
FC	Fuel Cell
FCC	Frequency Containment Control
GB	Great Britain
HV	High Voltage
ICT	Information and Communication Technology
IEEE	Institute of Electrical and Electronics Engineers
IRCP	(ELECTRA) Integrated Research Programme
IRPC	Inertia Response Power Control
KPI	Key Performance Indicator
LFC	Load Frequency Control
LV	Low Voltage
MV	Medium Voltage

NSGL	National Smart Grid Laboratory
OLTC	On-Load Tap Changer
OPF	Optimal Power Flow
PCC	Point of Common Coupling
PFC	Primary Frequency Control
PHIL	Power Hardware-in-the-Loop
PV	Photovoltaics
PVC	Primary Voltage Control
PPVC	Post Primary Voltage Control
RES	Renewable Energy Resource
RoCoF	Rate of Change of Frequency
SC	Study Case
SCL	Secondary Control Loop
SD	Standard Deviation
SG	Synchronous Generator
SGAM	Smart Grid Architecture Model
SuT	System under Test
TCR	Test Criteria
TPO	Transient Phase Offset
TRL	Technology Readiness Level
WoC	Web-of-Cells
WG	Wind Generator
VRB	Vanadium Redux Battery

Table of Contents

List of Figures and Tables

Figures

Tables

1 Introduction

1.1 Scope and Purpose of the Document

An important activity within ELECTRA IRP was to evaluate the proposed Web-of-Cells (WoC) real-time control approach and its corresponding control schemes which are described in corresponding deliverables D4.2 (functional architecture) [1], D5.3 (control architecture) [2], and D6.3 (control schemes) [3]. The objective of this activity was to conduct experimental proof of concept testing of the different ELECTRA controllable flexibility solutions for voltage and balancing control based on the outcomes of various simulation studies of the individual functions as discussed in Deliverable D6.4 [4]. This report documents and summarizes the implementation and integration work of the WoC concept and corresponding functions on selected validation and testing scenarios taking the capabilities (infrastructure, personnel) of the involved partners into account.

1.2 Structure of the Document

The validation goals and requirements for the WoC proof of concept evaluation are briefly introduced in Section 2 whereas the applied validation methodology, the available validation infrastructure and the selection of use case combination is discussed in Section 3. Achieved results for validation scenarios covering balancing and frequency control schemes are described and discussed in Section 4 and the corresponding voltage control results are presented in Section 5. Conclusions and an outlook about the future work is provided in Section 6. Finally, fact sheets of the selected and realized simulations and laboratory experiments of the involved partners are shown in the Annex.

2 Evaluation Goals and Requirements

The concepts for the control schemas developed within ELECTRA IRP are the aggregation of multiple control and observable functions acting together towards an ultimate goal; the stable frequency (balancing) and voltage control within the corresponding cells. In order to validate the aforementioned functions, they need to be integrated within the laboratory environments provided by the ELECTRA IRP partners.

These intelligent solutions comprise more than one inter-dependent function encompassing multiple domains that are developed independently by domain experts and brought together for integration within the laboratory for proof of concept evaluation. Therefore, the validation goals for analysing the WoC approach can be summarized as follows:

- Experimentally implement WoC-based distributed real-time control in a number of respected European laboratories,
- Proof that local problems can be solved locally within a cell,
- Demonstrate the effectiveness of distributed controls in relation to a number of selected grid scenarios taking laboratory evaluation capabilities of ELECTRA partners into account,
- Investigate the local coordination of numbers of devices when subject to uncertainty in system operation while maximizing the effective utilization of flexibility,
- Compare performance demonstrated across multiple laboratories and with traditional approaches (i.e., business as usual case), and
- Understand on the basis of experiments the implications of potential controller conflict(s) and the relative merits of different controls.

3 Proof of Concept Validation Methodology and Environment

In order to select suitable laboratories for the proof of concept evaluation a corresponding validation methodology has been developed which is outlined in this section. Also, a brief overview of the available research infrastructures and facilities provides by the ELECTRA partners for evaluating the WoC concept and the corresponding control schemes and functions is provided together with a brief overview of the finally selected validation scenarios.

3.1 KPI-based Validation Methodology

The integration of multiple software and hardware controllers into a consolidated solution for laboratory validation and testing – as for the ELECTRA IRP WoC concept – is complex due to the requirements of developing consistent functional interfaces between controllers and ensuring real-time operation. Therefore, a structured process should be followed when assessing the performance of novel solutions, which requires:

- Defining Key Performance Indicators (KPIs),
- Measuring the defined KPIs in simulations and laboratories, and
- Comparing the measured KPIs with a Business as Usual (BAU) case.

Testing activities are sometimes performed across multiple laboratories, which brings various benefits such as exposure to a wider variety of hardware testing environments, communication protocols and testing procedures that collectively have the potential to increase the robustness of the tested system. Therefore, it is of critical importance to formulate KPIs that do not depend on the peculiarities of individual laboratory setups and capabilities, in order to ensure that the results are comparable. This is a challenging task; for example, many relevant indicators of power system control performance, such as the Rate of Change of Frequency (RoCoF) during disturbances, are linked to time constants which are highly specific to the system inertia, unit capabilities and signal delays inherent to the physical power system being measured.

Typically, for laboratory validation and testing of power system controllers, multiple functions need to be integrated within the laboratory environment. These intelligent solutions comprise more than one inter-dependent function encompassing multiple domains that are developed independently by domain experts and brought together for integration within the laboratory for validation and testing. By using the Smart Grid Architecture Model (SGAM) the interdependencies of the different functions are more clearly exposed and therefore the development of the KPIs required for testing across multiple facilities can be performed in a meticulous manner.

Therefore, a methodology for developing suitable KPIs using the SGAM has been developed for the WoC proof of concept evaluation which is outlined in Figure 3.1. It consists of three main stages, whereas in the first stage a consolidated function description of the WoC controls are being mapped to the SGAM Function Layer. In a second stage, for each use case to be evaluated in the experimental infrastructure of a partner, the functions identified in the first stage along with the selected reference power system need to be mapped to individual laboratory components. In the last step experimentation descriptions and KPIs are being identified based on the aforementioned mapping. Further details about this structured approach are provided in [5] and [6].

The final derived KPIs for evaluating the WoC concept address mainly the objectives of showing that the proposed real-time control concept and its corresponding functions are working and can be better than today (i.e., compared with the BAU). The resulting test criteria based on these KPIs are provided in the corresponding Sections 4 and 5 where the achievements are presented and discussed.

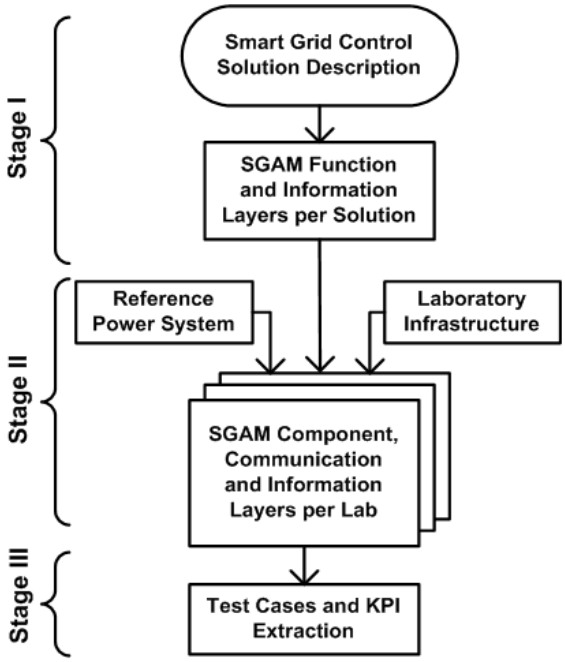

Figure 3.1: Structured methodology for validation of ELECTRA control concepts

3.2 Available Validation Environments and Competencies

In general, the available research facilities and infrastructures for the proof of concept evaluation of the ELECTRA WoC real-time control concept can be divided into:

- Pure simulation environments using of the shelf power system analysis tools,
- Pure hardware environments (i.e., power system and smart grid related laboratories), and
- Hybrid environments including simulation and controller/power components which are coupled in a Controller Hardware-in-the-Loop (CHIL) and/or Power Hardware-in-the-Loop (PHIL) manner in the laboratories of the partners.

Table 3.1 provides a brief overview of the available environments which are provided by the ELECTRA partners for the proof of concept evaluation. Details about the different facilities and tools are provided in the following sections.

Table 3.1: Available research infrastructures of the ELECTRA partners for the proof of concept evaluation

Environment	Partner	Details
Pure Simulation Environment	VTT	Modified CIGRE European MV distribution network model in *MATLAB/Simulink/SimscapePower* and *Matpower*
	IEE/DERlab	Modified CIGRE European MV distribution network model in *MATLAB/Simulink/SimscapePower*
	CRES	Modified CIGRE European MV distribution network model in *MATLAB/Simulink/SimscapePower*
	ENEA	Modified CIGRE European MV distribution network model within *PowerFactory*
	INESC P	Modified CIGRE European MV distribution network model in *MATLAB/Simulink*
	USTRATH	Reduced Great Britain power network model within RSCAD (RTDS)

Environment	Partner	Details
	TECNALIA	FLEXTEC ad-hoc developed grid model (LV/MV distribution grid; conventional and RES/DER units: 60% RES penetration), *PowerFactory* with Python scripts
Pure Hardware Environment	CRES	Experimental LV microgrid (controllable and uncontrollable DER: photovoltaics, batteries, battery inverters, loads)
	RSE	RSE microgrid (Distributed Energy Resources Test Facility-DERTF): controllable loads, PV, wind, CHP
	DTU	SYSLAB experimental facility (meshed configuration with the ability of opening tie-lines forming a radial network; resources: PV, wind, EVs, vanadium-redox battery, diesel, loads)
Hybrid Environment: Controller and Power Hardware-in-the-Loop	SINTEF	PHIL platform with CIGRE European MV distribution network (Opal-RT simulator; EGSTON 200 kW grid emulator; 2x 60 kW converter units; RT-Lab, *MATLAB* and *GAMS* software)
	AIT	SmartEST Lab: coupled HIL co-simulation with CIGRE European MV distribution network; *PowerFactory* with *Python* scripts; AIT smart grid converter (emulated power electronics + real converter controller); Typhoon HIL real-time simulator
	USTRATH	Dynamic Power Systems Laboratory (DPSL); 2 Cells emulated with real lab equipment and 3 within RSCAD (RTDS)

3.2.1 Pure Simulation Environments

Modified CIGRE European MV test grids used by VTT, IEE/DERlab, CRES, ENEA, and INESC P

For the simulation tests implemented by VTT a modified version of the CIGRE European Medium Voltage (MV) reference grid is being used [7]. The realized cell division together with the additional branch (i.e., Cell 3) is shown in the following figure.

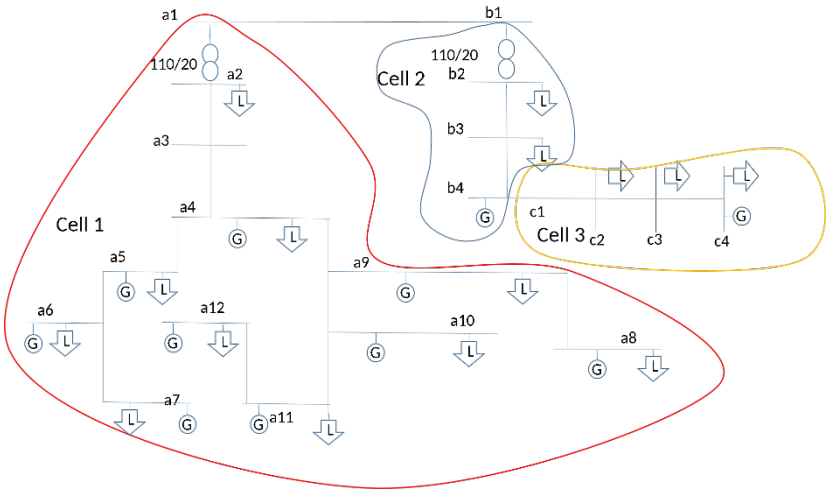

Figure 3.2: Cell division in CIGRE medium voltage model grid provided by VTT

The outside grid connection to the High Voltage (HV) system is at points a1 and b1. Renewable power resources are distributed to the system quite evenly. There is however one relatively larger wind turbine present in node a7.

The simulation environment for the ELECTRA tests is being realized via MATLAB/Simulink together with Matpower package in MATLAB. The grid model is implemented in Simulink whereas the calculation of the control algorithms is performed in Matpower.

Similar to the VTT set-up also IEE/DERlab is using the CIGRE European MV test network implemented in MATLAV/Simulink. For the corresponding tests the original version of the test grid is being used which is divided mainly into three interconnected cells. A similar approach has been chosen by CRES where the CIGRE network is divided into 4 cells.

In ENEA's case the reference grid is a modified CIGRE MV test grid developed within DIgSILENT PowerFactory divided into six cells as shown in the following figure. Each cell is composed of several devices such as load, Photovoltaics generators (PV), or synchronous machines. A generation loss of 2MW in Cell 1 is chosen as the reference event. The generation loss is emulated by means of a step increase in load.

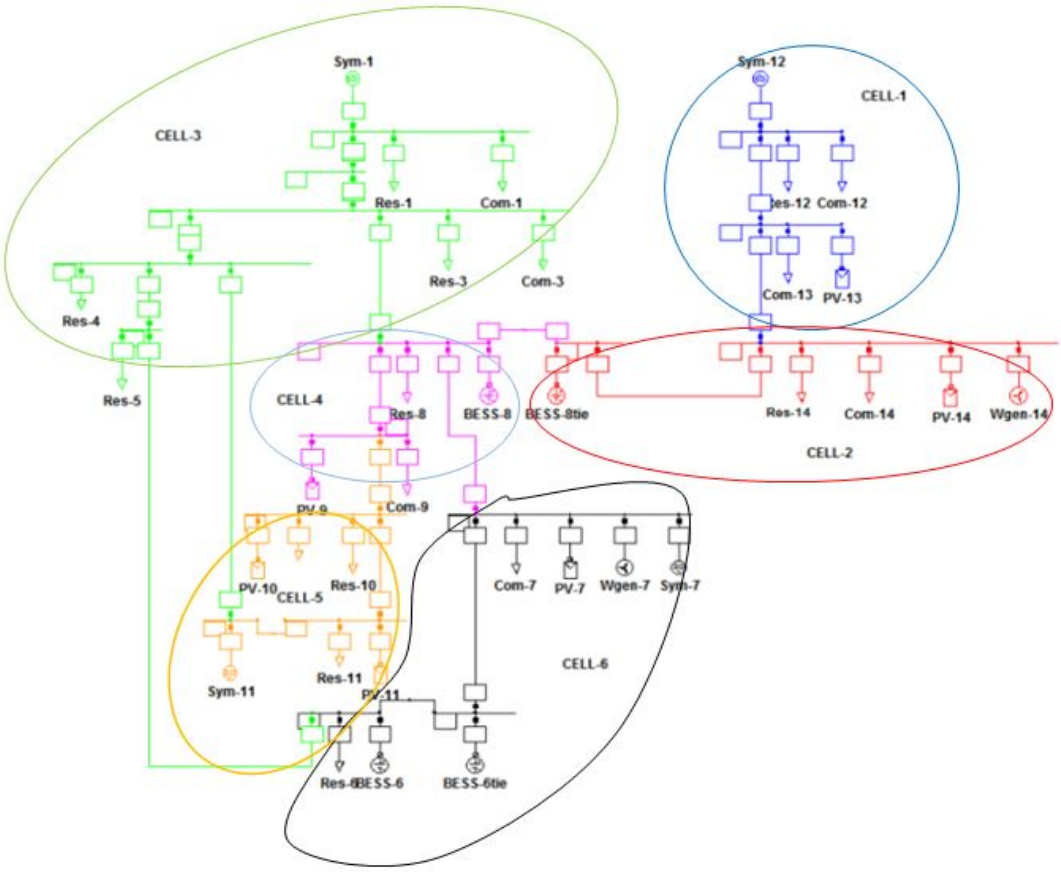

Figure 3.3: CIGRE European MV modified test grid provided by ENEA

INESC P also used the CIGRE MV grid as a reference which is modelled in MATLAB/Simulink with the following assumptions on the network configuration:

- All circuit breakers were considered closed in order to have a meshed network topology.
- The "slack node" that represents the HV grid is modelled as a synchronous generator with an inertia constant of H=5 s and equipped with primary frequency control (R=0.1). The nominal power of this generator is 500 MW.
- Cell 1 is composed by PVs, a battery, a wind turbine and loads.
- Cell 2 is composed by PVs, Fuel Cells (FCs), a battery, a Combined Heat Power (CHP) plant, a wind turbine and loads.
- Cell 3 is composed by loads.

All generators connected to the MV grid participate in the frequency control. A disturbance in a load from Cell 1, with an increase of its value by 1 MW at 30 s is chosen as reference event.

All this different simulation set-ups have been developed to study different aspects of the WoC and the corresponding control functions.

Reduced GB power network used by USTRATH

For analysing mainly frequency control implementations, a reduced five-cell dynamic model of the Great Britain (GB) power system has been chosen as the reference grid (see Figure 3.4). Each cell relates to a region developed around major generation sources, power flow corridors and load centres and the model is based on real power flow data. The model has been developed in RSCAD and simulated in real-time using a RTDS real-time simulation system, with each cell comprising an aggregated generator and an aggregated load. A number of occurrences of ~1 GW generation losses have been experienced by the GB grid within the last year and therefore a generation loss of 1 GW in Cell 2 has been selected as the reference frequency event.

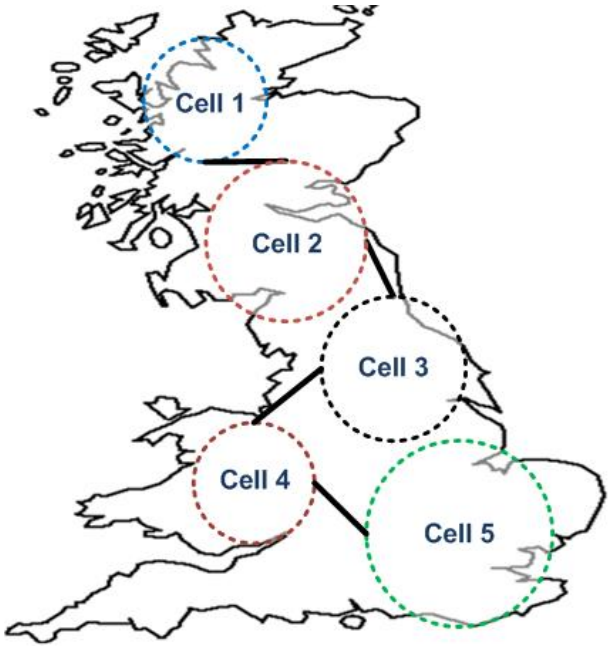

Figure 3.4: Reduced GB power network model provided by USTRATH

Extended test network "FLEXTEC" developed by TECNALIA

In context of the ELECTRA project an extended test grid has been developed by TECNALIA called FLEXTEC. This model (provided in DIgSILENT PowerFactory) due to the variety of distributed energy resources in MV and Low Voltage (LV) levels has been considered as representative of the WoC. This test grid is suitable for its use in the ELECTRA experiments. An overview of the implemented model is provided in Figure 3.5.

The test grid presents a meshed configuration in the MV levels and a radial structure typically representative of the LV feeders. The connection to the transmission network is done through a 255 MVA 220 kV/20 kV transformer. The MV distribution grid voltage is 20 kV. The conventional generation generates at 6.3 kV. The wind generators voltage is 690 V and the PV panels are connected to the 400 V LV grid.

In a first WoC approach, the grid has been divided into three main cells although the flexible structure of the grid and its size is enough to easily divide it into a bigger number of cells. In the framework of ELECTRA, up to 9 cells have been considered.

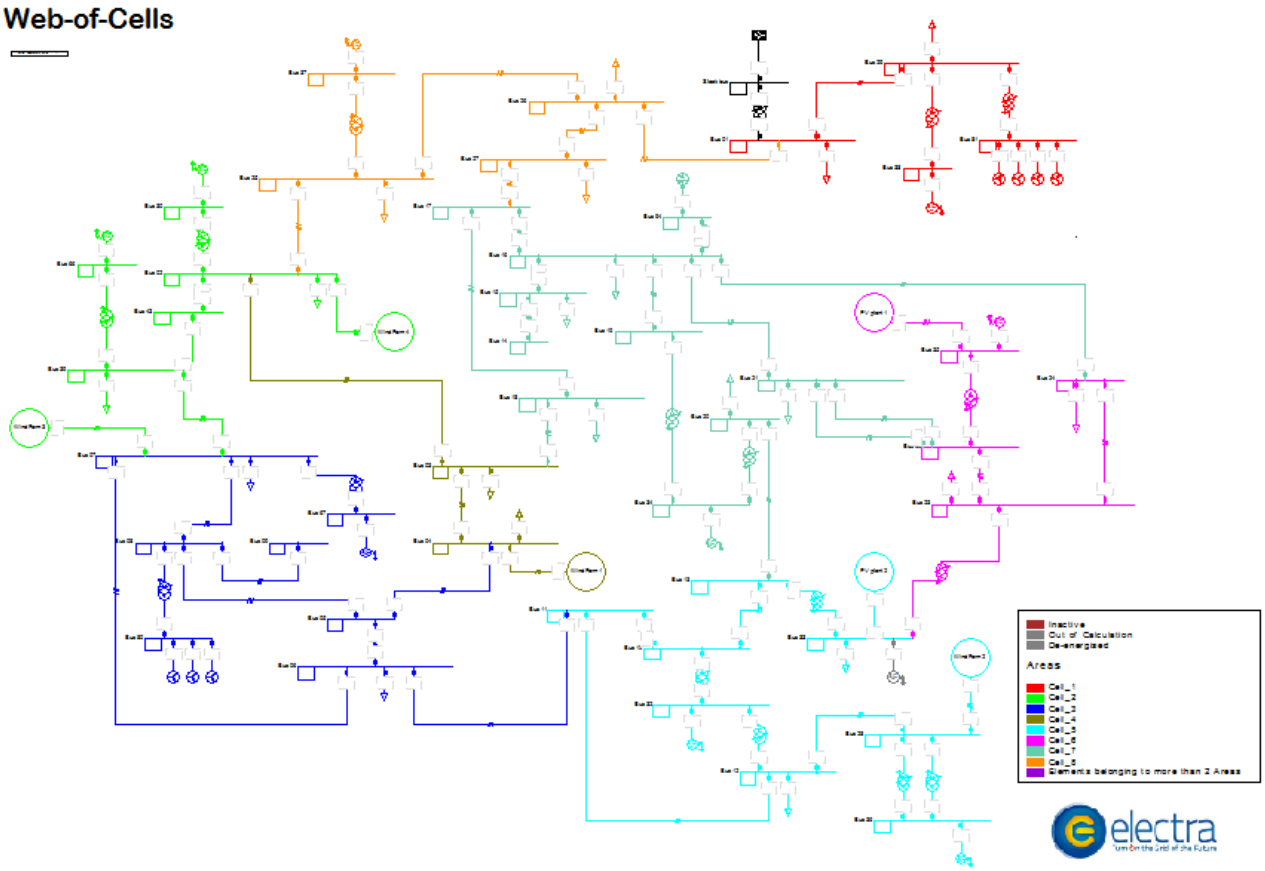

Figure 3.5: FLEXTEC test grid provided by TECNALIA

The distributed generation placed in the grid includes:

- 10 conventional renewable and non-renewable distributed energy sources (3 diesel groups + 5 hydraulic units + 2 gas generators) with rated powers between 2.7 MW and 10 MW.
- 20 wind turbines of 2.5 MW grouped into four big wind power plants.
- 7 medium power wind turbines of 240 kW each one.
- 27 PV systems with rated powers between 2.1 kW and 4.1 kW.

The loads have been modelled as constant PQ loads with variable profiles of around 10 % variation over their scheduled program. It has also been added to the profile the typical uncertainty that is characteristic of the very-short term techniques (15 min to 1 h ahead), 1 %. The same procedure has been followed for the definition of the generation profiles, considering that the uncertainty in generation forecasting is bigger compared to the uncertainty in the load (up to 5 %).

3.2.2 Pure Hardware Environments

CRES

The experimental microgrid of CRES was provided in the setup shown in Figure 3.6 for specific ELECTRA tests. This setup involves a number of controllable and uncontrollable renewables such as PV, batteries, battery inverters and loads. The system is configured to represent two LV, single-phase cells. During the tests the microgrid is operated in islanded mode in order to allow for the system to vary its frequency based on imbalances. The microgrid is supervised by a SCADA computer which communicates with a second machine. The latter is the host of the controllers which are mainly implemented in MATLAB/Simulink.

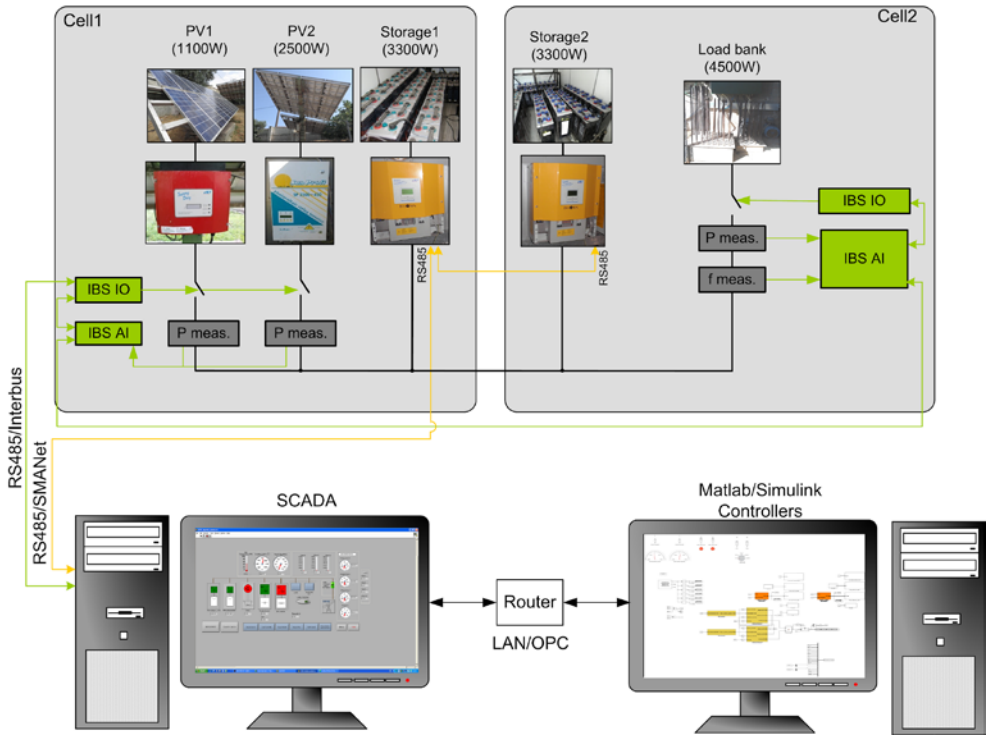

Figure 3.6: Experimental setup used by CRES

RSE

The RSE microgrid called DER-TF (see Figure 3.7), is a facility of distributed energy resources, capable of electrical and thermal power production. DER-TF includes a CHP natural gas engine of 50 kW, a 30 kW photovoltaic field, a 3kW micro wind turbine, a number of storage systems (Lithium, Lead, etc,) with energy from 30 kWh to 60 kWh and a 100 kW controllable load. DER-TF is electrically connected to the distribution grid, but it is possible to operate it in islanded mode.

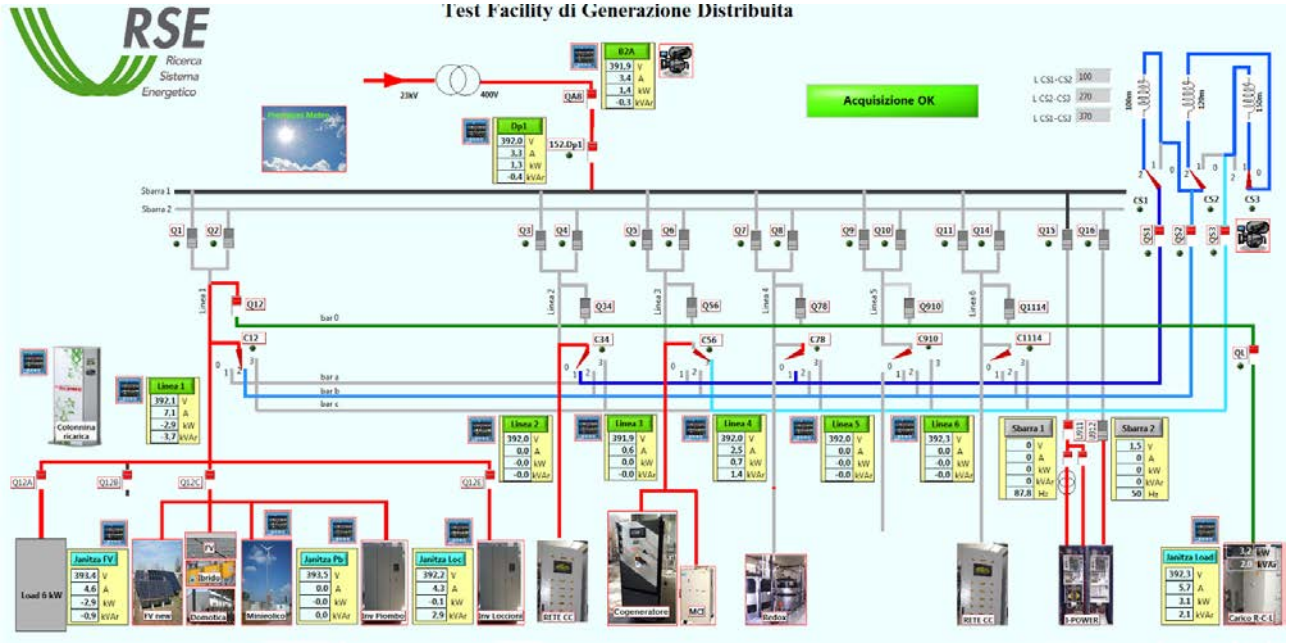

Figure 3.7: DER-TF microgrid of RSE

For the WoC experiments, the DERTF was set into three cells, each exchanging power with other cells by a single tie-line.

DTU

SYSLAB is an experimental facility at DTU Risø campus, designed as a testbed for advanced control and communication concepts for power grids. Rated at 400V, the 3-phase grid with a total of 16 busbars and 119 automated coupling points serves as the electrical backbone of the facility, allowing for tests to be undertaken under a large variety of different grid topologies.

Figure 3.8(a) shows the electric topology of the complete SYSLAB network. Marked in red is the setup used in the ELECTRA experiments. A single line overview of the simulation and experiment setup is shown in Figure 3.8(b). The grid is partitioned into three distinct cells in meshed configuration with the ability of opening tie-lines (tie-line 1-2) forming a radial network. The diagram also features the location of the Cell controllers running on the computer nodes, the communication links between the nodes as well as the communication between the devices. Devices providing the primary response are marked with I, and II indicates participation in the secondary control. The diesel operates at a fixed droop of 5 % as the grid-forming unit in island mode, and is the only component with a rotating mass. It covers, together with the four-quadrant inverter of the vanadium redox battery, the reactive power flows caused by cables and thyristors.

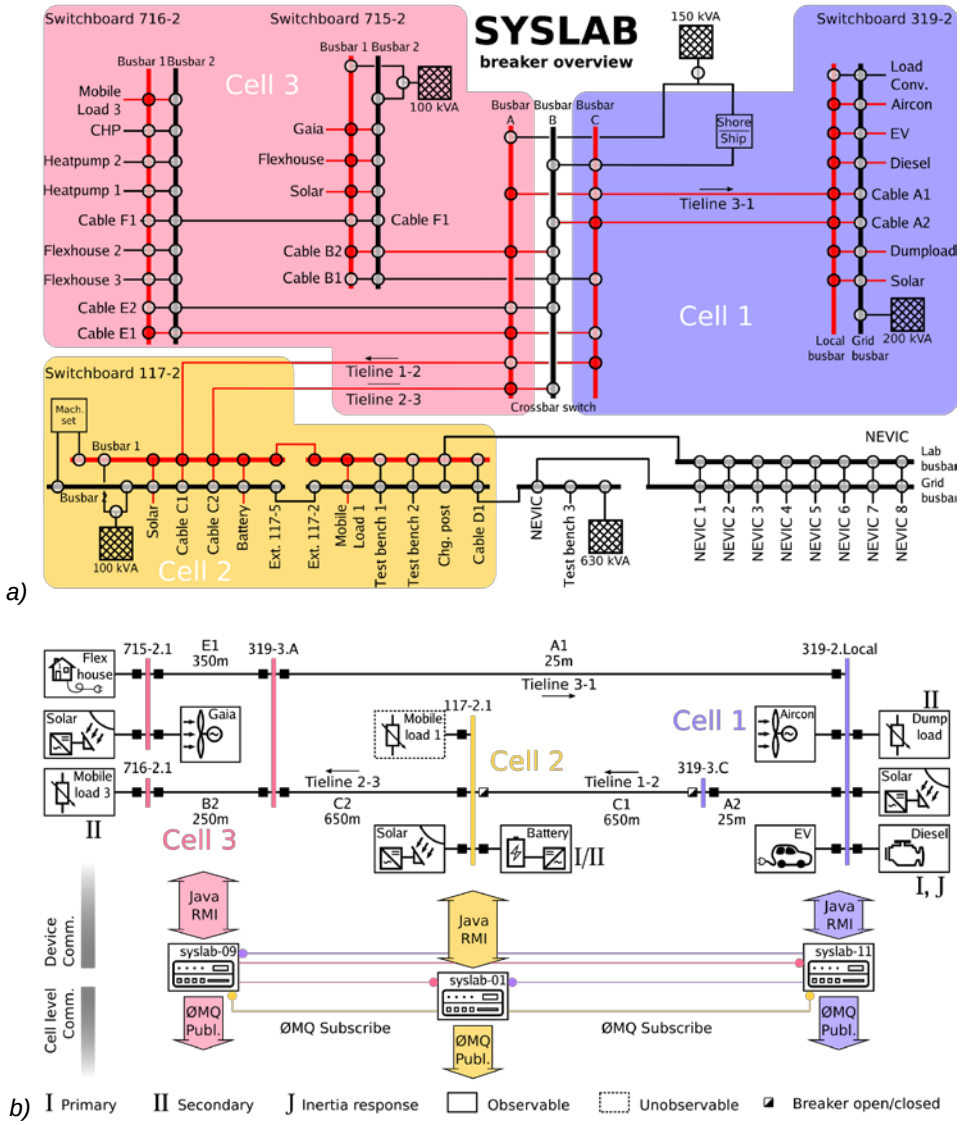

Figure 3.8: (a) Electrical topology of the SYSLAB laboratory network with the configuration used in ELECTRA experiments marked in red, and (b) the corresponding single line diagram together with the communication infrastructure

3.2.3 Hybrid Environments

SINTEF

The National Smart Grid Laboratory (NSGL) located in Trondheim is provided for the ELECTRA tests. The laboratory is equipped to perform real-time simulations of electrical systems and their controls. For the ELECTRA experiment the following equipment is utilized: OPAL-RT real-time simulator, 200 kW high-bandwidth (20 kHz) power converter operating as a grid emulator, and three 60 kW converter units as shown in Figure 3.9.

The CIGRE 15-bus benchmark network with eight PV connections and a wind turbine is utilized for the WoC proof of concept validation. While the converters at bus-10 and 7 are connected to the converter hardware, the rest of the PV panels are updated with “forecasted” (deterministic) minute level values.

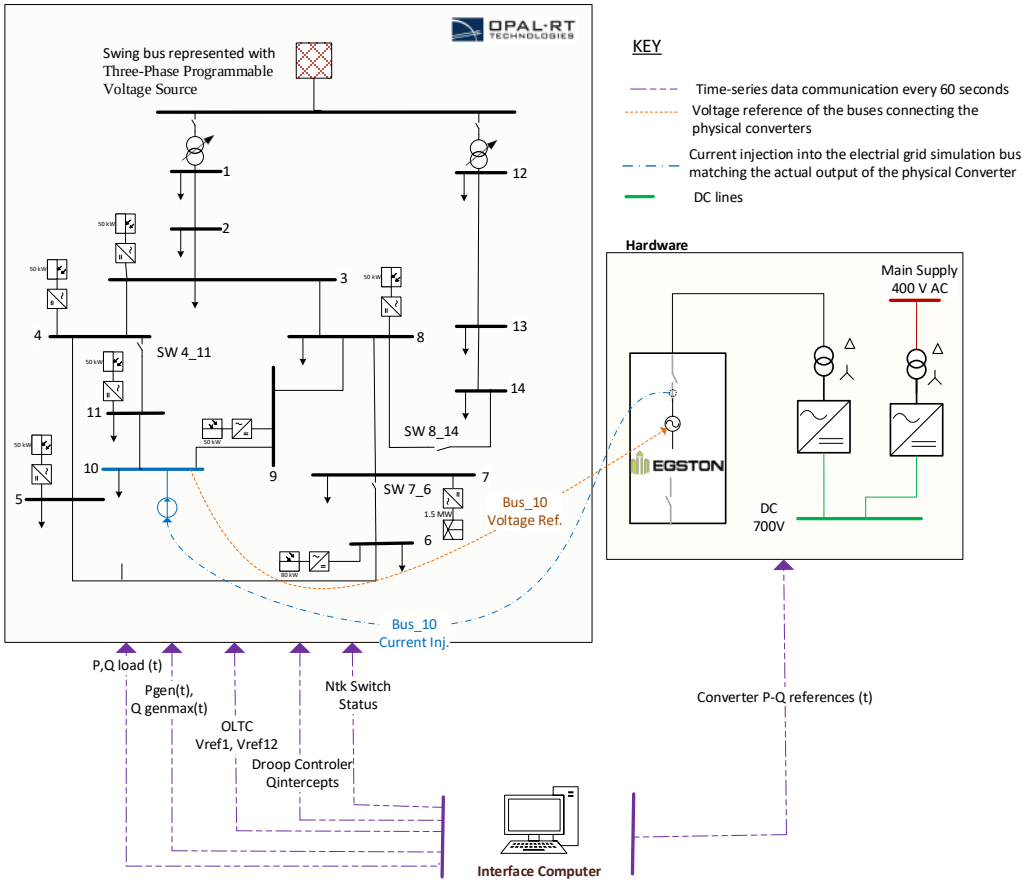

Figure 3.9: Power Hardware-in-the-Loop validation environment at SINTEF

AIT

A kind of HIL-based co-simulation set-up is provided by AIT in its SmartEST laboratory. The lab configuration contains the simulation of a power grid divided into several cells using the aforementioned CIGRE European MV reference grid implemented in PowerFactory. One of the distributed energy resources (i.e., a PV generator) is emulated in real-time simulation system (i.e., Typhoon HIL) where the real embedded controller platform is connected to it. An own developed inverter-based Distributed Energy Resource (DER) – called AIT Smart Grid Converter – is being used as basis; i.e., the power electronics of the converter are modelled and emulated in real-time and are controlled by the real controller board.

The proposed concept of this kind of real-time HIL-based co-simulation environment is shown in Figure 3.10. where the coupling framework LabLink has to provide a real-time signal exchange between automation and control applications, the power grid simulation, and hardware components

coupled to it. Additionally, a synchronization client is used to synchronise the execution of the different connected elements. Also, a real-time database and a visualization client is connected to this laboratory setup providing a comprehensive HIL-based setup.

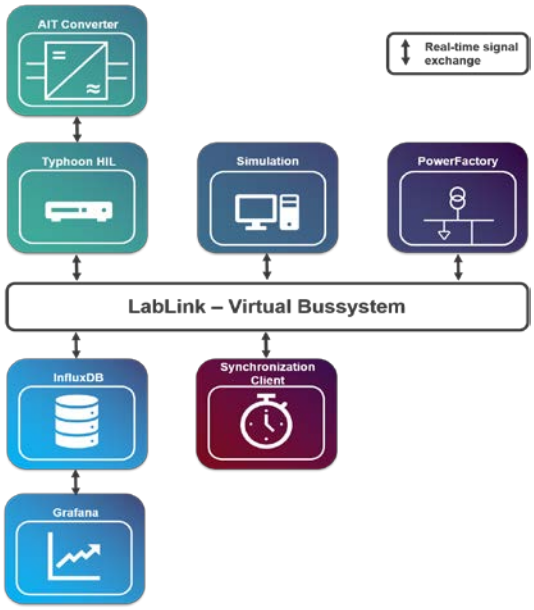

Figure 3.10: HIL co-simulation based validation set-up provided by AIT

USTRATH

The CHIL and PHIL validation environment within DPSL at USTRATH is presented in Figure 3.11. For testing the control algorithm in a more realistic environment, two of the cells (Cell 1 and Cell 2) are emulated with real laboratory equipment, a 15 kVA converter, a 10 kVA inverter and two 10 kW resistive load banks. The remaining 3 cells of the GB network are simulated in RTDS with a time-step of 50us. For coupling the laboratory hardware with the simulation, a 90 kVA bidirectional power converter unit is utilized as the power interface, amplifying the voltage at the point of common coupling with the simulation. The hardware equipment responds to the dynamics at the Point of Common Coupling (PCC), which is measured (usually in the form of currents) and fed into the simulation for closing the loop. For an increased accuracy of the PHIL implementation a time delay compensation technique is used.

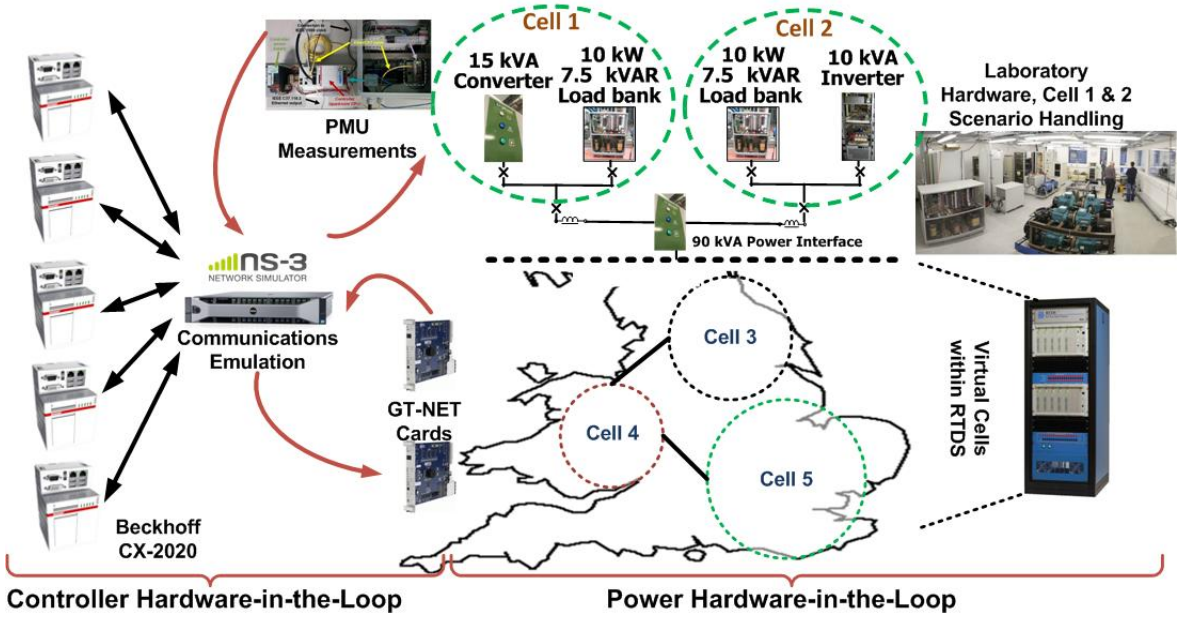

Figure 3.11: Controller and Power Hardware-in-the-Loop validation environment at USTRATH

3.3 Selected Validation Scenarios

With the usage of the above outlined KPI/SGAM-based validation methodology taking the laboratory and personnel capabilities of the ELECTRA partners into account, the nature of the six different control schemes for balancing and voltage control as well as the results of a survey from industrial stakeholders (which was performed during CIRED Workshop 2016), overall, 15 different experiments have been identified and finally selected for implementation and proof of concept evaluation.

Those testing scenarios addressing the combination of balancing and frequency control (i.e., IRPC and FCC; FCC and BRC; FCC, BRC and BSC) as well as voltage control (i.e., PVC and PPVC) use cases. They have been implemented and validated in selected partner's labs following mainly four phases as outlined in the following figure.

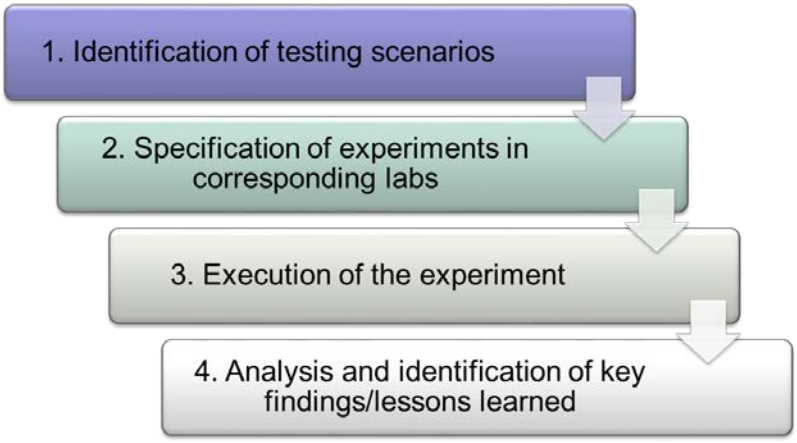

Figure 3.12: ELECTRA's evaluation approach for proving the WoC control concept

The identification of the testing scenarios has been carried out as outlined above. Based on this selection a detailed specification of the identified 15 experiments in the selected laboratory environments has been performed using the ERIGrid approach as outlined in [5]. Later on, the selected combinations of the control schemes and the corresponding observable and control functions have been implemented in (co-)simulations, Hardware-in-the-Loop (HIL), and pure laboratory set-up of the ELECTRA partners – as described above – for the proof of concept evaluation and analysis of the results. The achievements from this evaluation are summarized and discussed in the following Section 4 whereas details to each of the aforementioned experiments are presented in corresponding fact sheets in the Annex.

For the sake of feasibility and based on the analysis and selection of grid models in the ELECTRA consortium, the number of cells in the validation environments was selected in the range of small-scale (i.e., 1-3 cells) and medium-scale (i.e., 4 to 9 cells) set-ups. In the validation process, each involved partner was free to select the model of their preference based on simulation and laboratory capabilities, know-how, and limitations. Hence, the diversity in the selection of the validation environments and grid setups enhances the validation of the controllers since it shows their feasibility of different implementations while the achieved results are qualitative the same.

4 Balancing and Frequency Control Validation Achievements

Based on the above outlined validation methodology, the available validation environments, and the selection of use case combinations the following results have been achieved for the proof of concept validation of the balancing and frequency control schemes in ELECTRA IRP.

4.1 Validation Experiments "Use Case Combinations FCC and BRC"

In this section, the validation of two of the balancing and frequency control solutions, namely the FCC and BRC, by simulations and experiments is discussed in detail. First, a brief overview of the validation environments utilized is presented followed by setting the objectives for the validation. The key findings of the validation are then presented and a discussion on the achievements and future outlook concludes the section.

4.1.1 Chosen Validation Environments

An overview of the validation environments utilized for validation of FCC and BRC use cases are shown in Table 4.1.The detailed descriptions of the validation environments can be found in Section 3.2 and in the Annex.

Table 4.1: Used validation for proof of concept validation of use case combinations FCC and BRC

Environment	Partner	No of Cells	Details
Pure Simulation Environment	ENEA	6	Modified CIGRE European MV distribution network model within PowerFactory
	USTRATH	5	Reduced Great Britain power network model within RSCAD (RTDS)
	INESC P	3	Modified CIGRE European MV distribution network model within MATLAB/Simulink
Pure Hardware Environment	RSE	3	Test facility DER-TF
	DTU	3	Test facility SYSLAB
Hybrid Environment: Controller and Power Hardware-in-the-Loop	USTRATH	5	Test facility Dynamic Power Systems Laboratory (DPSL) using 2 Cells within DPSL and 3 within RSCAD (RTDS)

4.1.2 Test Criteria

In this section, the objectives of validation are set. The KPIs derived through the SGAM methodology were further refined to form the corresponding Test Criteria (TCR). The TCRs defined specifically for FCC and BRC validation are presented below:

- *Increased responsibilization*[1] *(TCR-FB01):* The reduction in divergence from planned system conditions (tie-line power flows) of remote cells following a disturbance, i.e., increased primary response from cell with imbalance event.
- *Bounded system frequency response (TCR-FB02):* The frequency response of the system should be within the exponentially decaying curves (referred to as trumpet curves) defined by

[1] The term responsibilization refers to the prioritization of remedial measures closer to the origin of an event, driving towards a new paradigm of increased decentralization.

ENTSO-E. When the frequency of the system following a disturbance is maintained within the trumpet curve, the response is considered apt.

- *Maximum frequency deviation (TCR-FB03):* Defined as the maximum deviation in frequency from its nominal value following a disturbance.
- *Settling time (TCR-FB04):* Defined as the interval between the occurrence of a disturbance and the point at which the frequency is restored within the set error margin (ε).

As is evident, the above set TCR can only be construed when compared to another existing control scheme or Business as Usual (BAU) practice. In this section, the primary frequency control and the automatic generation control employed by ENTSO-E are chosen as the reference implementation.

4.1.3 Performed Experiments and Results

The simulation results presented in Deliverable D6.4 [4] have shown the performance improvement of individual controllers, i.e., FCC and BRC, compared to the current state-of-the-art controllers employed in power systems around the world. However, the underlying design choices of the controllers have not been presented earlier. In this section, by means of simulation and experimental results, the design choices of the controllers are justified, followed by their validation within a laboratory environment. The results are presented in three parts; i.e., *(i)* FCC, *(ii)* BRC, and *(iii)* combination of FCC and BRC.

4.1.3.1 Frequency Containment Control (FCC)

The motivation of working towards development of a primary frequency control has been the need to achieve responsibilization. Two controls, namely, the *fuzzy FCC* and the *Const. FCC* were developed. The following subsections present the evolution and the development of the controls.

Fuzzy FCC

First, a fuzzy logic based responsibilizing FCC was developed. Observing the frequency and power imbalance across the tie-lines, the control adapts the droops of all the devices within the cell [8]. The droop of the cell with the imbalance remains unchanged while the droop of all other cells is increased. Through simulations [8] and experiments (see Figure 4.1) its ability to introduce responsibilization was proven. Figure 4.1(a) presents the frequency of a 3 cell system (RSE) in response to an imbalance within Cell 2 with the droops of the cells presented in Figure 4.1(b). As can be observed, with the implemented control, upon occurrence of the event, due to the increase in droop of non-event cells, the overall droop of the system increases.

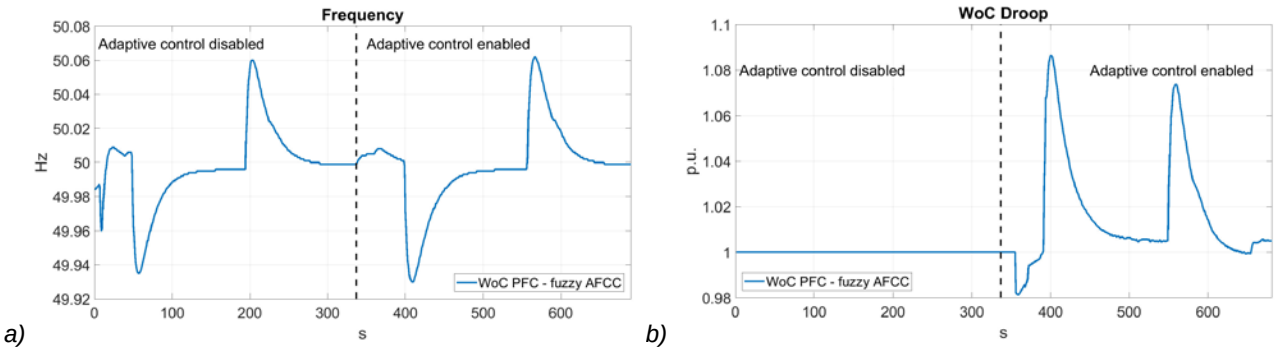

Figure 4.1: Behaviour of Fuzzy FCC – (a) frequency response, and (b) droop contribution

It is worth mentioning that the fuzzy FCC developed is centralized within a cell. The simulation and experimental evaluations at this stage did not involve any form of communications emulation. However, the developed fuzzy FCC prove its resilience towards requirement of meticulous tuning, as is evident from Figure 4.1(a), where the frequency response of the system with and without the adaptive droop is very similar, owing to the resilience of the fuzzy control to tuning. To demonstrate the motivation for

development of fuzzy FCC, consider the frequency traces of a 6 cell system (ENEA) and 3 cell system (INESC P) presented in Figure 4.2(a) and (b) respectively. The control implemented was a simple 0/1 logic for adaptation of droops, which without procurement of sufficient reserves within each of the individual cells deteriorates the response of the system in comparison to the conventional PFC.

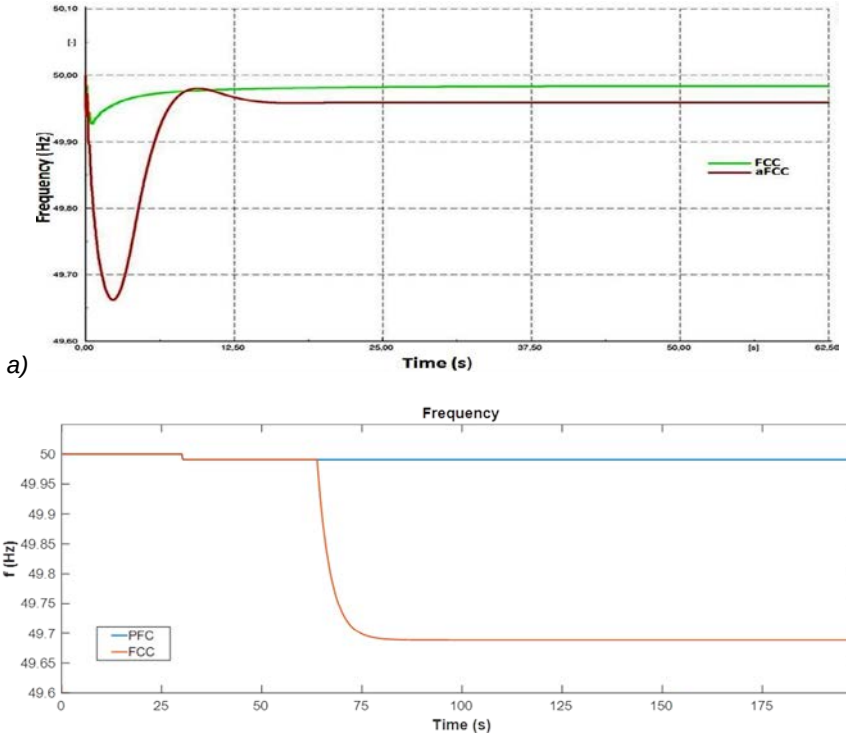

Figure 4.2: Examples of requirement of tuning for proposed fuzzy FCC –
(a) Frequency response from ENEA 6 cell system, and (b) Frequency response from INESC P 3 cell system

Const. FCC

A study was undertaken to understand if an alternative approach could be adopted that would ensure equivalent primary response before and after an event without the need to tune the controller. As a result, an additional controller was developed, referred to as Const. FCC, the performance of which is compared to the results of the fuzzy approach in Figure 4.3. The developed control (the detailed controller description can be found in the Annex) did not require tuning, however ensuring equivalent system response required coordination among all the cells (requiring information from all the cells in real-time), effectively turning the control into a centralized solution. As this was contrary to the objective of achieving a more decentralized and distributed solution, the equivalent FCC was not developed any further. However, the equivalent FCC can be used as a starting point for future research to develop a tuning-less adaptive primary controller using distributed computational algorithms.

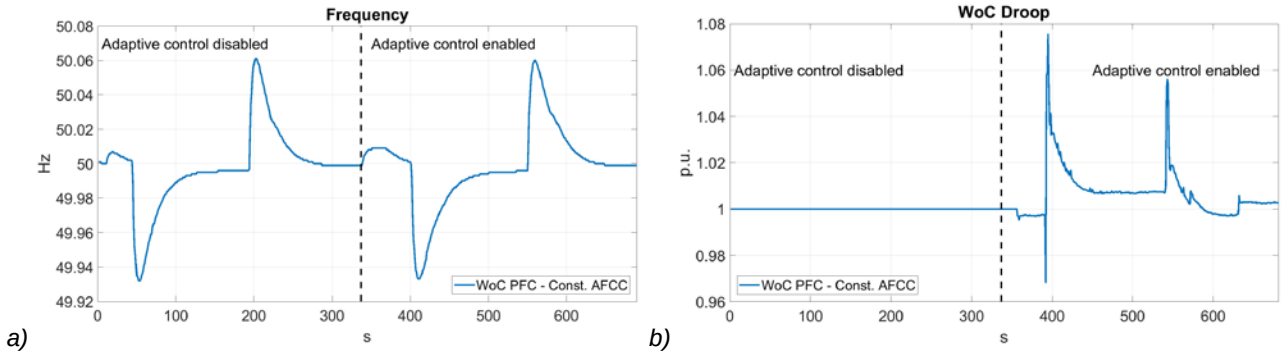

Figure 4.3: System response with const. FCC within RSE 3-Cell network –
(a) frequency response, and (b) droop contribution

Summary of Frequency Containment Control

Although, achieving responsibilization within the timescale of primary frequency control is difficult, the aFCC developed within ELECTRA has proven its feasibility. The responsibilization within the primary frequency control is achieved by means of adapting the droops of the cells that experience an imbalance. First, a fuzzy logic based FCC was developed that was capable of adapting the droops and introducing responsibilization. However, the control was centralized within a cell, relied on communications and required tuning. To explore if a tuningless control can be developed, the equivalent FCC was developed. The equivalent FCC was capable of ensuring equivalent primary response before and after responsibilization without requiring tuning but was effectively a centralized control (not just within the cell but within the entire web-of-cells). Therefore, for the purpose of evaluation, the fuzzy controller was adopted.

4.1.3.2 Balance Restoration Control (BRC)

Although responsibilization within secondary frequency control is inherent, the motivation of developing balance restoration control was to improve the speed of response of secondary control while at the same time ensuring enhanced responsibilization (use of more local observables and resources where possible). In the following subsections, the design process and validation of BRC is presented. First, the state-of-the-art secondary controller is presented followed by two case studies. With the focus on utilizing local variables, the first study was undertaken to understand if utilizing the tie-line power flow alone is sufficient to restore the balance and frequency of the network. The second study was undertaken to understand the implications of increasing the speed of the conventional secondary control. Drawing from the conclusions of the two studies, the design of BRC is presented and its performance is evaluated.

Automatic Generation Control (AGC)

Consider an interconnected power system with M control areas indexed by $i = 1, 2, \dots, M$. The Load Frequency Control (LFC) model of the i^{th} control area is presented in Figure 4.4. As shown, the LFC comprises a primary control loop and a secondary control loop, where the aim of primary control is to contain the frequency deviation caused by power imbalance in any control area, while the secondary control, i.e., Automatic Generation Control (AGC), is responsible to recover the frequency back to its nominal value [9]. The conventional LFC framework is widely employed in power systems around the world such as the Continental Grid of Europe, USA and Australia [9]-[11].

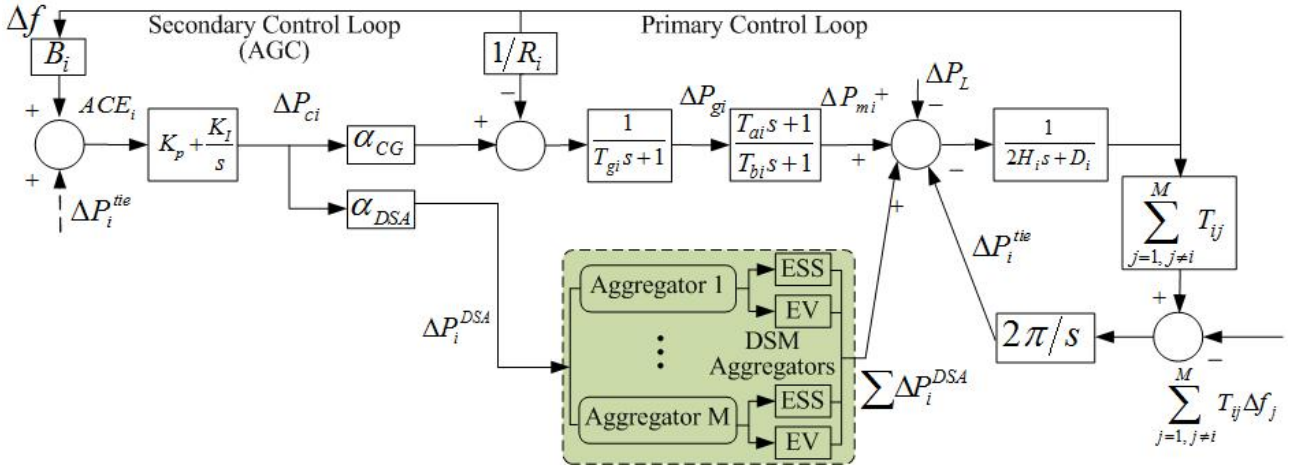

Figure 4.4: Load Frequency Control: A combination of automatic generation control and primary frequency control

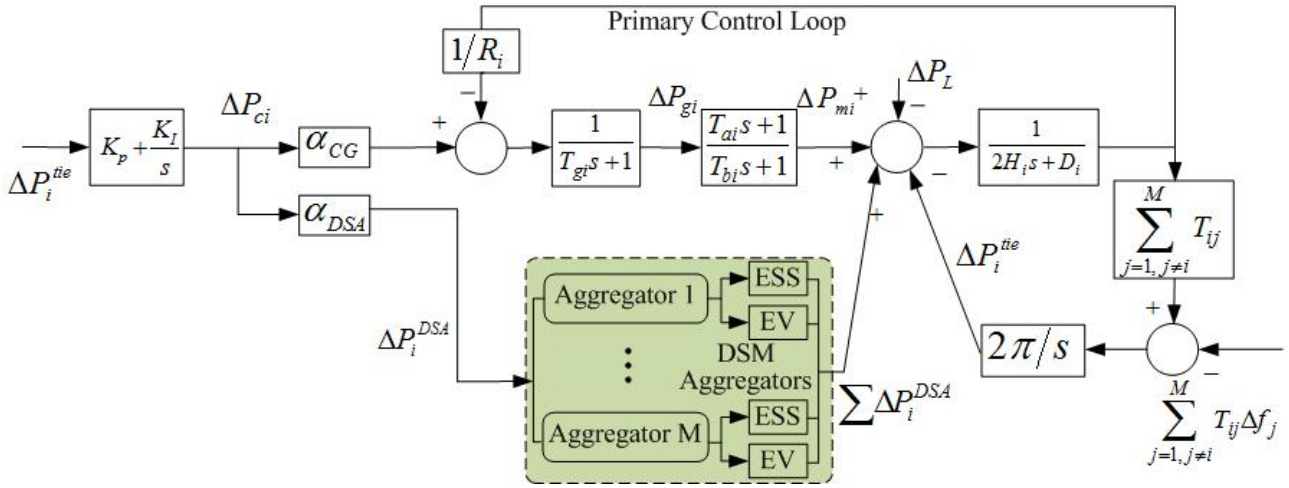

Figure 4.5: AGC with ΔP^{tie} as the error instead of ACE

Case Study I: Is restoring tie-line balance only sufficient?

First, as the focus of the WoC was on restoring the balance of the cells, an exercise to understand whether using tie-line balance (ΔP^{tie}) alone as an error signal within the secondary frequency control (as shown in Figure 4.5) would restore the system frequency was undertaken. The study was undertaken in a 3 Cell system (RSE) under the following three scenarios:

- In the first scenario (0 – 300 s), AGC control was disabled and the frequency was contained by the primary droop control of the generators, i.e. conventional primary frequency control only.
- In the second scenario (300 – 700 s), AGC was enabled but with the cell imbalance calculated without the $\beta\Delta$f term. In this way the frequency was contained by the Primary Frequency Control (PFC) and the tie-line power cell imbalance (ΔP^{tie}) was controlled by the AGC PI controller (as in Figure 4.5).
- In the third scenario (700 – 1000 s), AGC was enabled with the cell imbalance calculated as the sum of the tie-line power imbalance (ΔP^{tie}) corrected by the $\beta\Delta$f term (as in Figure 4.4).

The system frequency and tie-line power flow are presented in Figure 4.6. In Figure 4.6(a), we can see firstly from the left the frequency behaviour after the load event only in presence of generators droop control is as expected, i.e., the frequency reaches a new steady state value after the disturbance. As no secondary control is active, the tie-line flows do not return to their set-points as shown in Figure 4.6(b). In the second scenario, it can be observed that with the operation of the AGC based on tie-line error only deteriorates the frequency response (i.e., it continues to fall rather than being restored), although the tie-line errors have been restored to their set-points. Finally, at the last step (from 700 s), after the imbalance event, the frequency and tie-line power flows are restored to its nominal value.

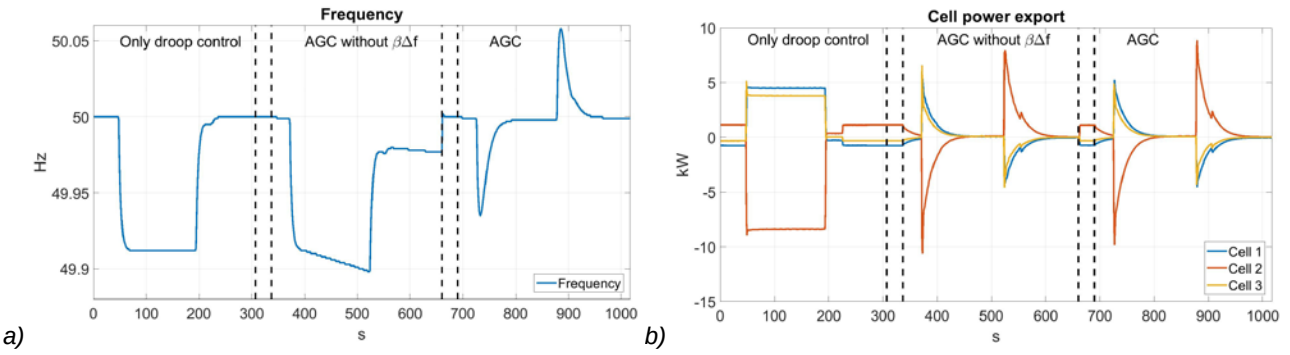

a) b)

Figure 4.6: AGC with and without $\beta\Delta f$ term – (a) Frequency, and (b) Tie-line power flow (ΔP^{tie})

In conclusion, it can be said that, the absence of the $\beta\Delta f$ term in the error signal not only prevents the correction of the frequency to its nominal value but can also introduce instabilities in grid frequency control.

Case Study II: Impact of increasing speed of conventional AGC

Once it has been established that balance alone cannot be utilized to restore the frequency, the focus was then turned to understand the impact of increasing the speed of AGC. Increasing the speed of AGC refers to increasing the gain K_I of the PI controller. A simulation and small signal stability analysis was undertaken on the 5 cell GB power system (USTRATH). The results of the small signal analysis are presented in Figure 4.7. The state-space model can be found in the Annex. The system is linearized around nominal frequency f_{nom} in steady-state. The input to the system is a disturbance in Cell 2 and the output is the system frequency.

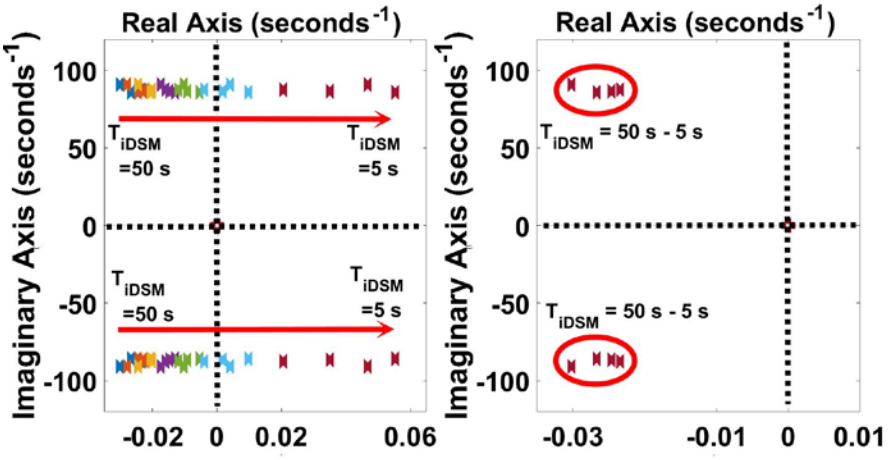

Figure 4.7: Pole-zero map from the small signal stability analysis of USTRATH's 5 Cell GB network

The time constant $T_{I,DSM}$ ($K_I = \frac{1}{T_{I,DSM}}$), Demand Side Management (DSM) signifying the use of fast acting demand side resources) of the integrator within the AGC varied from 50 s to 20 s in steps of 10 s and then to 5 s in steps of 5 s. Only the states that are impacted by $T_{I,DSM}$ are shown for clearer representation. As can be observed from Figure 4.7 (left), as the value of $T_{I,DSM}$ is reduced (i.e., the speed of AGC is increased), the poles move towards the imaginary axis. For $T_{I,DSM} = 10\ s$, the poles cross the imaginary axis representing an unstable system.

An alternative approach was explored, where $T_{I,DSM}$ of the cell where the imbalance has occurred is reduced while it remains same for all the other areas. It was observed that in the case where unilateral reserve activations only within the cell where the disturbance has occurred, the poles are very slightly impacted by the reduction in $T_{I,DSM}$ (see Figure 4.7, right), which therefore does not deteriorate the stability of the system.

From the two studies undertaken earlier, the following can be concluded:

- The use of ΔP^{tie} alone as the error signal is not sufficient.
- Activating reserves unilaterally allows for increasing the speed of secondary frequency control without deteriorating the system performance.

Balance Restoration Control (BRC)

To ensure unilateral activation of reserves to enable fast response, location identification techniques become necessary. Therefore, the objective was to focus on the development of fast location identification techniques that would allow for responsibilization. A location identification technique that

relies on measurement of ΔP^{tie} and RoCoF was developed and the details of the technique can be found in Deliverable D6.3 [3].

As the use of ΔP^{tie} alone as the error signal is not sufficient, a control architecture as shown in Figure 4.8 was proposed. The proposed controller, referred to as the BRC, incorporates a fast-acting Balance Control Loop (BCL) that utilized ΔP^{tie} as the error signal while at the same time, the secondary control loop utilizes Area Control Error (ACE) as the error signal. The fast acting BCL is enabled by a disturbance observer that incorporates the developed event location algorithm.

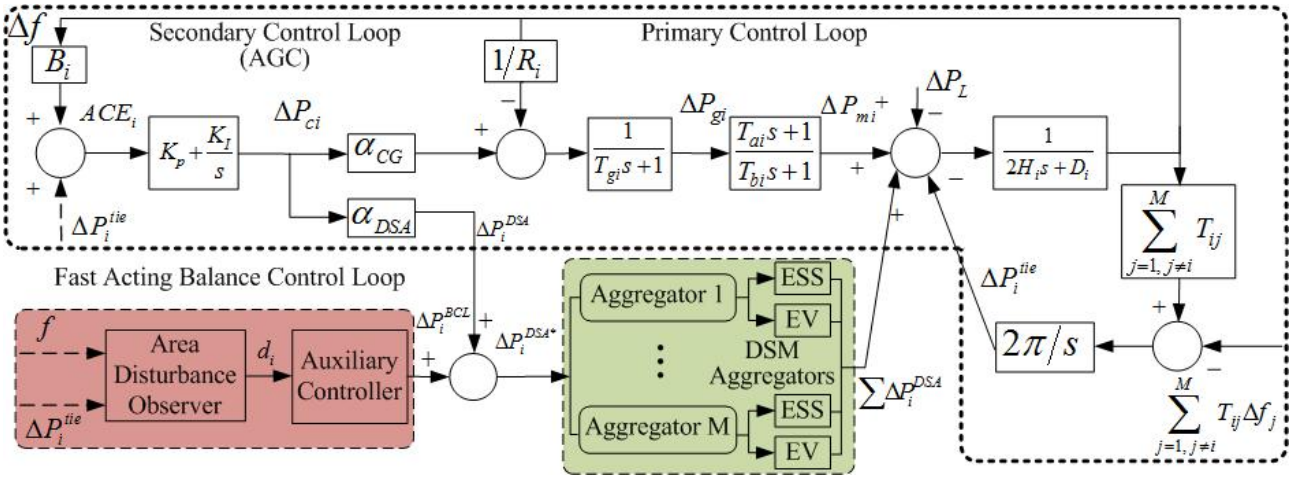

Figure 4.8: Proposed balance restoration control incorporated within LFC framework

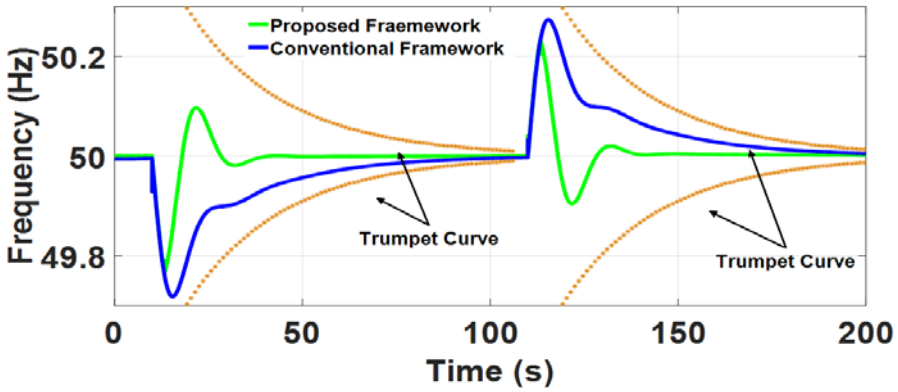

Figure 4.9: Comparison of frequency response of 5-Cell GB network with AGC and BRC

The frequency response of the 5 Cell system (USTRATH) when subject to generation loss at 10 s and a load loss at 110 s for the proposed BRC control and AGC is presented in Figure 4.9. Two performance indicators are used in the following investigations. Exponentially decaying functions $H(t) = f_0 \pm Ae^{-t/T}$ (so-called "trumpet-curves") as defined by the ENTSO-E in [9], which are used to monitor whether the frequency response of the system is exponentially bounded. In addition, the settling time is defined as the interval between the occurrence of a disturbance and the point at which the frequency remains within a 5 % band of the system's droop response for all times.

The settling time for conventional AGC is 83 s with no overshoot. The BRC, by means of fast and accurate detection of disturbance location, contributes to improving frequency nadir (frequency zenith for load loss) and leads to a faster settling time. With a settling time of 35.2 s, the proposed control is twice as fast. As can be observed, the BRC exhibits an overshoot compared to the AGC but is well within the bound defined by the trumpet curve.

The performance of the BRC was further analysed. Consider the frequency responses presented in Figure 4.10, with frequency bias factor β miscalculation of 5% for both the conventional and proposed control. As can be observed, a 5% miscalculation of β results in a ± 17 s variation in T^{set} for the conventional AGC while has no significant impact within the BRC. Larger generating units within the network are bound by the grid code to provide a set percentage response to a variation in frequency. However, if the units do not abide by the set droop, this will lead to miscalculation of β. Furthermore, presently it is normal practice to determine β on a yearly basis [10]. In future systems, it is expected that the characteristics of the network (e.g., system inertia) will vary vastly within a single day. It is also expected that the difference between the peak load and the base load will increase significantly [12], thereby resulting in the load offering a different damping effect at different times. Therefore, the proposed BRC utilizing ΔP^{tie} is more resilient to changes expected within the future power system.

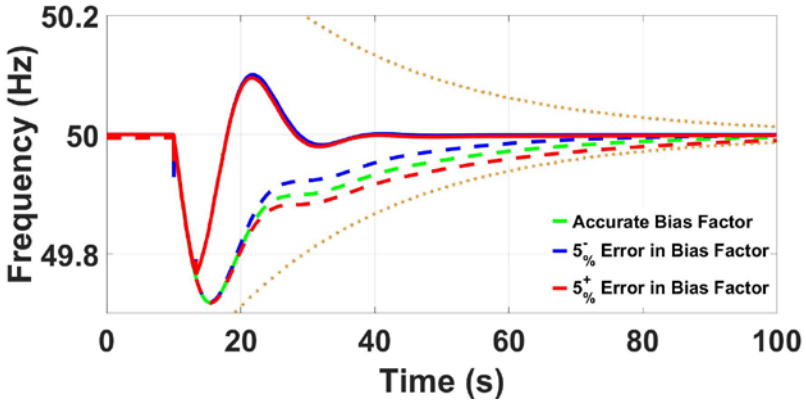

Figure 4.10: BRC performance analysis

Furthermore, if ACE is utilized within the BCL of the BRC (which is equivalent of increasing the speed of Secondary Control Loop (SCL) after event detection), although the activations of reserves are guaranteed to be unilateral within the cell where the disturbance has been detected, the miscalculation of β leads to nuisance activations as shown in Figure 4.11. It should be noted that utilizing ΔP^{tie} avoids any nuisance activations.

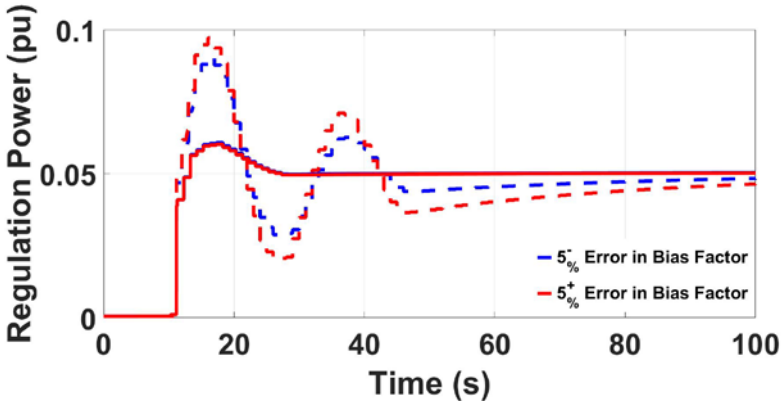

Figure 4.11: Usage of ACE within BCL

4.1.3.3 Enhanced Load Frequency Control (FCC and BRC)

The combination of the proposed fuzzy FCC and BRC is referred to as the Enhanced Load Frequency Control Framework (ELFC). The two controls were incorporated within the 5 Cell CHIL and PHIL environment at USTRATH. The performance of the combination of the controllers is compared to the present day state-of-the-art control scheme. The frequency response of the system subject to reference disturbance is shown in Figure 4.12.

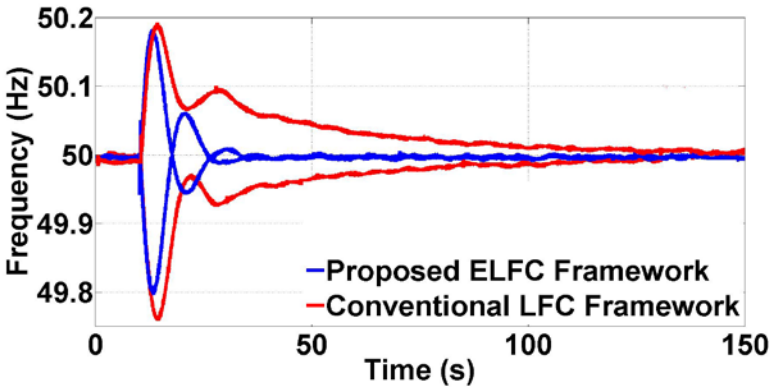

Figure 4.12: System frequency response comparison – proposed ELFC vs conventional LFC

The laboratory validation of the ELFC has proven the following:

- The ability of the fuzzy FCC to adapt individual cell droop contribution in real-time. The implementation of fuzzy FCC did not incorporate communications emulation, however the intrinsic communications between the controller and the participating devices was inherent.
- The ability of accurate event detection by the disturbance observer of BRC. The location identification is dependent upon the observable RoCoF, which in power systems community is regarded as a very noisy measurement. Any control utilizing this measurement should be validated in a laboratory environment. By the implementation of the control framework within the laboratory, the ability of BRC to detect the event with a measurement window of 0.02 s has been proven.
- The increased speed of frequency restoration under realistic communications delay. With the incorporation of delays under the communications architecture when utilizing demand side management devices as presented in [13], the proposed framework still exhibits better frequency dynamics and restores frequency faster than the conventional framework.
- The prototypical control implementation. The discrete controller implementation enabled the further improvement of control implementation, with minor implementation bugs being realized through its discrete implementation, serving the purpose of prototype testing.

4.1.3.4 Further Control Enhancements through Validations

In the previous subsections, the performance of the individual FCC and BRC controllers was presented followed by their combined validation. Throughout the process of validation, several opportunities for further development were realized. This subsection presents two such cases, one for FCC and one for BRC, where the enhancements are presented and the performance of the enhanced controls evaluated.

Enhancement to FCC: Decentralized Responsibilizing Transient Phase Offset (TPO) FCC

From the FCC discussion presented in the earlier section, it can be said that the fuzzy FCC has proven the feasibility of responsibilization within primary frequency control, both by means of simulations and experiments. However, the following potential drawbacks can be stipulated:

- The proposed approach is centralized within the scope of a cell, and
- The proposed approach relies on communications infrastructure.

To overcome the above potential drawbacks, an alternative decentralized responsibilizing FCC, referred to as Transient Phase Offset (TPO) FCC, was proposed. This proposed control relies on measuring the TPO and adapting the droops based on a simple droop curve proposed [14].

To demonstrate the responsibilization, consider the frequency response of a 5 Cell system (USTRATH) with an imbalance event of 1 GW within Cell 2 presented in Figure 4.13. Upon occurrence

of an event, the TPO is larger when measured geographically closer to the event than further away as shown in Figure 4.13(a) and (b). A TPO based droop curve designed to achieve responsibilization in FCC is presented in Figure 4.13(c).

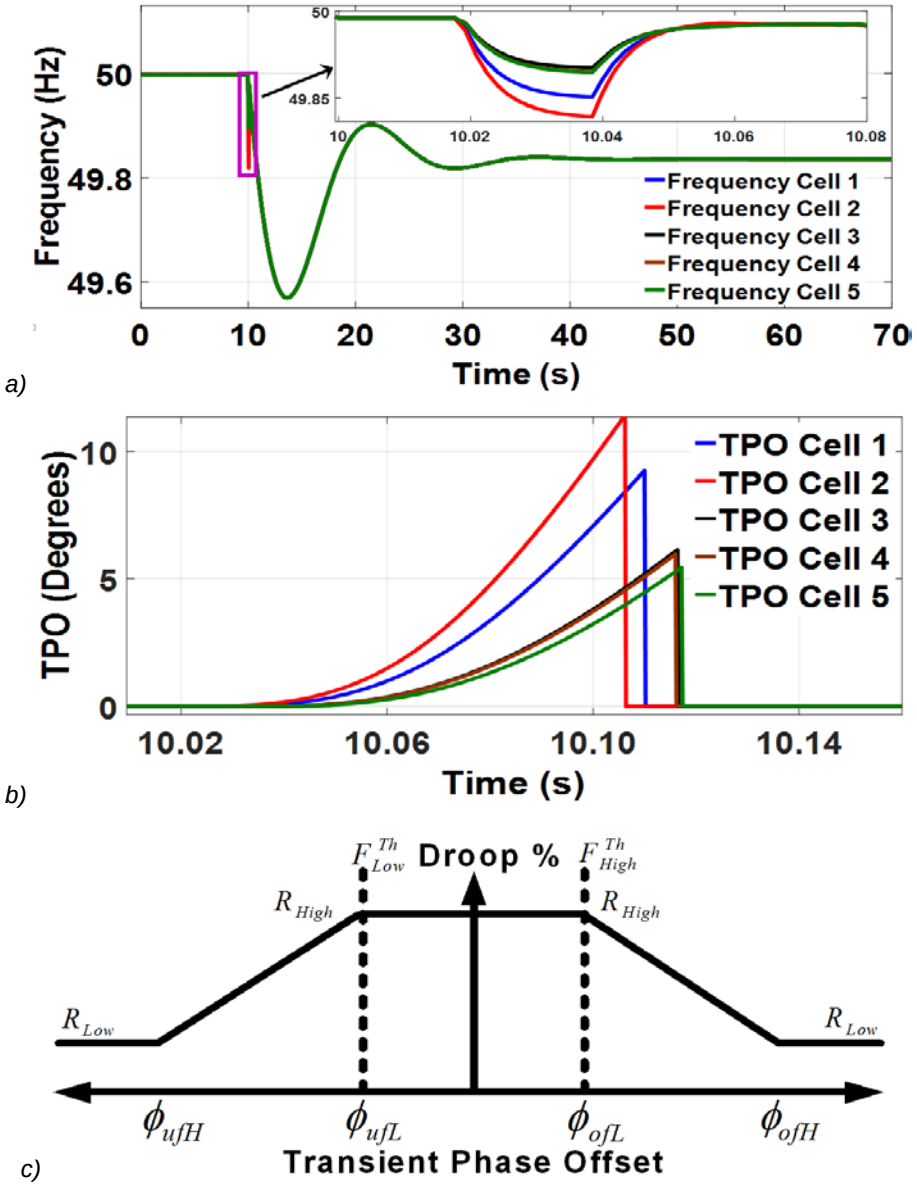

Figure 4.13: Reference event in Cell 2 – (a) frequency (b) TPO, and (c) proposed TPO based Droop Curve

The system frequency response is shown in Figure 4.14(b). As can be observed, the response of the system with proposed approach is stable and within the fixed droop responses. The FCC power contribution of each cell is presented in Figure 4.14(a). The solid line represents the system response with fixed droop and the dotted line represents system response with the proposed control. Cell 2 increases its contribution to the event, demonstrating greater responsibilization.

As the TPO FCC relied on local measurement only, it is a completely decentralized solution, does not require any form of communication, ensures near equivalent primary response at all times, and is scalable (given the autonomy and decentralized nature of the scheme).

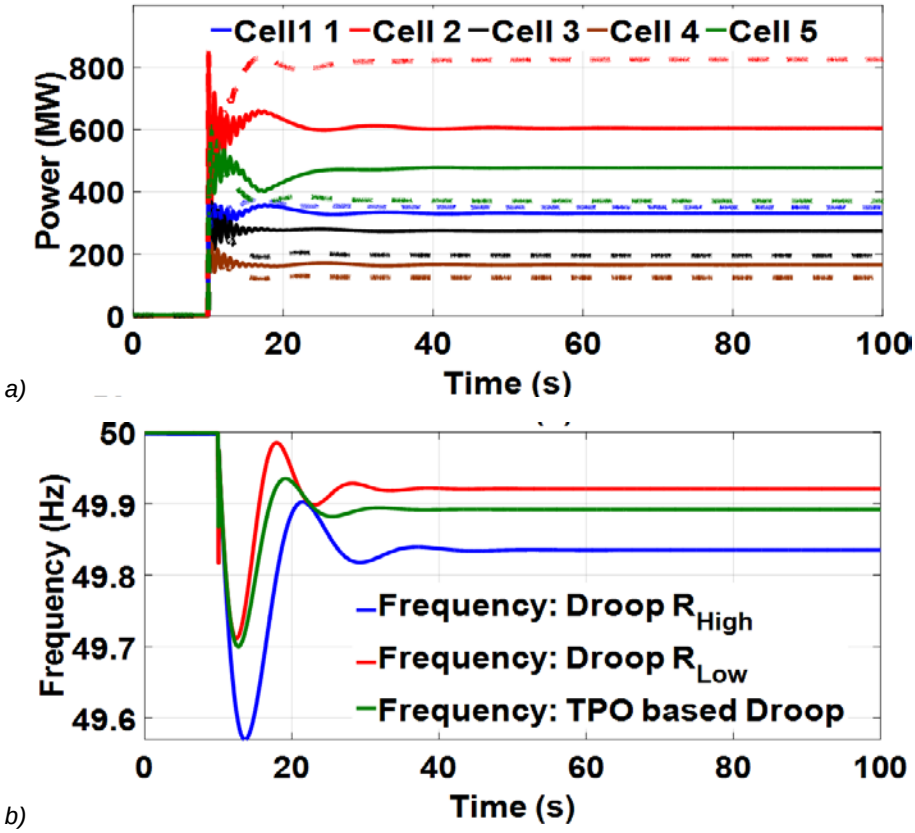

Figure 4.14: Reference event in Cell 2 – (a) frequency response and (b) cells power output

Enhancement to BRC: Direct Load Frequency Control – Direct Balance Restoration Control (DBRC)

The proposed BRC control presented in the previous section achieves the objectives of improving responsibilization while at the same time enhances the speed of frequency restoration, without deteriorating the system performance. An advantage of the proposed control is its ease of integration within the present-day control, allowing for transition to the paradigm of more decentralized and distributed control of power system, i.e., the WoC concept. The control has highlighted the importance of event detection ac accurate event detection allows for a faster, more robust (in terms of number of activations) frequency control. However, potential drawback of the proposed control is its reliance on accurate event detection.

Given the pace of current developments with regard to monitoring and Information and Communication Technology (ICT) infrastructure in power systems, new grid control concepts become possible that earlier were unfeasible due to technological limitations. The enhancement to BRC called Direct Load Frequency Control (DBRC) developed assumes significantly higher state observability within cells, which can be expected in future grids. The rapid expansion of Advanced Monitoring Infrastructure (AMI) together with optimal meter placement and (near-)complete topological knowledge will allow for the required state observability in the near future. Therefore, instead of looking at the power flows through the boundary of cells over the tie-lines and the system frequency as done by the ACE, the cell production and consumption is directly (hence the name) observed via AMI and state estimators as shown in Figure 4.15. The ability to monitor cell imbalances through direct observation replaces the need for accurate event detection. In addition, contrary to the ELFC, the DBRC is tuningless and does not employ an integrator, which is potentially unstable if tuned wrong or system parameters change significantly. Active communication with neighbouring cells is employed to coordinate control actions. The methodology has been analytically and numerically proven to be stable and was tested both in simulations and in experiments in SYSLAB. The details of the control and its implementation can be found in [15].

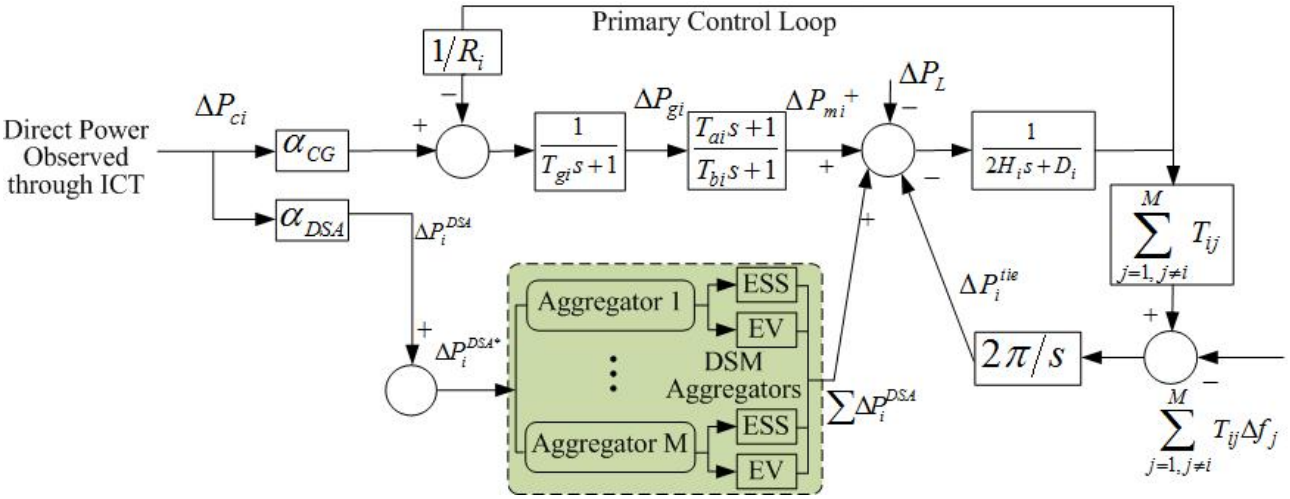

Figure 4.15: Proposed balance restoration control in its DBRC variant incorporated within the LFC framework

Simulation results

The simulation model of SYSLAB as described in the Annex was developed in MATLAB/Simulink. Each cell is modelled using one swing equation and incorporating the following constraints: Output saturations, ramping rate P_{ramp} limiting the change of primary and secondary power, and the reaction time T_{delay}^{sec} of secondary resources. Tie-lines are modeled as serial admittances. The DBRC is compared with the AGC for a range of Cell inertias, ramp rates, and control delays. In the Annex the table with the corresponding parameters for two scenarios are listed:

- The high inertia scenario J_{hi} with long delay times and comparatively low ramp rates of primary and secondary resources, representing mechanical fuel-driven generators.
- The low inertia scenario J_{lo} resembling SYSLAB setup with fast, inverter-based devices. Cell 3 offers in both scenarios only secondary power control, as it lacks primary resources. Despite Cells 2 and 3 having only inverter-coupled devices in the laboratory, a very small inertia value is necessary for the simulation model.

Table 4.2: Events in the DBRC simulations

Event	Time (s)	Parameter	Parameter change	Description
1	10	ΔP_1^{obs} (kW)	0 → -5	Load in Cell 1 increased
2	50	ΔP_1^{obs} (kW)	-5 → 0	Load in Cell 1 decreased
3	90	ΔP_3^{obs} (kW)	0 → 5	Load in Cell 3 decreased
4	130	ΔP_2^{uo} (kW)	0 → 5	Load in Cell 2 decreased, unobs. by DBRC
5	170	ΔP_2^{uo} (kW)	5 → 0	Load in Cell 2 increased, unobs. by DBRC
6	210	δ_{12}	1 → 0	Tie-line 1-2 opens, tie-line setpoint sums for Cells adjusted
		$P_{0,1}^{tie}$ (kW)	-8.08 → -4.04	
		$P_{0,2}^{tie}$ (kW)	8 → 4	
7	250	ΔP_3^{obs} (kW)	5 → 0	Load in Cell 3 increased

A series of events is applied in each scenario to the system for a simulation period of 300 s are summarized in Table 4.2. Figure 4.16 shows the system frequency response for both scenarios and controllers. As the AGC was tuned for ±5 kW steps for optimal performance and no overshooting,

its performance is similar for all events, with a settling time of around 20.02 s. The DBRC with a 26.08 s settling time is about 25 % slower in comparison, and exhibits around 40 % overshooting due to the two concurrent control actions for the observed load events 1 to 4. Both controllers' responses are exponentially bounded by the trumpet-curves. For the case of the slowest DBRC responses (events 1 and 2), the trumpet parameters are A = 0.21 Hz and T = 14.5 s. This results in a decay time of 34 s to cross the ±20 mHz margin around the nominal frequency f0 after the event, which is well under the 900 s restoration time demanded by the ENTSO-E.

The primary reference frequencies f_r, necessary for frequency control under partial observability, are depicted in Figure 4.17. Changes in the reference signals follow the primary responses immediately after the load events. As the secondary balancing resources start acting, f_r returns to f_0 as the primary powers approach their nominal operating points P_0^{pri}.

No overshooting occurs for unobserved events 5 and 6 because no direct power balancing takes place, and f_r differs from f_0 as long as the unobserved power persists. Opening the tie-line at event 7 makes Cell 3, which does not participate in primary control, the only physical neighbour of Cells 1 and 2. Hence, the reference frequencies start to diverge because of the different local ramp rates. Load sharing between the Cells is no longer proportional, but stable frequency control is maintained. The situation between the controllers turns in the Jlo scenario where the DBRC only needs 16.2 s to settle. Overshooting drops to around 14 %. The AGC does not benefit from the faster system response and its performance gets even worse, causing even longer frequency excursions.

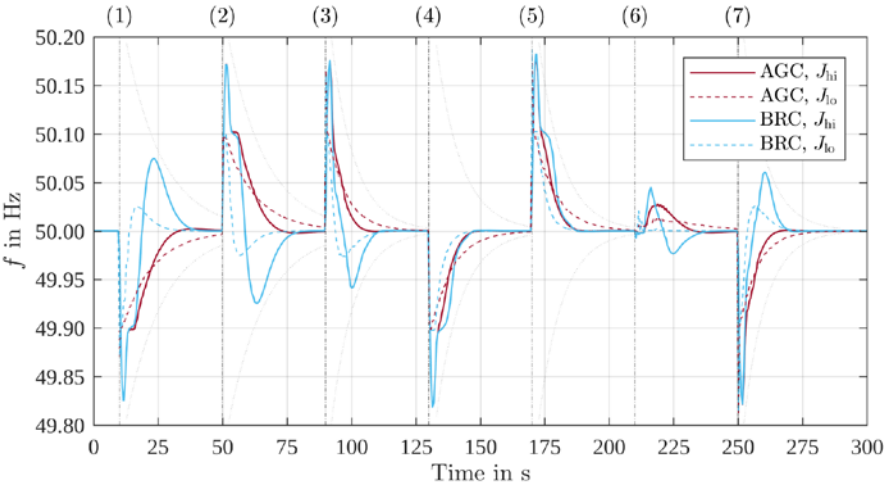

Figure 4.16: System frequency response caused by AGC and DBRC actions for the high- and low-inertia scenarios

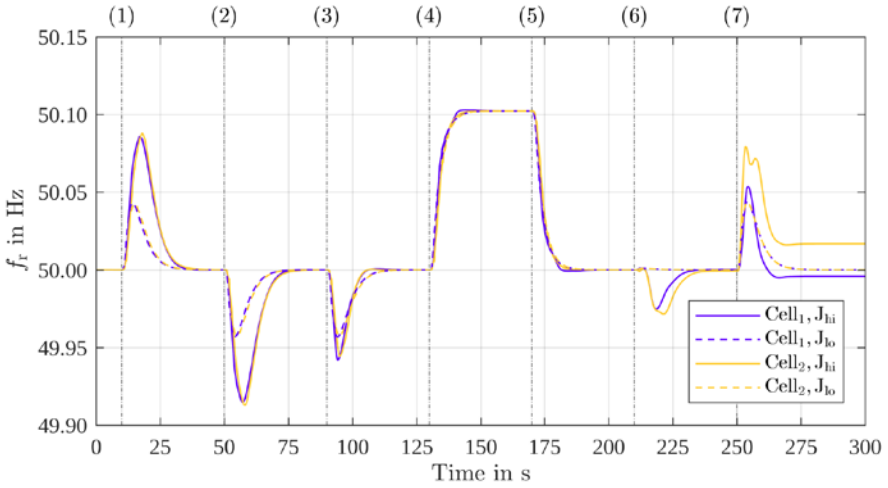

Figure 4.17: Reference frequencies by the DBRC of Cell 1 and 2 in the high- and low-inertia simulation scenarios

Sensitivity and Small Signal Stability Analysis

The performance of the DBRC was further evaluated by means of conducting a sensitivity and small signal stability analysis. The results of the sensitivity analysis with parameter variations of disturbance magnitude μ_{step}, inertia, ramp rates and secondary delays μ_{speed} is presented in Figure 4.18. The AGC naturally exhibits good performance around the operating point for which they were tuned. However, moving away from that point reveals peculiarities of applying PI-controllers to nonlinear systems. First, the AGC's settling time does not necessarily decrease with smaller load steps, and second, neither does it benefit from faster systems. Instead, its performance gets even worse because of the fundamentally changing system response. The DBRC on the other hand has a slightly worse performance than the AGC in the considered high inertia scenario but responds much more predictably to changing environmental conditions. Smaller load steps and/or faster system responses lead to short settling times in virtually all considered cases, without the need for tuning.

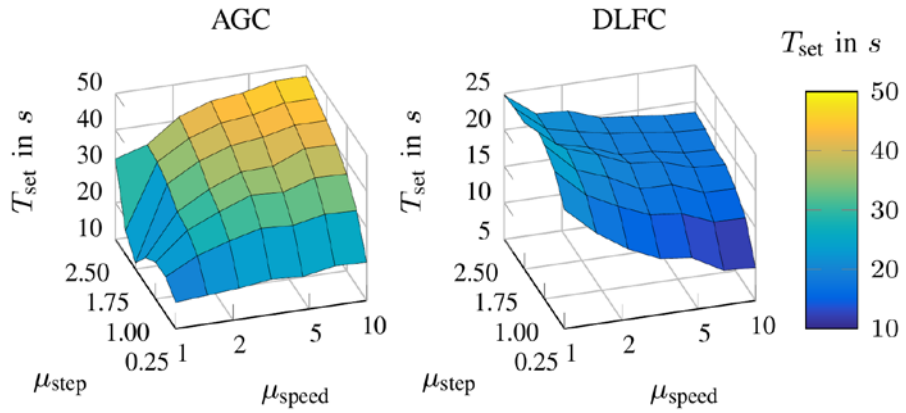

Figure 4.18: Comparison of the settling times of AGC and DBRC for variations of the disturbance magnitude and reaction speed of the system

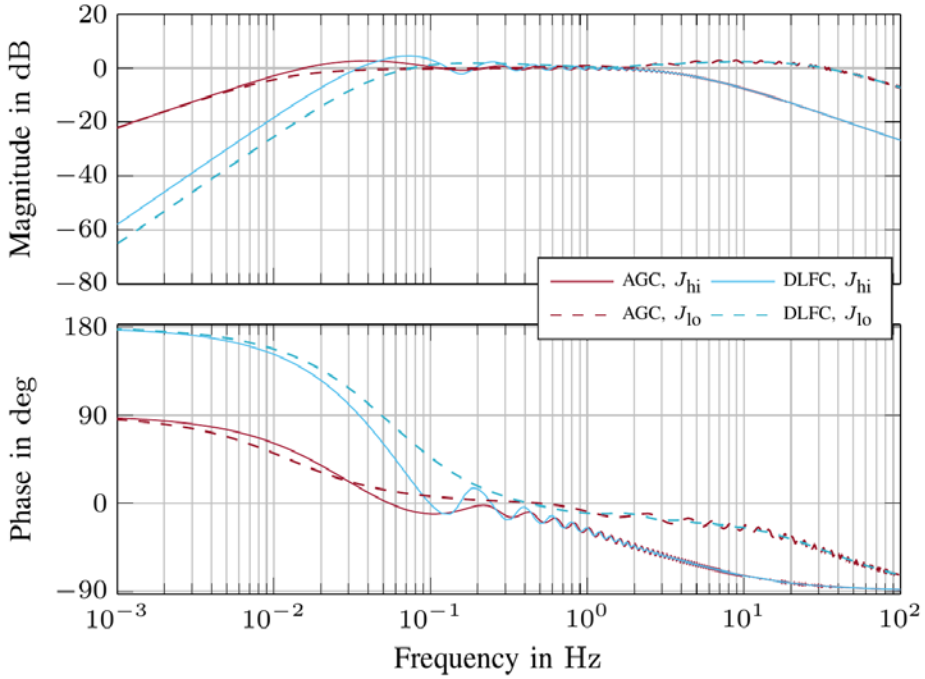

Figure 4.19: Small signal stability investigation of AGC and DBRC

A small-signal analysis has been conducted on SYSLAB's three-area system, with the system linearized around f_0 in steady-state, input as the load disturbance in Cell 1, the output as the system frequency and the bode plot is presented in Figure 4.19. The performance gain of the DBRC over

the AGC is apparent for lower frequencies, where the AGC shows a −20 dB falloff due to its integrator, while the DBRC has −40 dB because of the concurrent power matching and reference frequency control mechanisms. Additionally, the DBRC takes advantage of the faster system dynamics in the low inertia case, confirming the findings of Figure 4.16 and Figure 4.18. The DBRC's speed manifests in a higher initial phase compared to the AGC, but both controllers remain between −90° to 180° and operate stably.

Experimental results

Figure 4.20 shows the system and reference frequencies resulting from the events in Table 4.3. Similar to the simulation analysis, it can be observed that the DBRC is able to maintain the frequency of the system under varied conditions (Wind turbines, solar panels, and the randomly charging and discharging EV created additional disturbances on the islanded system. Cloudy and gusty weather during the experiment caused low PV output and highly fluctuating power production on the part of the wind turbines). In fact, the average frequency between 215 s to 750 s is exactly 50.0 Hz.

Table 4.3: Events in the DBRC experiment

Event	Time (s)	Parameter	Parameter change	Description
1	60	ΔP_2^{uo} (kW)	0 → -5	Unobserved load in Cell 2 on
2	148	---	---	Controllers on
3	210	---	---	Communication on
4	296	ΔP_2^{uo} (kW)	-10 → 0	Unobserved load in Cell 2 off
5	450	δ_{12}	1 → 0	Tie-line 1-2 opens, tie-line setpoint sums for Cells adjusted
		$P_{0,1}^{tie}$ (kW)	-8 → -4	
		$P_{0,2}^{tie}$ (kW)	8 → 4	
6	632	δ_{12}	1 → 0	Tie-line 1-2 closes, tie-line setpoint sums for Cells adjusted
		$P_{0,1}^{tie}$ (kW)	-4 → -8	
		$P_{0,2}^{tie}$ (kW)	4 → 8	

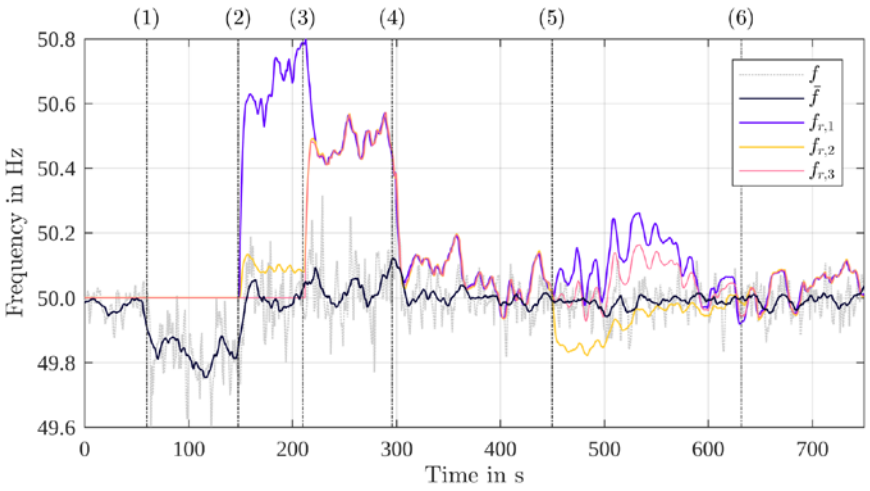

Figure 4.20: System frequency response caused by the DBRC in the SYSLAB experiment

The experimental evaluation was an important step towards proving the ability of the proposed control to perform under real-world conditions. In particular, the inherent tolerance to non-linearities like

ramping limitations following the stability proof needed to be demonstrated, as this characteristic is one of the main features that set the DBRC apart from the AGC. The unsparing laboratory environment allowed to prove that the DBRC assumptions are valid and implicit model considerations of common non-linearities are sufficient. The IT facilities in SYSLAB enabled rapid prototyping of the controller, allowing for an efficient iterative development process by feeding back experiences made under real conditions into the theoretical method. The most noteworthy result is perhaps the fact that SYSLAB's off-the-shelf laboratory equipment like the Diesel generator provide necessary functionality for implementing the DBRC. Despite the unorthodox approach of directly involving primary resources (which the Diesel was used as) for secondary frequency control, the utilised components were perfectly applicable for that purpose.

4.1.4 Discussions

In the previous subsections, the validation of FCC and BRC has been dealt with in detail. This subsection presents a discussion by summarizing the achievements thus far and presenting a forward outlook.

The analytical and experimental assessments in the work undertaken has demonstrated the aptness of the proposed control approaches for dynamically changing power system of future. The experimental evaluation was an important step towards proving the ability of the proposed controls to perform under real-world conditions. While the simulations already highlighted the benefits of these controls over state-of-the-art, it remained unclear whether these fundamentally new approaches would perform satisfactorily outside idealised simulated conditions. Therefore, the conducted experiments where imperative to highlight the real-world applicability of the proposed controls. The resilience of the proposed controllers to communications asynchronicity, finite measurement and control step resolution, various noise sources, parameter uncertainties, and other factors not explicitly incorporated in the mathematical model were tested in the process as well. The deployment of the controllers on dedicated controller hardware enabled rapid prototyping, allowing for an efficient iterative development process by feeding back experiences made under real conditions into the theoretical method.

As has been described earlier, the controls have been under development throughout the process of validation. The ELFC framework presented will remain the frequency control method of choice when only tie-line measurements are available, the prospect of a significantly higher degree of observability in future power systems will enable the incorporation of DBRC within ELFC, leading to the control framework referred to as the DBRC.

With the development of the balancing control functions (FCC and BRC) and their validation in a laboratory environment, the promise of Web-of-Cells concept has been delivered, i.e., the ability of more decentralized and distributed operation of power system has been proven. Furthermore, the developed controls, in essence work towards the objective of solving local problems locally. Beginning with the speculation of advantages of more local control, this exercise has proven some merits of prioritizing of local response to a local imbalance, such as improved dynamic response, robust reserve activations and reducing the divergence from planned system conditions and hence minimizing the operational implications of the disturbance. In addition, the developed controls support enhanced scalability in the future grid given the autonomy of the approaches.

4.2 Validation Experiments "Use Case Combinations FCC, BRC, and BSC"

The specific combination of use cases was originally selected in order to assess the performance of BSC and its impact on the WoC operation. Based on the BSC use cases it is evident that this is not an independent control loop but it is a subset of functions which extends those of BRC. Therefore, in order to evaluate the performance of this controller it was necessary to incorporate it into one of

the BRC variants developed during the project. The selected BRC variant makes use of the local (at cell level) signals of tie-line power and frequency in order to make the most efficient use of the local reserves. By this combination it is possible to assess the effectiveness of BSC in terms of imbalance netting exploitation. The basic idea of BSC is to benefit from the fact that adjacent cells may undergo imbalances that can counteract each other in a way that the BRC reserves can be deactivated if the control process simply modifies the selected tie-line set-points.

On the other hand, this process may have some significant impact on the stability of the system. Therefore, in order to have a clearer view of the system stability a very representative scenario had to be implemented. In this respect, the adaptive version of FCC (aFCC) was also incorporated in the combination. From this viewpoint, the focus of the analysis is chiefly on the BRC and FCC behaviour and how they react to the "disturbances" caused by the change in the tie-lines set-points by BSC. It is noteworthy that by simply combining the three above mentioned use cases the test setup becomes challenging enough because all these controllers are novel strategies developed in ELECTRA and only tested as standalone implementations before. Despite these challenges, the implementation and testing of this combination in both simulation and experimental environments showed the real benefits of these controllers' use, together with the fact that the stability of the system is always ensured.

4.2.1 Chosen Validation Environments

An overview of the validation environments utilized for validation of FCC, BRC, and BSC use cases are shown in Table 4.4.The detailed descriptions of the validation environments can be found in Section 3.2 and in the Annex.

Table 4.4: Used validation for proof of concept validation of use case combinations FCC, BRC, and BSC

Environment	Partner	No of Cells	Details
Pure Simulation Environment	CRES	3	Modified CIGRE MV grid in a meshed topology modelled using MATLAB/Simulink
	USTRATH	5	5 cell GB test system implemented in RSCAD
Pure Hardware Environment	CRES	2	CRES Microgrid consisting of two cells; scenario implemented incl. unequal imbalances

A close examination of the selected controllers reveals that all of them act based on the state of a cell's boundary, namely its tie-lines. Therefore, the environments selected for the validation of the combination had to incorporate at least two cells. On the other hand, these use cases do not have any limitation with regard to the upper limit.

4.2.2 Test Criteria

As mentioned in the introduction of this section the objective of this use case combination test is twofold: the effectiveness of BSC on the one hand and the stability/behaviour of BRC/FCC on the other. The test approaches followed by each partner was also from a different viewpoint. Thus, CRES' implementation emphasized mostly on the BSC performance with the assessment of some stability criteria as well. USTRATH, by contrast, investigated chiefly the performance of BRC and FCC in the presence of BSC emphasizing more elaborate stability criteria. The two approaches are complementary with each other and combined together provide a more holistic assessment of the use case combination.

In order to meet the evaluation requirements, the following test criteria were assumed. These criteria also illustrate the sequence of actions that take place during the process:

- *Effective operation of the proposed BRC technique (TCR-FBB01):* The two aspects addressed by this KPI are the capability of the controller to identify the location of the disturbance as well as how fast both balance and frequency are restored.
- *Effective operation of the proposed aFCC (TCR-FBB02):* Similarly, to BRC there are two important aspects addressed by this TCR. There is the capability of aFCC to contain frequency and the adjustment of reserves activation (in real time) in order to increase the FCC contribution of the disturbance cell and to decrease that of the neighbouring cells.
- *Effective negotiation between cells (TCR-FBB03):* This KPI represents the ability of BSC to lead to an effective negotiation between cells. This negotiation effectiveness illustrates the ability of BSC controllers to detect the correct amount of imbalance, to communicate it to their neighbours, and to respond to their neighbours with the right values of power adjustment.
- *Imbalance netting exploitation (TCR-FBB04)*: Even if the negotiation of the previous is effective, it is necessary to validate that once the setpoints of the tie-lines change, the BRC reserves are led to deactivation. In such a case the imbalance netting is fully exploited.
- *System stability (TCR-FBB05):* The deactivation of BRC reserves must be done in a system-secure manner. The changes in the power balance should always ensure that the stability of the system is not jeopardised.
- *Tie-lines operating limits (TCR-FBB06):* The adjustment of the tie-lines setpoints should not lead to power flows outside the acceptable capacity limits.

In order to assess the system's behaviour based on the above TCRs the following signals have to be monitored:

- Output signal (binary value) of the imbalance location detection block of BRC/frequency (TCR-FBB01)
- Frequency/tie-line power deviations (TCR-FBB02)
- Output signals of the Cell Setpoint Adjusting functions of each cell (TCR-FBB03)
- Active power of all BRC reserves (TCR-FBB04)
- Frequency (TCR-FBB05)
- Active power of tie-lines (TCR-FBB06)

4.2.3 Performed Experiments and Results

As mentioned previously the experiments conducted for the assessment of this combination of use cases included both simulation and experimental tests. In this section, an extended summary of the achieved results is presented. This summary provides an overview of the most important scenarios and the corresponding test results which highlight the significance of the WoC concept in general as well as the proposed controllers.

For the simulation tests conducted at CRES with the modified CIGRE MV European test grid we can distinguish for different scenarios:

- Test 1: System response under two nearly equal imbalances in two adjacent cells
- Test 2: System response under two unequal imbalances in two adjacent cells
- Test 3: Behaviour of the BSC functions when the capacity limit of a tie-line has been reached
- Test 4: Response and impact on the stability when the adjustment is deployed with some time delay between two cells

For the Tests 3 and 4 the amount of imbalance in the cells is nearly equal while in all cases the two disturbances result in imbalances of the opposite sign. Thus, for Tests 1-3 the considered imbalances were disconnection and reconnection of a 500 kW load in cells 1 and 2 respectively with a

time difference of 50 s. Similarly, Test 2 assumes the same initial incident of 500 kW load disconnection in cell1, however the load connected to Cell 2 is only 250 kW. The execution of the tests and the analysis of the results show that in all tests the Cell Set-point Adjuster (CSA) controller is capable of correctly estimating the amount of imbalance in each cell. Also, the correct adjustment request and acceptance is communicated to all neighbouring cells. This is true even in Test 3 where one tie-line of cell1 has already been exhausted in terms of capacity. In this case the controller was capable to exclude the tie-line from the negotiation and instead, it redistributed its part to the adjustment in the other two tie-lines that interconnect Cells 1 and 2. All in all, the controller's behaviour seem always to lead to a correct negotiation thus satisfying TCR-FBB03.

Some key test results regarding Tests 2 and 4 are also shown in Figure 4.21 and Figure 4.22 respectively. These results, together with the results from the other tests validate the concept of imbalance netting exploitation (TCR-FBB04) in a stable and system-secure manner (TCR-FBB05). More in detail, the results in Figure 4.21 show that the output power of the BRC reserve is reduced to 0 for Cell 2 or to the half of its initial value in Cell 1. This is due to the fact that the set-point in the tie-lines between Cell 1 and 2 changes in order to allow an extra 250 kW of power from Cell 1 to Cell 2. At the same time the BRC output of the other two cells (3 and 4) that do not participate in the negotiation are only briefly activated due to the system dynamics and in steady state their output is 0. Moreover, the frequency response in Test 4 (as well as in all other tests) in Figure 4.22 shows that even with the significant time delay of 2 s in the adjustment deployment the system is capable of maintaining the frequency within strict operating boundaries.

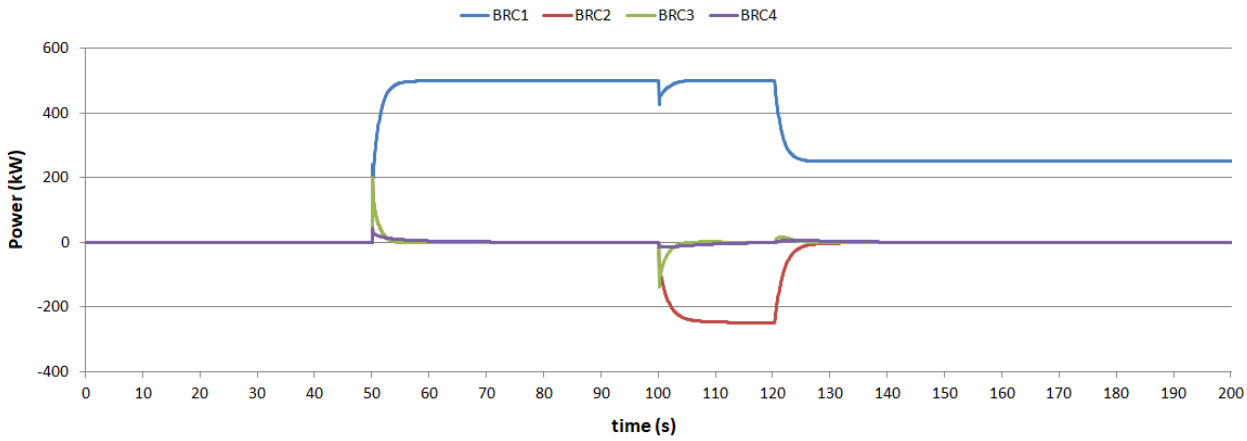

Figure 4.21: Simulation results showing the deactivation of BRC reserves in Test 2

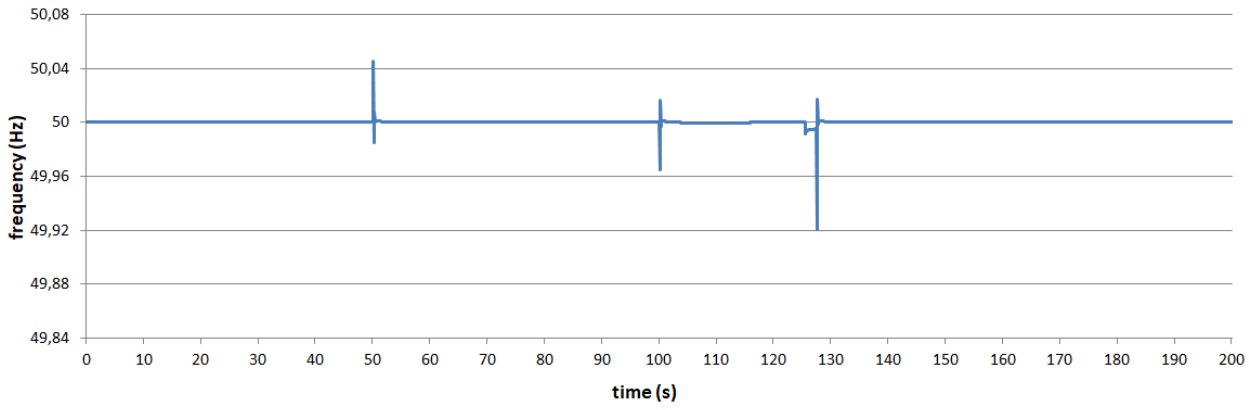

Figure 4.22: Simulation results showing the frequency response of the system in Test 4

Last but not least, it is important to mention that the actual power of the individual tie-lines connecting Cells 1 and 2 vary significantly from the expected values (TCR-FBB06) even though the net balance

of each cell is always the correct one. This is an intrinsic characteristic of BRC which appears also in classical AGC. This is due to the fact that by definition BRC acts on and corrects the total imbalance of a cell and not each tie-line's deviation separately. In such a case, the restoration of power flows through the tie-lines can only be achieved by controlling the voltage at the tie-lines terminals. This combination of controllers is out of scope for these tests.

The simulation tests conducted by USTRATH with the 5 cell reference grid can be distinguished the following scenarios:

- Test 1: Comparison of FCC controller variations
- Test 2: Validation of FCC and BRC controller effectiveness
- Test 3: FCC vs BRC in terms of frequency containment
- Test 4: Compatibility of FCC and BRC with the BSC scenario

It is worth noting that from the above tests, only the fourth one is specifically oriented to BSC performance. The other three tests were conducted, however, more a more comprehensive investigation of the FCC and BRC controllers' behaviour since the same controllers were also used in the FCC and BRC combination of use cases.

In Test 1 two fuzzy logic based variants of aFCC were investigated in terms of their frequency response and Cell Power-Frequency Characteristic (CPFC) modification during imbalances. The comparison of the two variants showed that the performance of aFCC can be improved by allowing the increase of CPFC within the cell of disturbance. This way it is possible to maintain a constant droop slope for the WoC prioritising only the use of reserves in the faulty cells. The performance of both variants satisfies the TCR-FBB02 criterion. Also, in Test 2 the performance of aFCC and BRC are compared against baseline scenarios, which involve the deactivation of one of both controllers, or the presence of AGC in the system. For a 2 GW imbalance incident in Cell 2 the experiments showed that the introduction of the proposed BRC improves the dynamic frequency deviation, thus satisfying TCR-FBB01, yet with the introduction of aFCC the dynamic response slightly worsens due to a net reduction in the overall droop slope of the system. The latter problem could be mitigated with fine-tuning of the FCC controller. In terms of comparing the primary response of BRC versus FCC, Test 3 showed again that the dynamic response (frequency nadir) improves with the use of BRC only. However, the trade-off in this case is the loss of local primary reserves activation something that is achieved only by means of FCC.In other words, although a fast BRC could completely substitute the use of FCC there will always be the need for some FCC reserves used as a safety net in order for the system to cope with large-scale incidents

Regarding Test 4, which involves the combination of FCC, BRC and BSC some key results are shown in Figure 4.23 and Figure 4.24. Specifically, for two consecutive imbalances of +2 GW in Cell 1 and -2 GW in Cell 2 the deactivation of BRC reserves is achieved as shown in Figure 4.23.

In this particular diagram, the response of the SG in Cell 2 is depicted. As it can be seen, the steady-state output power of the Synchronous Generator (SG) is modified when the second imbalance takes place at 80 s). At 400 s when the adjustment of the tie-lines setpoint takes place the output power of the generators is restored to its original schedule. That means that the action leads to deactivation of the BRC reserve provided by the specific generator. More importantly, this is achieved while the system maintains stability in terms of frequency as shown in Figure 4.24.

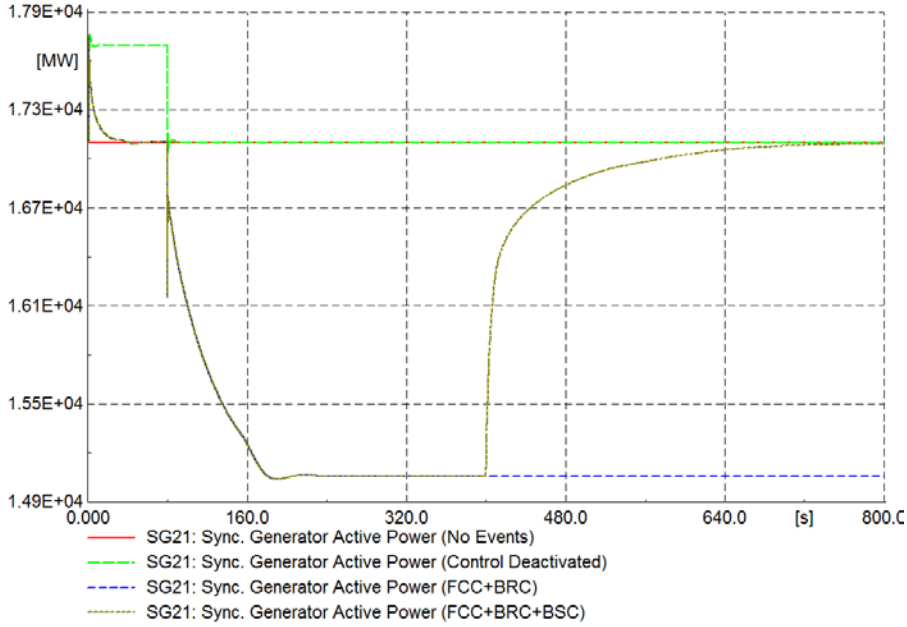

Figure 4.23: Cell 2 synchronous generator response to BSC scenario

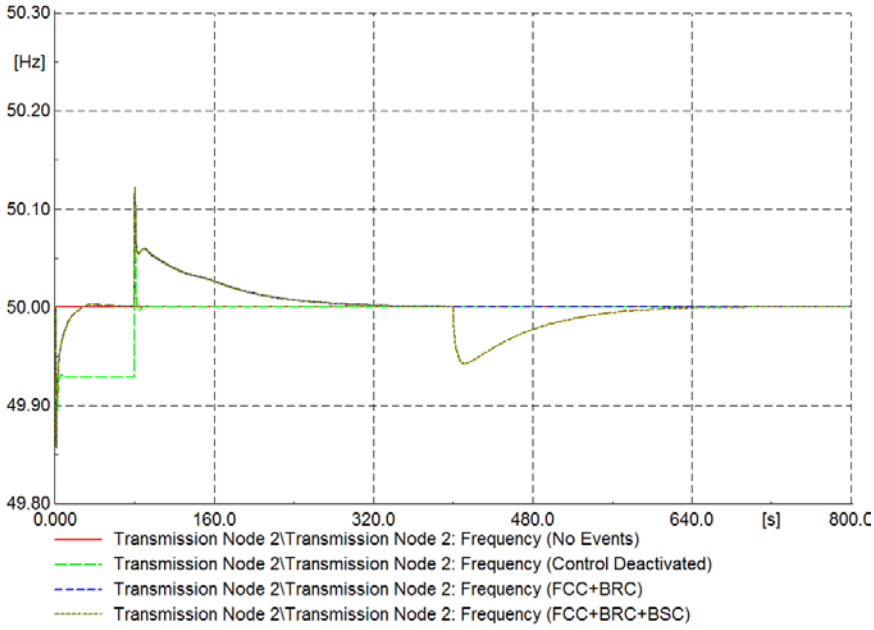

Figure 4.24: Full frequency response of BSC scenario

The experimental implementation at CRES showed that all four above mentioned KPIs are satisfied by the implemented control scheme. The results in Figure 4.25 and Figure 4.26 show the power/frequency response under a scenario of unequal imbalances. In the specific test the load in Cell 2 increases to 1500 W and this results in activation of the BRC reserves in Cell 2, namely Battery 2. After that the Photovoltaic (PV) units in Cell 1 start producing a significant amount of power that creates imbalance netting exploitation conditions. This also results in activation of Battery 1 which is the BRC reserve in Cell 1. Once a nearly-steady state is reached the BSC controller modifies the set-point of the tie-line in order to allow the PV power from cell 1 to flow to cell 2. This results in the BRC deactivation. In Figure 4.26 it is shown that the frequency of the system remains stable throughout the process.

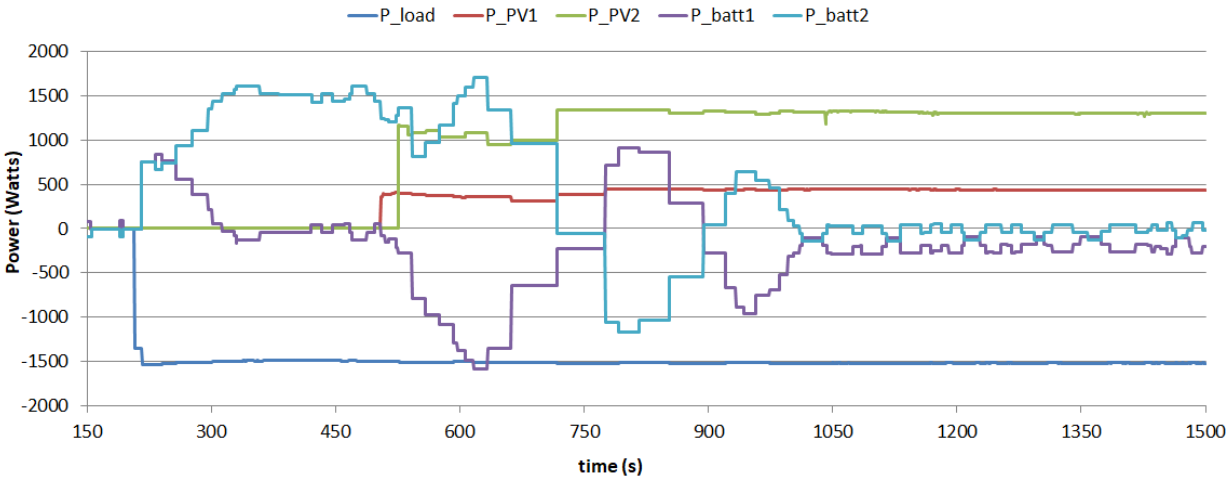

Figure 4.25: Experimental results showing the power profiles of all resources in the system

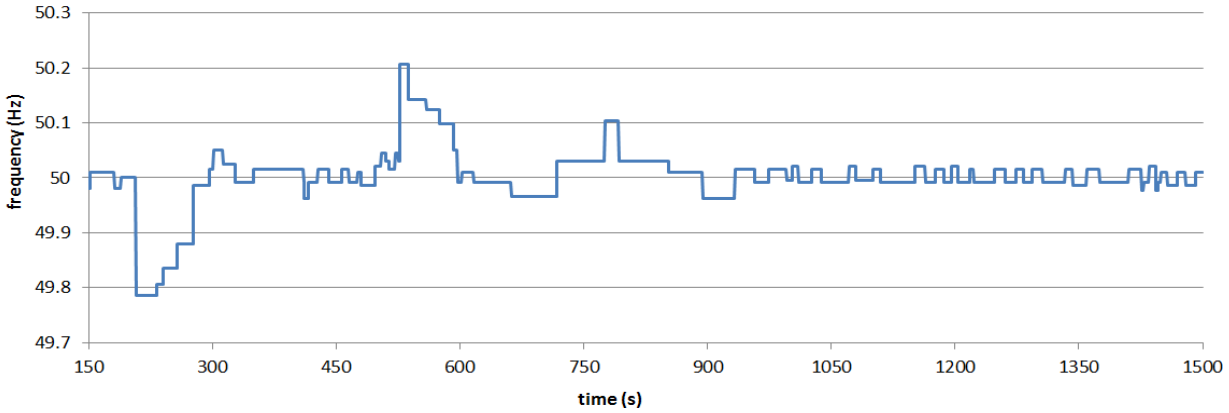

Figure 4.26: Experimental results showing the frequency response of the WoC

4.2.4 Discussions

Investigating the results from the BSC perspective we realise that this controller manages an effective negotiation and, in addition, the system is benefiting from the imbalance netting effect of two adjacent cells without jeopardising the stability in all simulation scenarios as well as in the experimental implementation. The negotiation is always successful even in the case of unequal imbalances or exhaustion of one tie-line's capacity. Moreover, in all implemented scenarios the BRC controller deactivates the output power of the reserves, thus benefiting from imbalance netting exploitation. In all cases, the frequency stability is maintained, and overall, the frequency dynamics are limited proving that the combination of the proposed controllers is secure for the system operation. This is true even in the case of significant time delays such as in the simulation scenarios or the experimental implementation. The only issue identified during the tests was the unsuccessful restoration of the power of each individual tie-line. However, this issue is related to the absence of a voltage control strategy from the scenario that would control the power flow on the grid lines. This controller was deemed out of scope for this combination of the use cases and, therefore, is a potential scenario for further analysis.

In terms of FCC and BRC effectivity in all scenarios the two controllers were capable of identifying the location of imbalances and acting towards successful frequency containment and frequency/balance restoration respectively. The presence of aFCC always slightly worsens the dynamic frequency deviation something attributed to the non-optimized design of the fuzzy controllers (in most of the above tests, the aFCC function was only curtailing the CPFC value. Performance improvement can be achieved by upscaling this value). Otherwise, the controller effectively modifies the droop slope of all FCC reserves in order to increase the contribution of the faulty cell and decrease that of its neighbours.

4.3 Validation Experiments "Use Case Combinations IRPC and FCC"

The control functions IRPC and FCC influence the short-term frequency stability of a power system. IRPC provides contribution from decentralised resources to the overall power system inertia, which limits the RoCoF after disturbances and herewith the frequency nadir. Protection devices for the purpose of plant protection are sensitive to both measures. In case of tripping due to high RoCoF after a loss of generation, additional generators will disconnect from the grid and herewith impair the power system stability massively. FCC mainly influences the steady state frequency deviation after a disturbance and will be taken over by integral control functionalities as BRC and BSC later on. The activation of IRPC and FCC is crucial for power system stability.

Accordingly, the experiments investigate the short-term frequency stability of different chosen power systems considering different test specifications.

4.3.1 Chosen Validation Environments

An overview of the validation environments utilized for validation of IRPC and FCC use cases are shown in Table 4.5.The detailed descriptions of the validation environments can be found in Section 3.2 and in the Annex.

Table 4.5: Used validation for proof of concept validation of use case combinations IRPC and FCC

Environment	Partner	No of Cells	Details
Pure Simulation Environment	IEE/DERlab	3	CIGRE European MV test grid
	CRES	4	Based on the modified CIGRE European MV test grid in MATLAB/Simulink
	DTU	2	Simulation model of test facility SYSLAB
Pure Hardware Environment	DTU	2	Test facility SYSLAB

The validation environment was chosen by each partner according to the planned tests in simulation or laboratory environment. Starting with the simulation environment, the IEE and CRES have made use of the CIGRE European MV test grid which has been described in detail in Section 3.2.

DTU chose a simulation environment according to their testbed, which has been utilized also for experimental validation. The testbed SYSLAB has been described in detail in Section 3.2.

4.3.2 Test Criteria

Following test criteria have been considered for the validation:

- Overall frequency stability; assessment of stability criteria related to short-term frequency stability (RoCoF, frequency nadir/zenith, steady state frequency deviation) *(TCR-IF01)*
- Conflicting use of resources: conflict of use of resources was investigated twofold, conflict between provision of power for IRPC or FCC and conflict between actual operating point of the resources and provision of additional power for IRPC/FCC *(TCR-IF02)*
- Impact on voltage: influence of additional power injection of the resources due to reserves activation on voltage at points of connection *(TCR-IF03)*
- Maximum RoCoF *(TCR-IF04)*
- Maximum frequency deviation *(TCR-IF05)*
- Virtual inertia contribution *(TCR-IF06)*

4.3.3 Performed Experiments and Results

The following groups of test specifications have been performed via simulations with the modified CIGRE European MV test grid and a model of the experimental infrastructure SYSLAB of DTU.

a) Investigation of controller combinations: comparative assessment/sensitivity analysis of the short-term frequency stability related KPIs with consideration of all possible controller combinations including a baseline case with no additional IRPC or FCC control, monitoring of impact on voltage.
b) Controller conflicts/resource limitation due to operational point before disturbance.
c) Impact of different inertia conditions on IRPC reserve activation.

The experimental validation of IRPC and FCC controller performance has also been conducted at SYSLAB using Electric Vehicles (EVs) to provide synthetic inertia and frequency containment control under condition with only load steps and secondly additional wind power injection as a more challenging and realistic configuration.

Firstly, simulation results from test specifications under a) are presented. Especially the test implementations from CRES and IEE with the CIGRE European MV test grid showed improvements in frequency deviation due to FCC activation and improvements in RoCoF or inertia time constant due to IRPC activation after a disturbance compared to a baseline case without any FCC or IRPC. FCC's impact on RoCoF could be determined as small compared to the IRPC's impact on RoCoF. Accordingly, the influence of IRPC on steady state deviation after disturbance is negligible (see Figure 4.27, Figure 4.29, and Table 4.6).

Additionally, two different activation methods of FCC have been considered. A constant droop characteristic and in contrast an adaptive FCC. The specific controller for adaptive FCC is described in Deliverable D6.3 [3] and is based on a fuzzy logic controller that curtails the total droop of a cell (named as Cell Power-Frequency Characteristic) if the imbalance takes place outside of the cell. In this approach, it is expected that a lower and, more precisely, local use of FCC reserves is achieved with all benefits that this strategy may entail such as:

- Avoidance of activating reserves away of the incident the contribution of which is less significant. Especially when the FCC service is provided by Renewable Energy Resources (RES) like PVs and Wind Generators (WGs) the activation of such reserves would lead to curtailment of their useful output power. By contrast, with the introduction of adaptive FCC the curtailment of the droop slope in real time leads to less rejection of the remote RES.
- Less power losses since the power deviation is covered locally and there is no need to transfer high amounts of power from remote areas.
- Potential improvement of voltage deviations because less power changes take place in remote cells.

On the other hand, the use of a strategy that adaptively reduces the droop of some units may lead to increased frequency deviations. However, improvement can be achieved by increasing the droop of the cell where the disturbance happens by an amount that is equivalent to the curtailment of the neighbouring cells. To this end, this test aims at assessing the impact of adaptive control in combination with IRPC in the system's frequency. To this end, this test aims at assessing the impact of adaptive control in combination with IRPC in the system's frequency. The resulting frequency deviations for comparison of fixed and adaptive FCC are shown in Figure 4.27 and Figure 4.28. The measured frequency deviation with adaptive FCC compared to fixed FCC is very small. In simulations performed the steady-state frequency is 49.24 Hz with the use of adaptive control whereas it is 49.29 Hz when fixed droop slope is used (reduction by 0.1 %). The simulations results obtained by IEE showed a reduction in steady state frequency deviation of 0.2 % for fixed droop compared to adaptive droop (see Table 4.6).

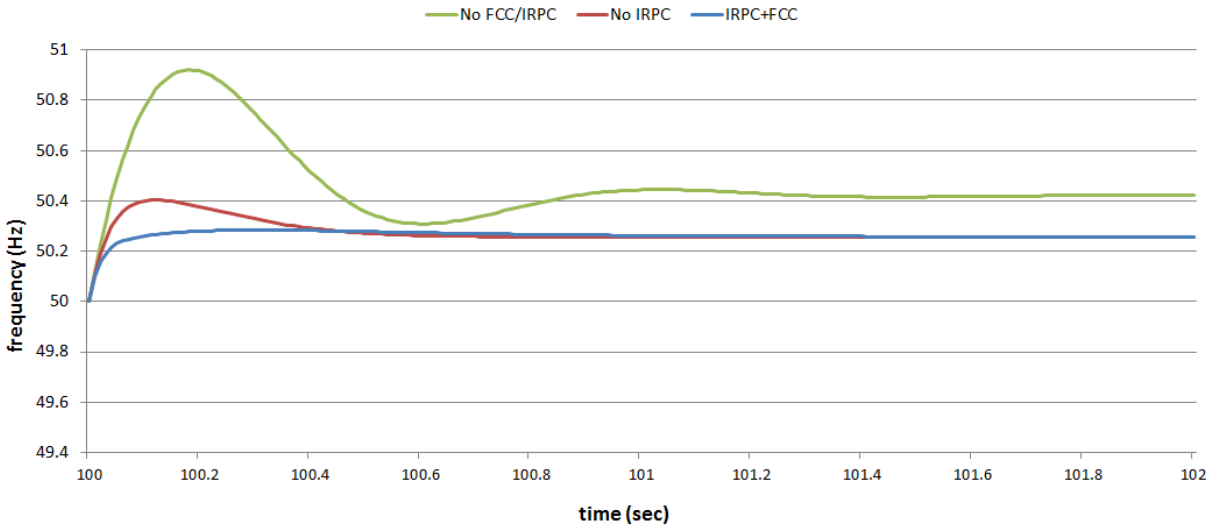

Figure 4.27: Frequency after load decrease of 1 %
(based on total system load) at bus 1 with different controller combinations, CRES

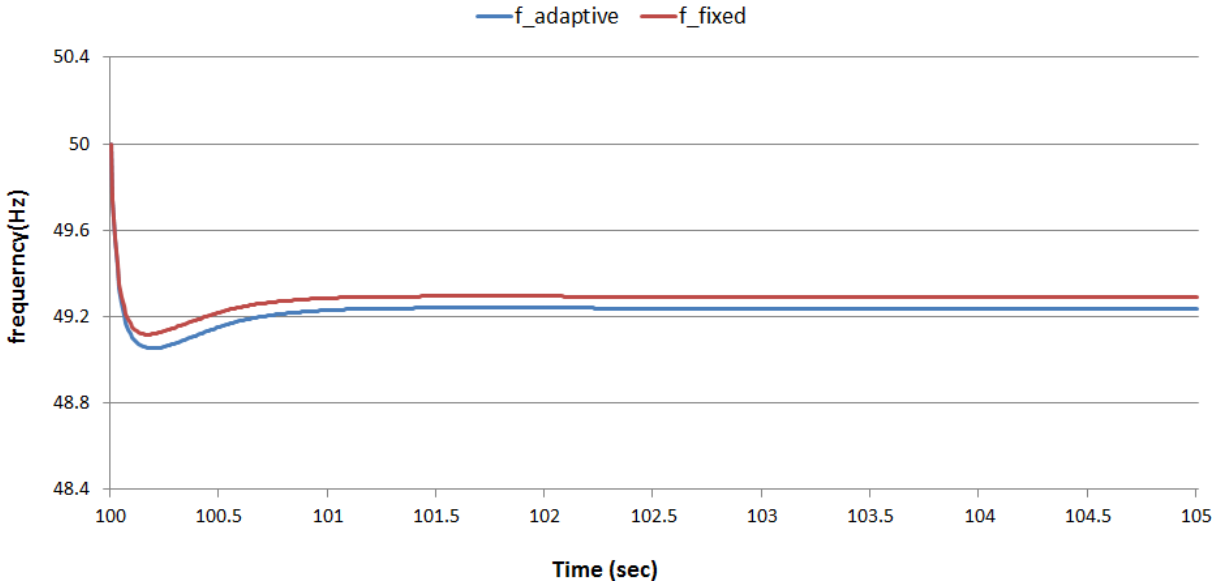

Figure 4.28: Frequency after load increase of 3,4 %
(based on total system load) at bus 1 with fixed and adaptive FCC, CRES

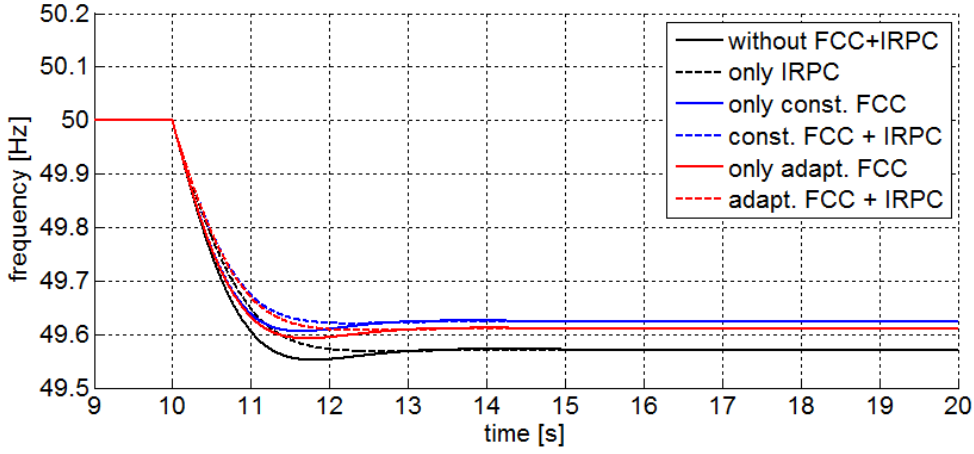

Figure 4.29: Frequency after load increase of 6,6 %
(based on total system load) at bus 9 with different controller combinations, IEE

Table 4.6: Result overview for controller combinations, IEE

Controller Combination	Frequency Nadir [Hz]	Frequency Deviation [Hz]	Max RoCoF [Hz/s]	Inertia Time Constant [s]
	TCRIF01, TCRIF05	TCRIF01	TCRIF01, TCRIF04	TCRIF01, TCRIF06
Without FCC and IRPC	49.55	0.43	0.55	5.42
IRPC	49.57	0.43	0.50	5.96
FCC	49.61	0.38	0.55	5.47
FCC and IRPC	49.62	0.38	0.50	6.01
aFCC	49.59	0.39	0.55	5.47
aFCC and IRPC	49.61	0.39	0.50	6.01

Reasons for the impact of FCC on mainly frequency deviation and nadir and in contrast the influence of IRPC on RoCoF are the implemented controller functions at device level. The following Figure 4.30 shows the reserve activation due to FCC and IRPC for storage 1 connected at bus 5 with an installed capacity of 600 kW. The instantaneous peak reaction with zero steady state injection of IRPC directly after disturbance is obvious. In contrast, FCC activation shows a delayed behaviour with a non-zero steady state value, which influences the steady state frequency deviation. the different peak time of both reserve powers is also reason for the possibility to include both controller functions, FCC and IRPC, within one device. Therefore, droop statics need to be designed accordingly. Per se, the controller functions do not conflict with each other.

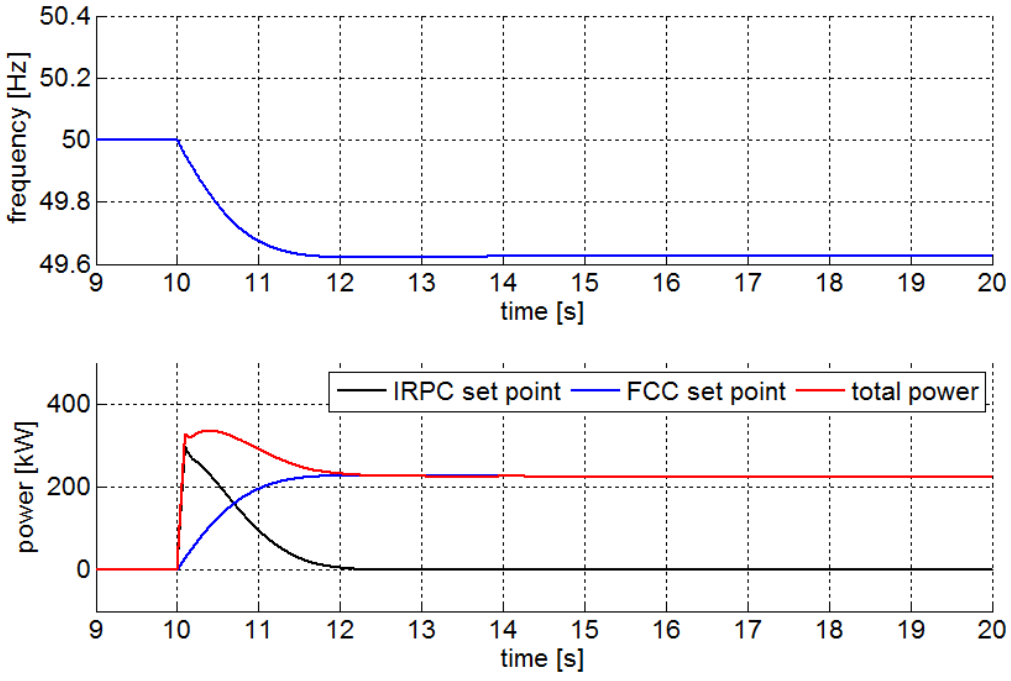

Figure 4.30: Reserves activation after load increase from storage 1 at bus 5 with installed capacity of 600kW, IEE

During the same test scenarios also, voltage has been monitored. The effect on bus voltage deviations resulting from additional power injection due to reserve activation for FCC and IRPC was found to be negligible (see Figure 4.31 and Figure 4.32).

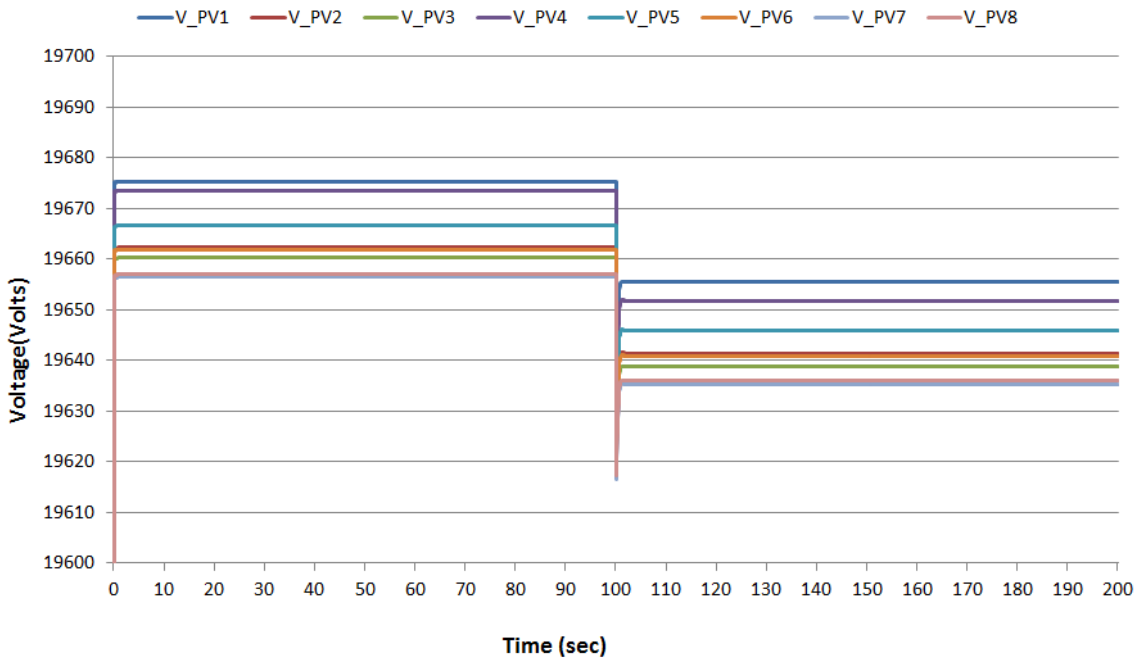

Figure 4.31: Voltage response at the connection point of each PV, CRES

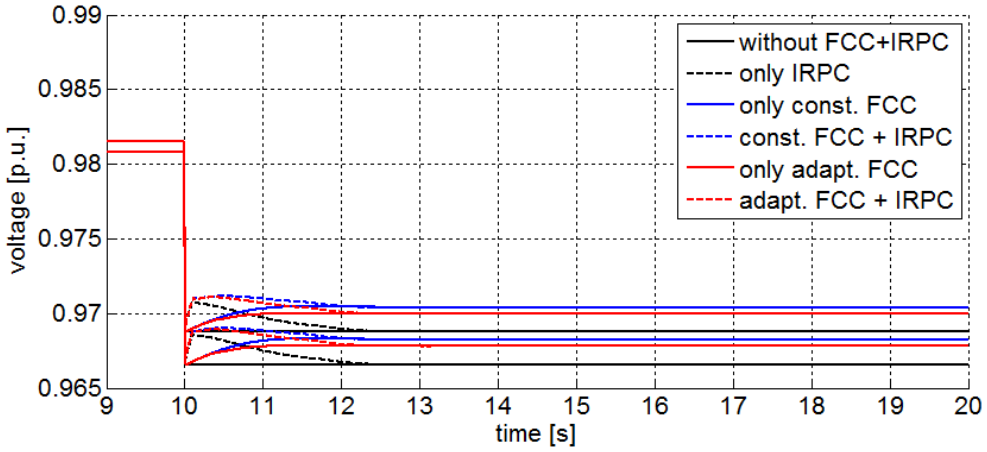

Figure 4.32: Minimum and maximum voltage response over all busses with different controller combinations, IEE

Coming to performed tests according to test group b), resource limitation due to operational setpoints has been investigated. Figure 4.33 shows the power set points from IRPC and FCC controller modules before limitation and the total power which is injected into the grid for two operating points: the solid line belongs to a high wind condition, where the turbine with rated power of 1500 kW injects 1450 kW. The second scenario is a low wind condition, where the power injection is half compared to the high wind condition, plotted with dashed line in Figure 4.33. In the high wind condition, nearly no additional power can be activated. As result of less inertia contribution of the wind turbine to the system, the RoCoF is higher. The summary of the results is provided Table 4.7.

The FCC contribution is zero, because this functionality is only in case of a load decreasing, where the output power can be reduced. Inertia contribution was considered due to the capability of wind turbines to provide additional power from the rotating turbine. After inertia contribution the rotational energy of the rotor needs to recover. Hence, after providing additional power, the turbine needs to consume power in order to accelerate the rotor again. The recovery effect was neglected for these investigations. However, the necessity of availability of resources for provision of IRPC services is obvious.

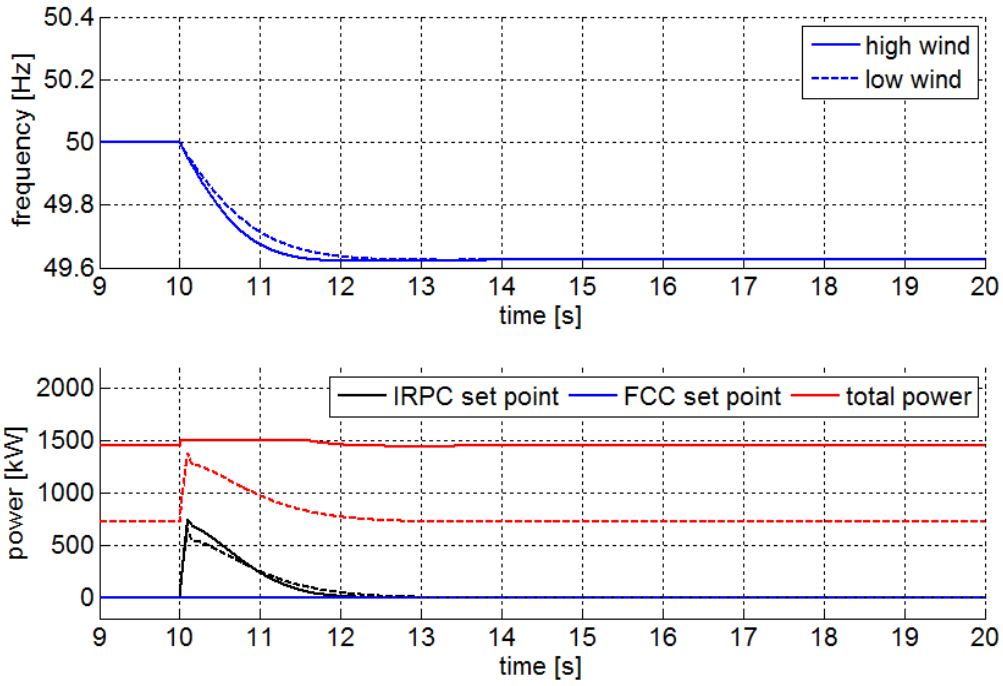

Figure 4.33: IRPC and FCC contribution of the wind turbine after load increase, IEE

Table 4.7: Result overview due to resource limitation due to initial power injection, IEE

Wind Condition	Frequency Nadir [Hz]	Frequency Deviation [Hz]	Max RoCoF [Hz/s]	Inertia Time Constant [s]
	TCRIF01, TCRIF05	TCRIF01	TCRIF01, TCRIF04	TCRIF01, TCRIF06
High wind	49.62	0.38	0.50	6.01
Low wind	49.62	0.38	0.44	6.80

Figure 4.34 shows the resource activation of a 600 kW storage for different inertia time constants. Table 4.8 shows accordingly the energy demand for balancing as integral of the power curves over the simulation time of 20 s.

From Figure 4.34 and Table 4.8 can be concluded, that higher inertia constants of the overall systems prevent high peaks of inertia contribution of the Distributed Energy Resources (DER) and herewith aging effects of batteries and mechanical loads on wind turbines could be reduced. Furthermore, the higher the inertia constant, the less energy is needed from DERs to balance disturbances.

DTU performed simulative validation related to test group a) with a different test network (SYSLAB) and gained in general similar results: FCC improved the frequency behaviour in terms of frequency nadir and steady state value. But in contrast to the findings from simulative validation with the CIGRE European MV test grid the simulations with EVs providing FCC and IRPC showed that FCC had a better performance in terms of RoCoF compared to IRPC (see Figure 4.35).

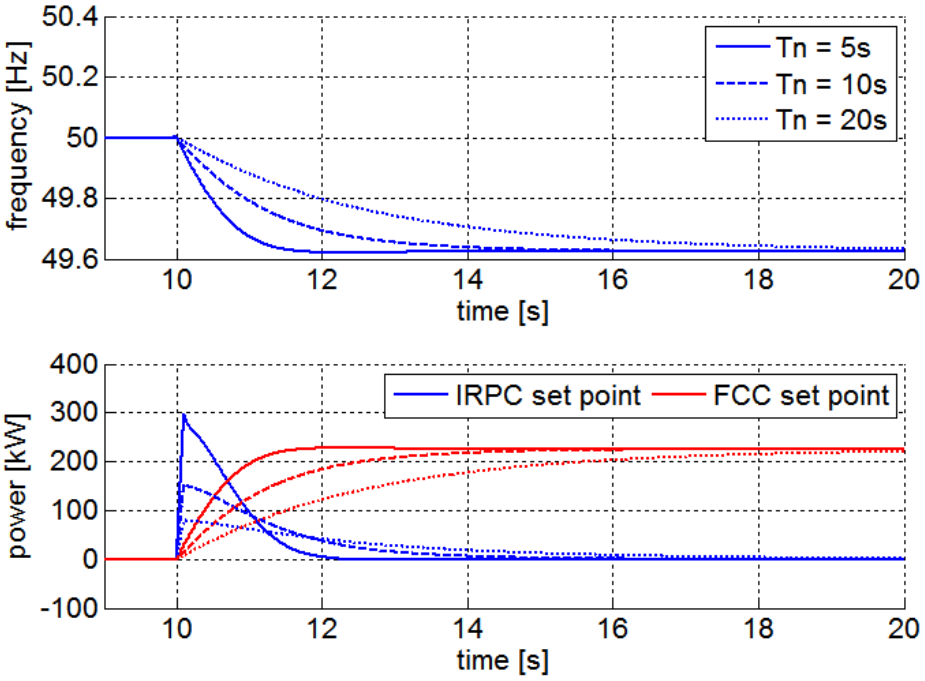

Figure 4.34: IRPC and FCC contribution of storage 600 kW under consideration of different system inertia, IEE

Table 4.8: Result overview for different inertia time constants of the HV-area, IEE

Inertia Time Constant	Tn = 5s	Tn = 10s	Tn = 20s
Energy consumption due to IRPC [kWh]	62.53	61.26	59.55
Energy consumption due to IRPC [kWh]	594.47	550.27	466.74
Total energy consumption for balancing [kWh]	657.00	611.54	526.29

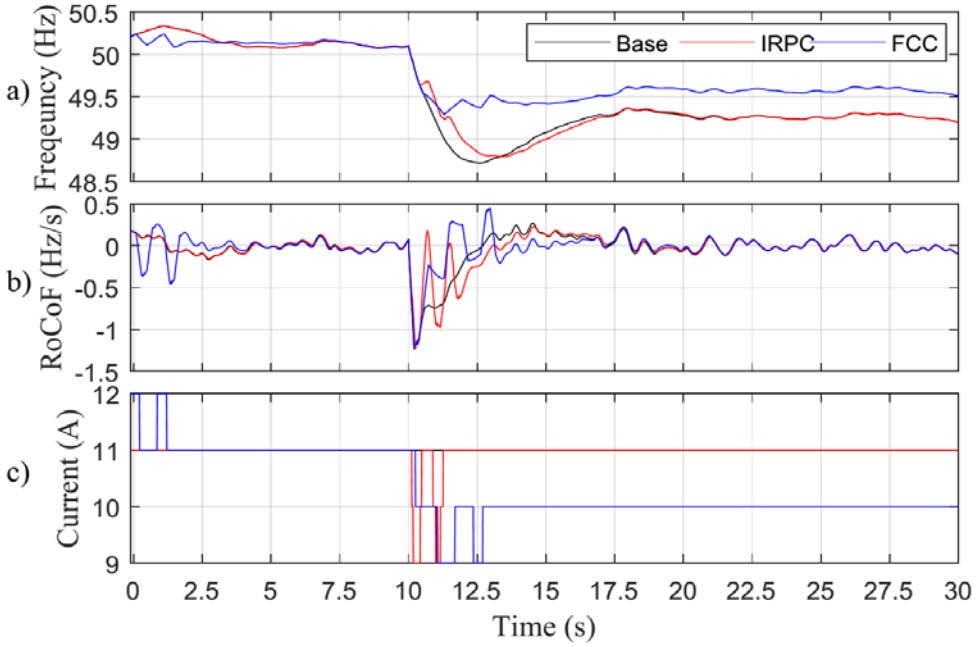

Figure 4.35: Frequency a), RoCoF b) and, current c) after load increase with different controller combinations, DTU

A sensitivity analysis is performed to better understand the effects of the 1 A granularity imposed by the standard IEC 61851 on the performance of the two controllers. A series of simulations are carried out employing different load steps and different granularities. Frequency drops have been obtained

by increasing the active power absorbed by the Vanadium Redux Battery (VRB) by 20 %, 40 %, and 60 %. They represent a load event of 8.7 %, 15.7 % and 23.5 % of the total consumption, respectively. For the evaluation of the influence of the granularity, the following values of granularity have been applied, which are expressed as fraction of the actual granularity of 1 A: ¼, ½ and 1. Moreover, for the sake of completeness, the case of continuous regulation (no granularity) and the uncontrolled case have also been included in the analysis.

Figure 4.36 reports 3D bar plots of the results for all of the performed simulations. The results are reported by means of Standard Deviations (SD) for both Frequency and RoCoF for FCC and IRPC. As expected, Figure 4.36 shows that in all of the cases the SD depend on the size of the load step. On one hand, they are mostly constant for the different considered granularity, on the other hand higher values are found in the uncontrolled cases. Moreover, it is noticeable that beneficial effects on the frequency are found in case of FCC.

Following the results obtained during the simulations, DTU investigated the EVs capability to provide synthetic inertia and frequency containment control in an islanded grid in real circumstances. Two study cases are analysed, in the first Study Case 1 (SC1), the system is studied involving a set of load steps. An alternate load-increase and load-decrease are applied, so that both over and under frequency dynamics can be analysed. In the second Study Case (SC2), wind power generation is added to the system. It adds random power fluctuations over the tested period and it allows the possibility of investigating the behaviour of the two controllers and the EVs in a more realistic and challenging situation.

In the first study case, the frequency variation is triggered by several load steps. A set of load events from the VRB of the same amplitude is applied (±2 kW), namely, 8.7 % of the initial installed load. To better investigate the controllers as well as the frequency dynamics, an additional set of load events with a different amplitude is applied, specifically (±4 kW), 17 % of the initial installed load.

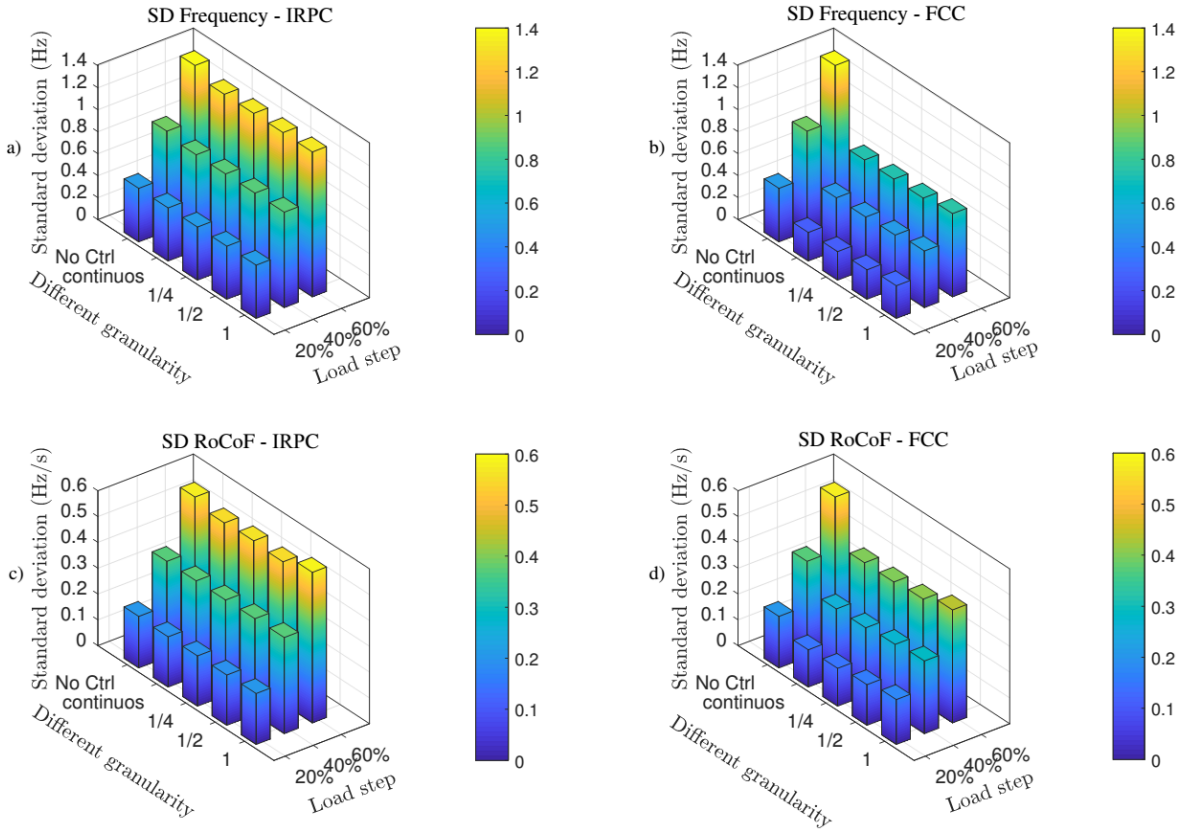

Figure 4.36: (a) SD of the frequency applying IRPC and (b) SD of the frequency applying FCC, (c) SD of the RoCoF applying IRPC, (d) SD of the RoCoF applying FCC, DTU

The results of the experiments are presented in Figure 4.37. Figure 4.37(a) shows the system frequency for the three scenarios. Figure 4.37(b) shows the RoCoF measured over 200 ms in grey and the filtered signal after applying the deadband in red (±0.8 Hz/s deadband is considered). In Figure 4.37(c) the controllers' current setpoint is plotted versus the EVs' absorbed current. Since the three EVs act similarly, only the current of EV1 is presented.

Figure 4.37(c) shows that the EVs change the absorbed current as desired by the different controllers. However, due to the 1 A granularity, the implemented droop and the operating point, the 2 kW load event implies the FCC to oscillate between 12 and 13 A, and between 9 and 10 A. A 6 kW load event is only introduced for Study Case 3 (SC3), at which a stable operating point was found. In fact, Figure 4.37(c) shows that the EVs current did not oscillate for this load event (i.e., around 450 s). However, this oscillation can be reduced by implementing a hysteresis function. Figure 4.37(c) shows that FCC limits the maximum frequency deviation compared to the base case, while the IRPC does not have an effect on it. On the other hand, due to the oscillation between the different set-points in case of FCC, Figure 4.37(b) shows that the RoCoF was outside the deadband more frequently when compared to SC1 and 2. Due to the response delay of the EVs and the dynamics of the diesel, which led to a continuous frequency oscillation, it is difficult to perceive a valuable improvement in terms of the RoCoF from IRPC.

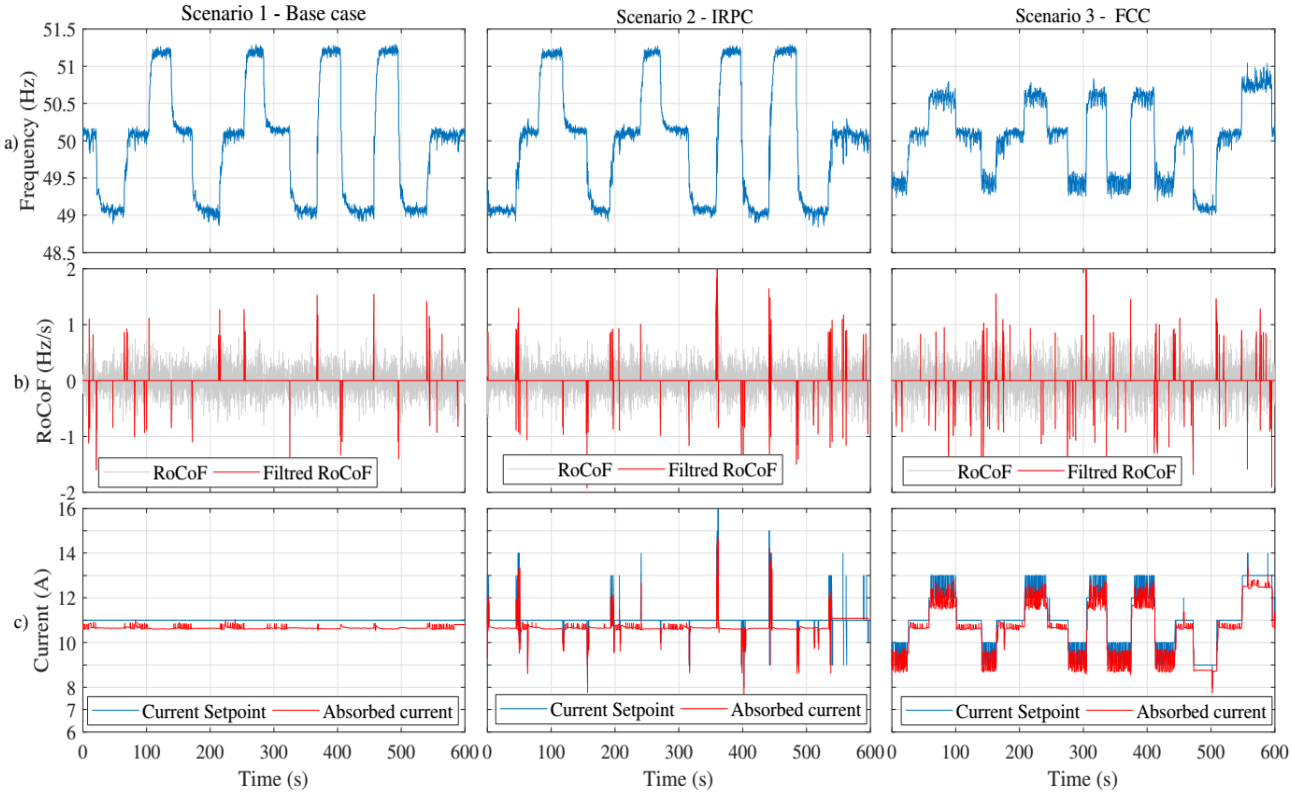

Figure 4.37: Study Case 1 (load steps) – (a) Frequency, (b) RoCoF, and (c) EV1's set-pint vs. absorbed current, DTU

In the second study case, the two controllers are analysed during wind power production. The VRB set-point is set to zero during this study case. The same scenarios and droop characteristic as the previous study case are applied. Due to the random stochasticity of the wind generation and the diesel dynamics, the initial and boundary conditions are not exactly identical. Nevertheless, this study case aims to investigate the performance of each controller and the EVs in a more challenging and realistic configuration rather than comparing the different scenarios. The results for SC2 are presented in Figure 4.38.

Figure 4.38(a) shows the grid frequency for the three scenarios. Figure 4.38(b) shows the RoCoF measured over 200 ms in grey and the filtered signal after applying the deadband in red. In Figure 4.38(c) the controllers' current set-point is plotted versus the EVs' absorbed current. Since the three EVs are acting similarly, only the current of EV1 is presented. Figure 4.38(a) shows that the FCC does have a remarkable effect in limiting the maximum frequency deviation. Figure 4.38(b) shows that by applying the IRPC, the RoCoF is outside the deadband more frequently.

This work, on a simulation level, presented the ability of FCC in improving the frequency in terms of nadir, steady state value and RoCoF. It also presented the ability of IRPC to improve the frequency nadir and slope following an event. While it was acknowledged that EVs could quickly and almost precisely respond to fast changing current set-points, some technical limitations in employing EVs for such services were found.

Moreover, an experimental validation was conducted, presenting the capabilities and limitations of the two controllers under two different circumstances: following load events in both directions and exogenous wind generation profiles. Employing the FCC, the simulations results showed a remarkable improvement of the frequency nadir and steady state value. It showed also a very limited improvement in terms of RoCoF. The controller did not limit the maximum RoCoF following the event but it did improve the overall behaviour compared to the base case. Similarly, the experiments showed the ability of FCC in limiting the maximum frequency deviation, both following a series of load events or considering a wind power generation.

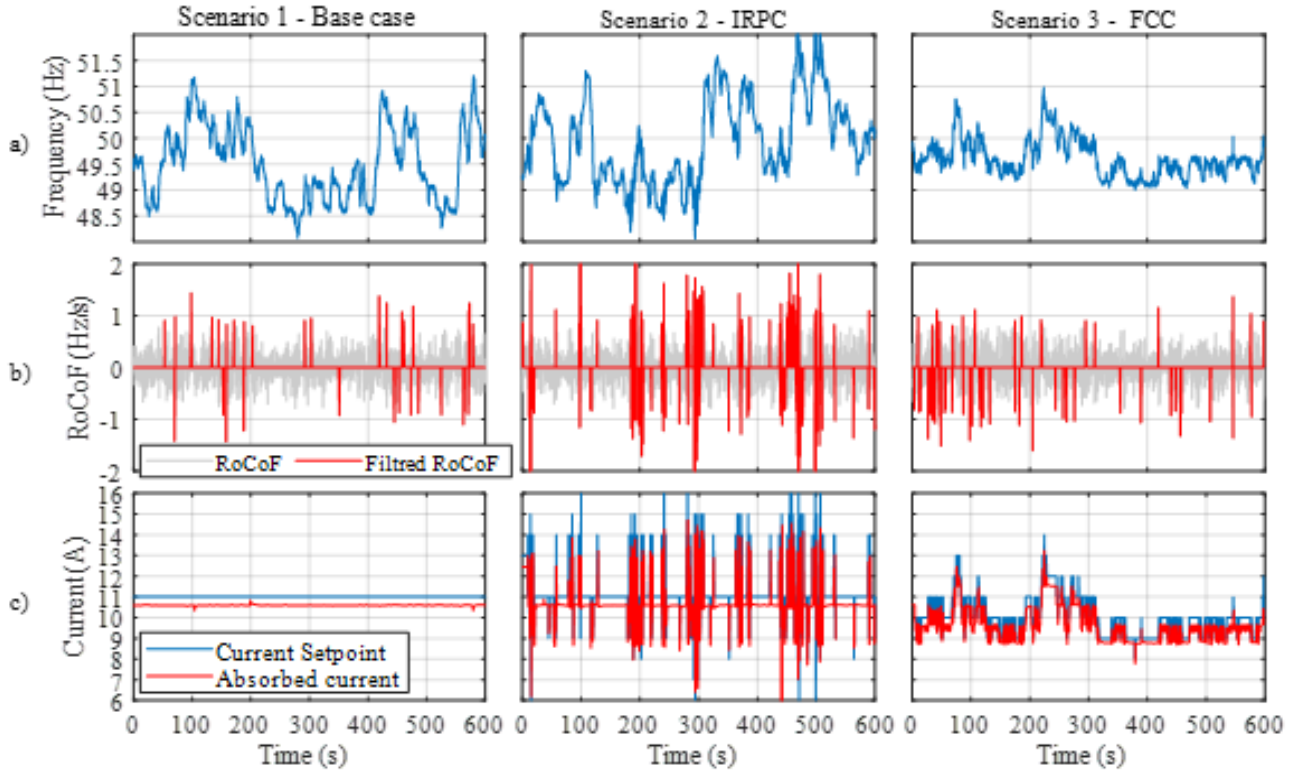

Figure 4.38: Study Case 2 (wind power) – (a) Frequency, (b) RoCoF, (c) EV1's set-point vs absorbed current, DTU

By applying the IRPC, the simulations presented limited frequency improvements in terms of frequency nadir and frequency slope. On the other hand, the smaller deadband worsened the RoCoF trend when compared to the base case. However, in both cases, the controller did not limit the maximum RoCoF value. As mentioned, the IRPC slightly improved the frequency slope but worsened the RoCoF. Nevertheless, considering the derivative characteristic of the IRPC, its implementation might easily lead to frequency oscillation and this limits the ability to exploit the resource (e.g., large deadband).

4.3.4 Discussions

The ability of FCC to improve short-term frequency stability of the investigated networks has been shown. Implementations of FCC in simulation and hardware implementation showed improvements of frequency nadir and steady state frequency deviation after a disturbance. In addition, the ability of an adaptive FCC to improve frequency stability metrics was proven. The higher frequency deviation in case of an adaptive FCC was found to be rather small, but with the advantage of less FCC contribution from reserves, which are located in cells, where no disturbance has happened. If, however, the system operation requirements specify that the frequency deviation should not be worsened, improvement in steady state frequency deviation can be achieved by increasing the droop of the cell where the disturbance happens.

Furthermore, the ability of IRPC to improve RoCoF/inertia time constant has been presented through simulations. In experimental validation the positive impact of IRPC was not obvious. Reason for this is the chosen droop slope and deadband. These parameters are very important and need to be designed according to the ability of the chosen devices and the power system requirements.

Anyway, in a future power system with reduced inertia a contribution from other DERs is needed. Other implementations to provide inertia, like virtual synchronous machines, need to be understood, integrated and validated in further investigations.

If reserves are not available for balancing services, the metrics for short-term frequency stability could not be influenced. Vice versa, system stability is endangered, if relevant reserves could not be activated. In order to avoid critical situations, relevant reserves need to be free in order to react with reserve power in case of a disturbance.

If the overall system inertia is very small, distributed devices need to provide more inertia by activation of IRPC reserves. Therefore, more balancing energy is needed from distributed resources and the peak power injection needs to be higher. This could have negative impact on mechanical loads (wind turbines) or life-cycle of batteries. For this reason, overall system inertia should remain over a minimum in order to guarantee power system stability. Investigations under a) showed that the combination of FCC and IRPC and their distributed reserves contribute sufficiently to balancing control and improve the short-term frequency stability of a future power system.

5 Voltage Control Validation Achievements

Essentially, the voltage control approach in ELECTRA IRP enables the preparation of reserves for near future requirements of voltage control. PPVC foresees near future voltage violations by using forecasts of load and generation from historical data. It also deploys all available resources after disturbances to take corrective measures of voltage level violations.

The primary purpose of the proof of concept validation is to investigate the capability of the PPVC concept in replacing the existing secondary and tertiary voltage control techniques. The key PPVC proof of concept questions to be addressed are:

- What are suitable cells from a voltage control point of view?
- Can PPVC replace the present secondary (local) and tertiary voltage control (global) schemes existing in power grids by a decentralized control located at a cell level?
- How would PPVC interact with PVC and respond to different network conditions?

Based on the above outlined validation methodology, the available validation environments, and the selection of use case combinations the following results have been achieved for the proof of concept validation of the voltage control schemes in ELECTRA IRP.

5.1 Identification of Cells

From the voltage control point of view, it is important to have a tool in hand which helps in the identification of potential cell set-ups. In the following sections such an approach is briefly outlined.

5.1.1 Clustering-based Identification of Cells

In order to identify the optimal configuration of an ELECTRA cell a clustering approach has been chosen which consists of the following two main stages:

Step 1: Calculation of the Normalized Electrical Distance

For defining cell objects, the clustering approach is based on the normalized electrical distance as outlined below following four steps [16]:

a) Calculate the Jacobian matrix and use it to obtain the *∂Q/∂u* matrix.

$$\begin{bmatrix}\Delta P\\ \Delta Q\end{bmatrix} = \begin{bmatrix}\frac{\partial P}{\partial \delta} & \frac{\partial P}{\partial u}\\ \frac{\partial Q}{\partial \delta} & \frac{\partial Q}{\partial u}\end{bmatrix}\begin{bmatrix}\Delta \delta\\ \Delta u\end{bmatrix}, \qquad J_4 = \frac{\partial Q}{\partial u}$$

b) Calculate the sensitivity matrix B by calculating the inverse of J4.

$$B = J_4^{-1} = \frac{\partial u}{\partial Q} \text{ where } b_{ij} = \frac{\partial u_i}{\partial Q_j}$$

c) Calculate the attenuation matrix α by dividing the non-diagonal elements by the diagonal elements using the following equation.

$$\alpha_{ij} = b_{ij} / b_{jj}$$

d) Calculate the electrical distance and obtain the normalized electrical distance matrix

$$D_{ij} = -\log(\alpha_{ij} \,.\, \alpha_{ji})$$

$$D_{ij}^{norm} = D_{ij} / \max(D_i)$$

Step 2: Hierarchical Clustering

Hierarchical clustering is one method of defining clusters from a data set. It requires distance matrix and linage criterion as input and generates a hierarchy of clusters. A user can then decide upon the best number of clusters based in additional and/or prior information. One method for choosing the best number of clusters is plotting a Dendrogram and a Scree plot. In literature the knee point in the scree plot is commonly used as the reference point for the best number of clusters

5.1.2 Example: CIGRE MV European Test Grid

In order to show how the above outlined clustering approach works, the CIGRE MV European Test Grid has been chosen which is also being used in a various of ELECTRA validation scenarios as outlined in Section 3.2. By using this approach, the normalized electrical distance matrix presented in Figure 5.1 shows that the CIGRE MV European test feeder has strong voltage coupling. This is essentially because the line lengths at the start of the feeder are much longer than the line lengths at the end of the feeder. This means that the nodes most susceptible to over voltage have tight voltage coupling and dividing the feeder into cells might not be possible. Ensuring cells have weak voltage coupling is important as it would limit the impact of one cell's regulations on its neighbours.

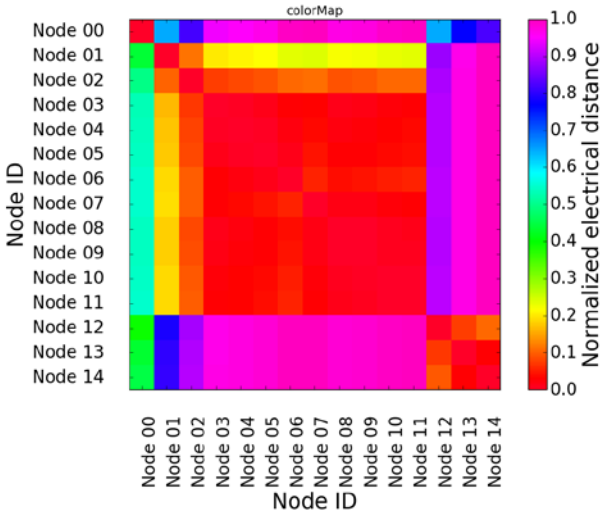

Figure 5.1: Colour plot of the normalized electrical distance matrix for the CIGRE European MV test network

The corresponding Dendrogram and a Scree plots are shown in the following two figures.

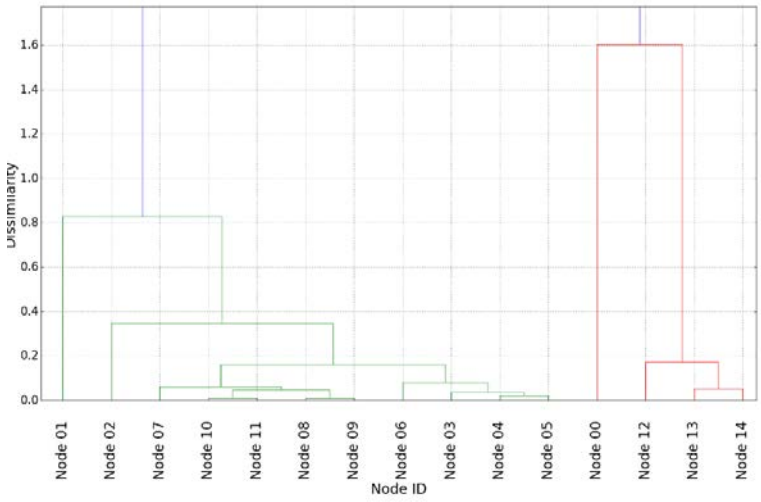

Figure 5.2: Dendrogram for clusters produced using ward linkage based agglomerative hierarchical clustering (original CIGRE European MV test grid)

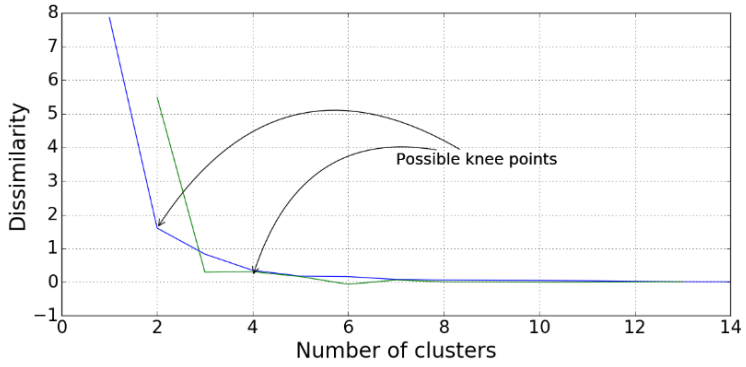

Figure 5.3: Scree plot for the dendrogram (original CIGRE European MV test grid)

As a result, the cell configuration with two main elements as shown in Figure 5.4 can be derived.

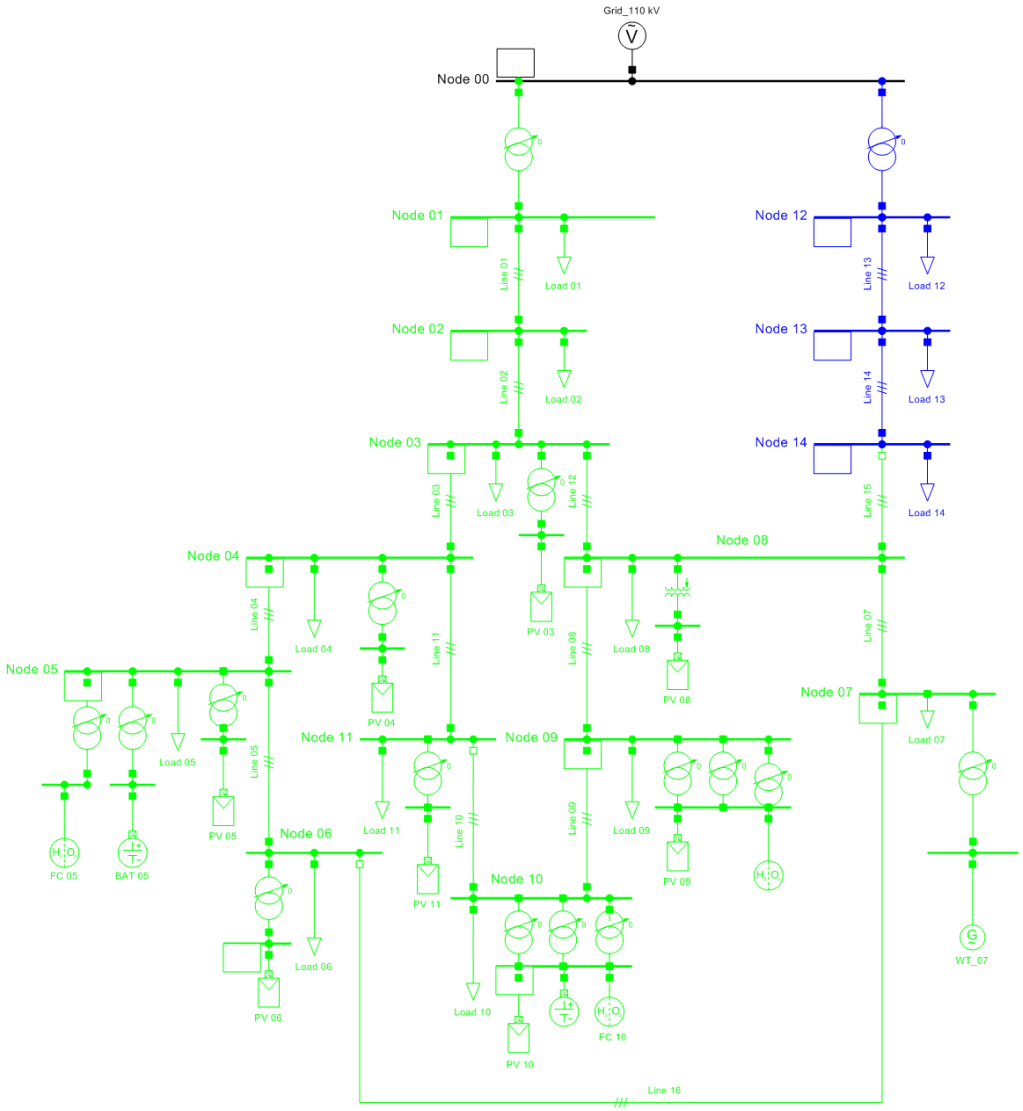

Figure 5.4: CIGRE MV European test grid divided into two cells (i.e., Cell 1 in green, Cell 2 in blue)

One way to emphasize the utility of a cell-based approach is to modify the line lengths such that voltage zones with weak voltage interdependence are created. For example, three-line lengths have been modified (Line 1: from 2.8 km to 0.8 km, line 2: from 4.4 km to 1.4 km and line 12: from 1.3 km to 6.3 km) to create regions with weak voltage interdependence as shown in Figure 5.5.

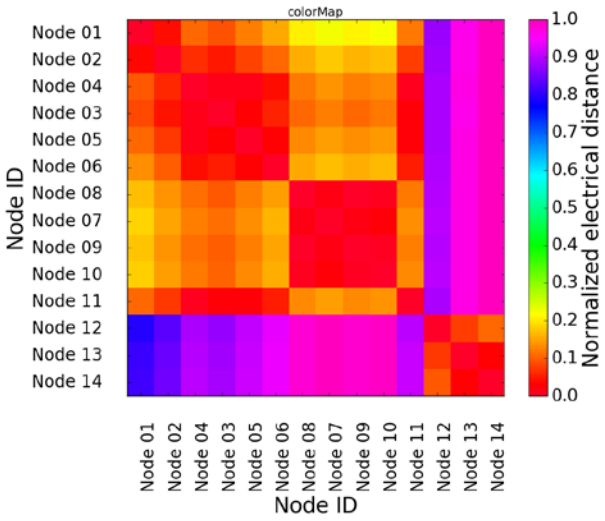

Figure 5.5: Colour plot of the normalized electrical distance matrix for modified line lengths

As a result, the cell configuration with three main elements as shown in Figure 5.6 can be derived.

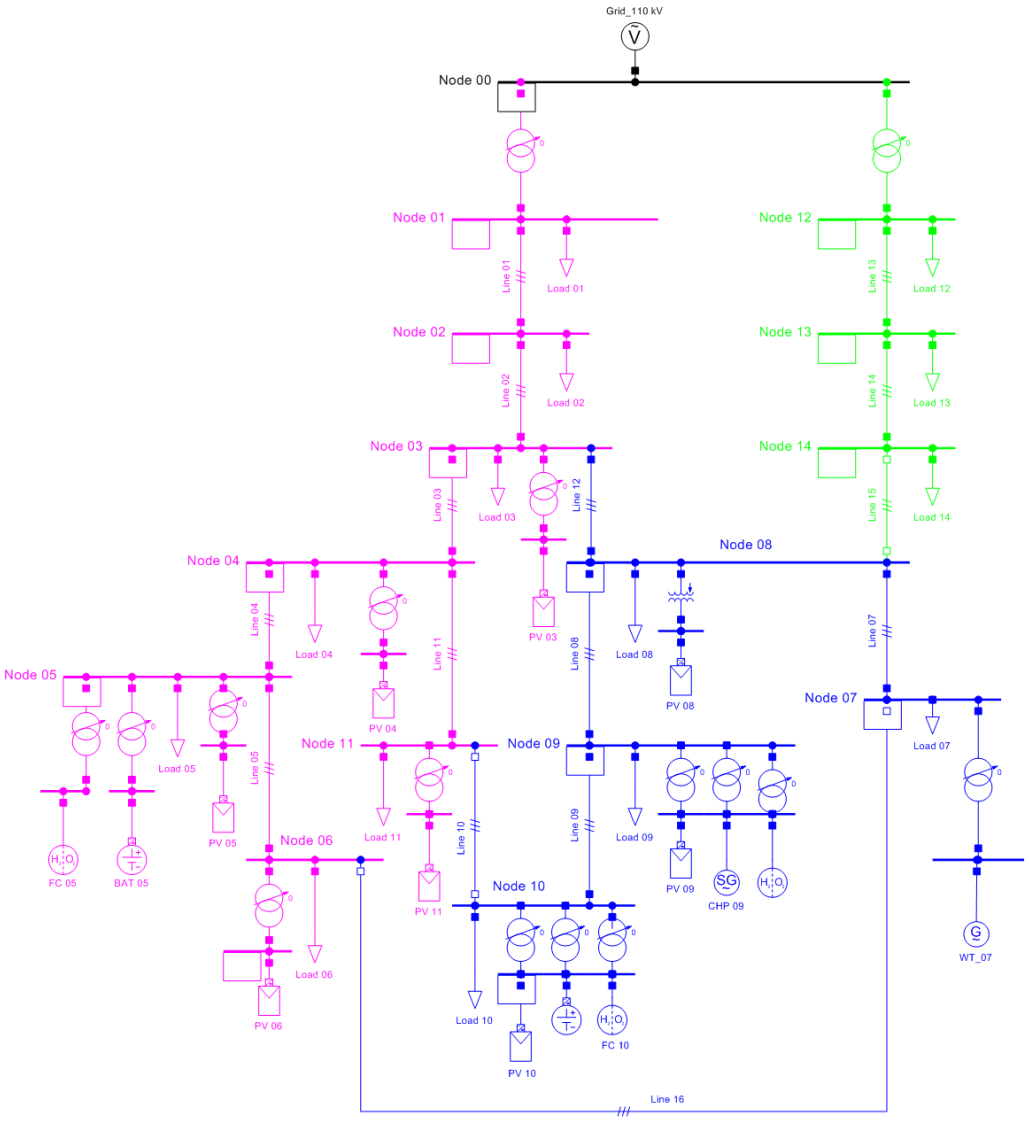

Figure 5.6: CIGRE MV European test grid divided into three cells (i.e., Cell 1 in cyan, Cell 2 in blue, Cell 3 in green)

5.1.3 Discussion

The above described clustering-based approach provides a suitable tool for the identification of potential ELECTRA cells from a voltage control point of view. Identified clusters can serve as a starting point for defining a ELECTRA cells together with the rules for defining cells as described in Deliverable D5.3 [2]. However, as expressed above this approach takes only the voltage sensitivity between the different nodes in a power grid into account and therefore doesn't include any information from the balancing and frequency control side. Moreover, local flexibility is also not taking into account.

Potential future work should seek for including the ELECTRA rules for defining a cell and balancing issues in a combined approach.

5.2 Validation Experiments "Use Case Combinations PVC and PPVC"

In this section, the validation of the voltage control solutions, namely the PVC and PPVC, by simulations and experiments is discussed in detail. First, a brief overview of the validation environments utilized is presented followed by setting the objectives for the validation. The key findings of the validation are then presented and a discussion on the achievements and future outlook concludes the section.

5.2.1 Chosen Validation Environments

An overview of the validation environments utilized for validation of PVC and PPVC use cases are shown in Table 5.1.The detailed descriptions of the validation environments can be found in Section 3.2 and in the Annex.

Table 5.1: Used validation for proof of concept validation of use case combinations PVC and PPVC

Environment	Partner	No of Cells	Details
Pure Simulation Environment	TECNALIA	1, 3, 9	Flexible test grid FLEXTEX developed within ELECTRA IRP and modelled in PowerFactory
	VTT	1, 3	CIGRE European MV distribution grid simulated in MATLAB/Simulink
Hybrid Environment: Controller and Power Hardware-in-the-Loop	AIT	2, 3	Modified CIGRE European MV distribution network model within PowerFactory coupled in a CHIL co-simulation with an emulated inverter-based DER in Typhoon HIL
	SINTEF	2	PHIL setup with simulated CIGRE European MV test grid in OPAL-RT and connected real converters

5.2.2 Test Criteria

Based on the KPIs derived through the SGAM approach the following test criteria have been considered for the validation of the voltage control schemes:

- *Optimal cell division for voltage control (TCR-PP01):* Optimal configuration of a cell taking the voltage sensitivity of the grid nodes into account (see also Section 5.1).
- *Power losses due to reserves activation (TCR-PP02):* The losses (in kWh) due to the additional power flows in the lines created by the reserves activation.
- *Cost of voltage restauration (TCR-PP03):* The cost (in €/kWh) of activating the resources for reserve provision.

- *Minimum power losses in the cell (TCR-PP04):* Network losses [kW]: sum of all the real power generated in the cell and/or imported from other cells and then subtracting all real power consumed by the cell loads in the evaluated period of time.
- *Safe and robust voltage for all nodes (TCR-PP05):* The voltage setpoints are within deadbands with additional margins in order to avoid undesirable (excessive) OPF calculations.
- *Time for voltage restauration (TCR-PP06):* Time between the instant the fault occurs (voltage crossed the threshold of 90%/110% of its nominal value) and the instant the voltage is back within 10% of its desired value.

5.2.3 Performed Experiments and Results

The experiment for the validation of the combined PVC and PPVC use cases has been accomplished by simulations and later on by laboratory-based testing using CHIL and PHIL set-ups. The objective of the experiment itself is the demonstration of the PPVC control scheme as valid voltage control structure for the WoC. The PPVC must ensure voltages within the safe band in their optimum values for power losses minimization in the current timeframes for secondary voltage control. PVC and PPVC are naturally coupled because the PVC controllers directly receive the set-points from the PPVC. The system configuration scheme for the experiment (see Figure 5.7) shows the existing relationships in terms of domains between the cell-centralized PPVC controller and the DER controller, that is the responsible for the PVC operation.

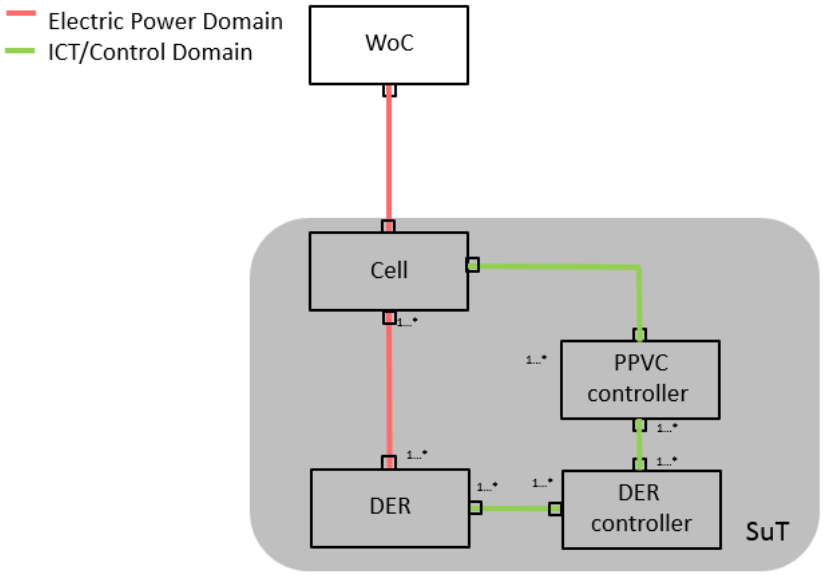

Figure 5.7: Voltage control system configuration with System under Test (SuT)

For the system configuration above, the following proof of concept tests have been identified and implemented:

- Test 1: Simulation-based proof of concept for the WoC approach controlling DER devices and corresponding loads (e.g., ZIP load model to emulate real grid dU/dP responses) under different renewable production scenarios and different test grid set-ups.
- Test 2: CHIL-based proof-of-concept analysis of the PVC and PPVC use case combination using an emulated inverter-based DER (incl. clustering concept for the identification of potential cells and comparison of different cell-configurations).
- Test 3: PHIL-based evaluation of response time sensitivity of PVC and PPVC controller in the face of topology changes in the network incl. a comparison of the WoC control approach against the traditional way of voltage control under similar circumstances.

Simulation-based validation achievements

First experiments related to voltage control are based on the CIGRE European MV test grid which have been implemented by VTT in simulations. Under different penetration levels of renewables (i.e., 1 %, 20 %, and 50 %) the behaviour of the proactive and corrective mode of PPVC has been tested mainly with three different configurations (i.e., without PPVC, one cell and three cells).

The corresponding simulations consist of evaluating performance of loss optimized reactive power injection with optimum power flow tool Matpower using cell division and single cell (not cell division). Result of the OPF tool is fed also to Simulink transient model to see interaction with tap changer dynamics.

In addition, ZIP[2] load effect is also analysed on loss optimization and how should it be taken into account. If there is permanent impedance style response of load to increased voltage, savings in transmission losses can be erased by increased load.

Power losses due to reserves activation (TCR-PP02) and cost of voltage restauration (TCR-PP03)

A selection of results is provided in Figure 5.8, Figure 5.9, and Figure 5.10 mainly addressing mainly test criteria TCR-PP02 and TCR-PP03. From the achieved results for the CIGRE model it can be concluded that the PPVC provides significant improvements in terms of grid loses, voltage restauration time and lower sags.

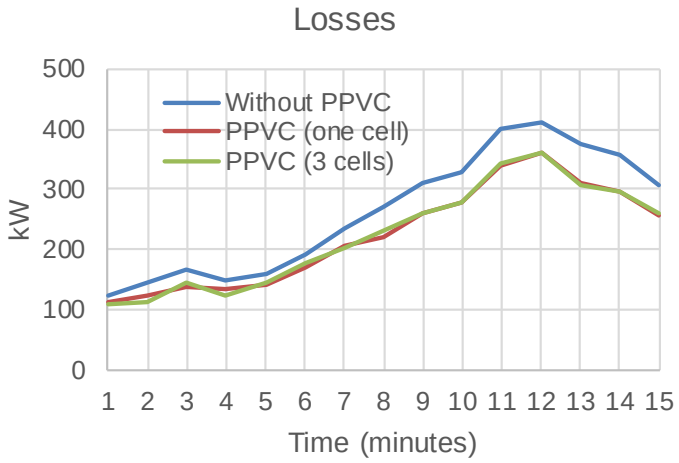

Figure 5.8: Differences between one and three cell grids in losses

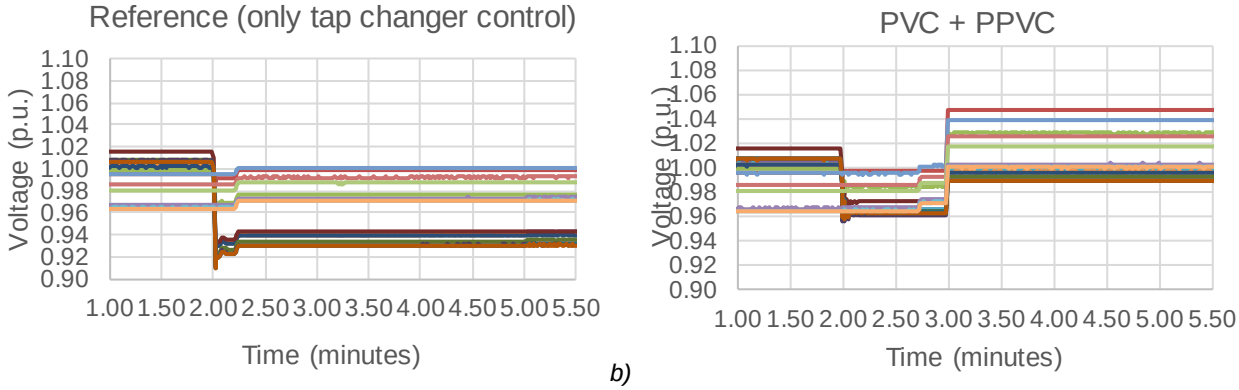

a) *b)*

Figure 5.9: Comparison of BAU with PPVC – (a) reference case with only tap changer reacting, (b) selected node voltage before voltage drop, corrective method reacting and proactive activating again when voltage is stabilized

[2] Z stands for impedance, I for current and P for power.

For the validation of PVC and PPVC use case combination with a larger test grid (i.e., FLEXTEC), three test criteria (i.e., TCR-PP04 – TCR-PP06) have been selected by TECNALIA. For each of them, dedicated simulations have been accomplished. All of them have been done considering a scenario with a significant penetration ratio of renewable energy sources (i.e., 75%). Three different topologies have been tested along the project: considering the WoC as a single cell, divided into 3 cells and into 9 cells. Key results for the 3-cell case and for the validation of the three selected test criteria are shown below.

Minimum power losses in the cell (TCR-PP04)

One of the objective of the ELECTRA voltage control approach is the minimization of active power losses in the system. For validating it, a comparison between the proactive operation of the PPVC and the BAU have been compared. Results of the total losses in the WoC are shown for both active and reactive power in Figure 5.10(a) and Figure 5.10 (b) respectively.

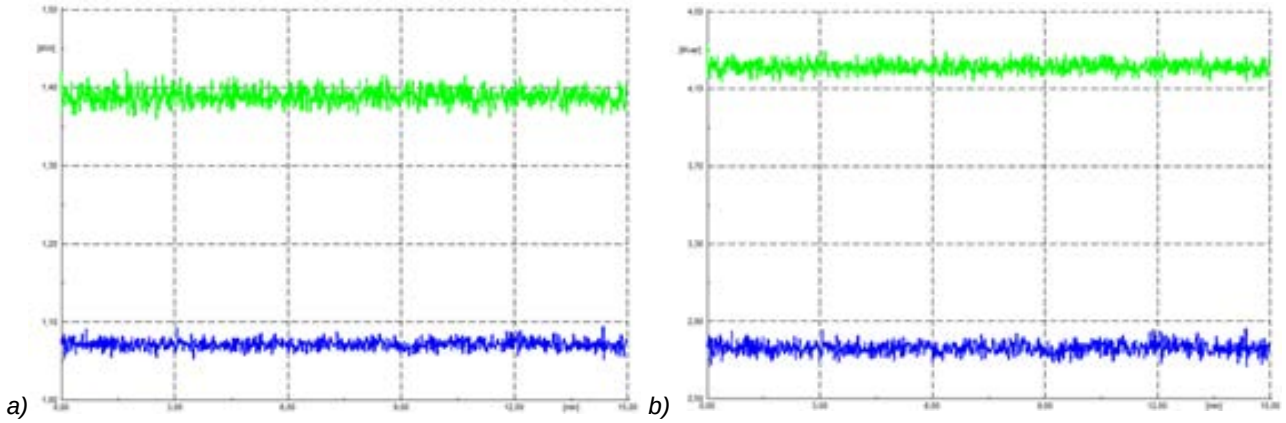

a) *b)*

Figure 5.10: Comparison of power loses between BAU (green) and PPVC (blue) – (a) active power losses, and (b) reactive power losses

The BAU case is plotted with green lines while the ELECTRA results are shown with blue lines. It can be clearly observed that important reductions can be achieved by using the proactive PPVC. For the scenario selected, up to 21% decrease in active power losses can be obtained. Even not in the primary focus of the use case, a very important reduction of the reactive power losses is achieved (up to 31%).

Safe and robust voltages for all the nodes (TCR-PP05)

The proactive set-points calculated before the real-time must be contained within the safe bands defined by the Regulations while keeping enough safe margins to avoid excessive Optimal Power Flow (OPF) calculations. This test criteria summarizes that the proactive PPVC is intended to reduce the number of corrective PVC/PPVC activations by an optimal calculation of the voltage set-points. In Figure 5.11 can be seen the comparison between the set-points calculated with the BAU case and those resulting from the application of the PPVC. The voltage set-points are shown in representative nodes of the grid, where the dashed lines correspond to the BAU case and the solid lines are the PPVC results. It has also been plotted the 0.95 p.u. line that would trip the corrective PVC/PPVC activation.

It can be clearly observed that, the set-points calculated from the BAU case would lead to values below the 0.95 p.u. established as limit for the PPVC corrective operation in real-time operation. The use of the proactive PPVC in the planning phase would have avoid the recalculation of the OPF in such circumstances.

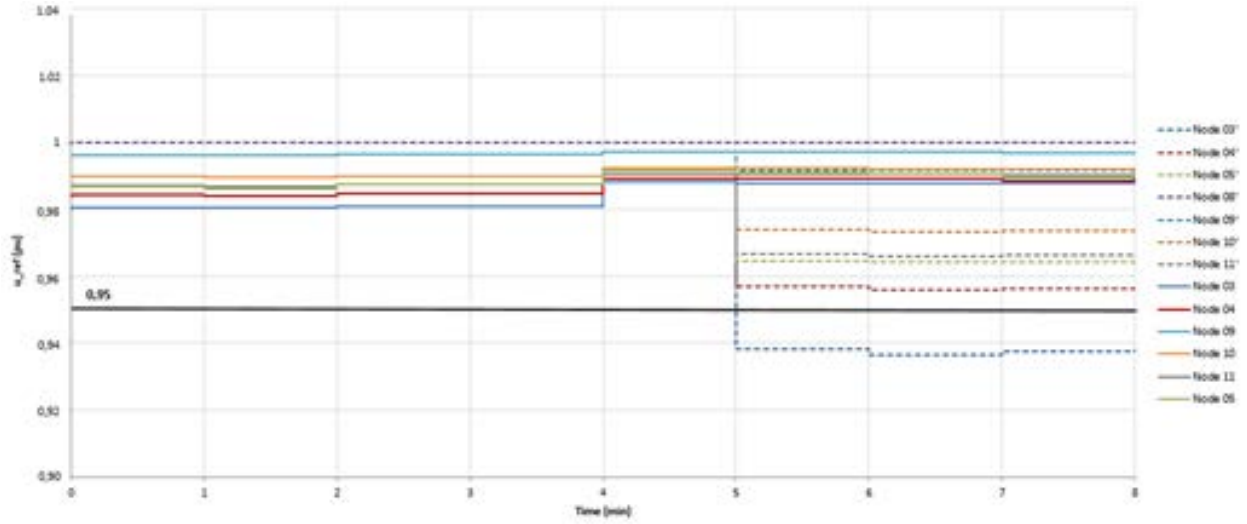

Figure 5.11: Comparison of voltage set-points for BaU and proactive PPVC

Time for voltage restoration (TCR-PP06)

For the last validation test criteria considered in the simulation tests, it has to be compared the improvement of the corrective PPVC versus the current traditional secondary and tertiary voltage control scheme. One of the objectives for the PPVC (corrective), as referred in the use case description, is the commitment to restore the voltage levels in the grid to their optimal values in the time frames of current secondary control [1]. Instead of simply validating the capacity to fulfil that objective, it has been compared the system response in case of an absence of voltage control, only with PVC or with the combined PVC and PPVC action. In the abovementioned scenario, with a 75% of renewable energy installed, at 20 s from the beginning of the proactive time window, an unexpected load increase is detected at load 11. This causes a voltage drop below the 0.95 low limit safe-band in bus 33. Results of the voltage profiles is shown in Figure 5.12.

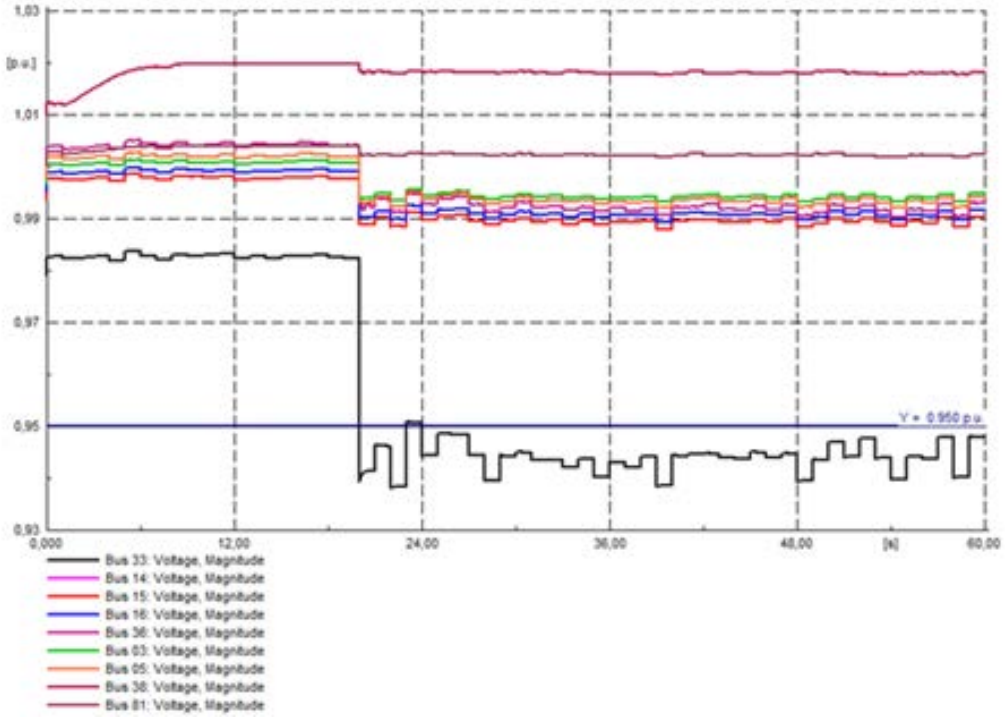

Figure 5.12: Voltages in representative nodes in the WoC

In Figure 5.13 it is shown the evolution of the voltage in the bus 33 depending on the voltage control scheme implemented: *(i)* Case 1 (green line) where no control is implemented in the generation sources, *(ii)* Case 2 (black line) showing the PVC response, and *(iii)* Case 3 (red line) showing the PPVC response.

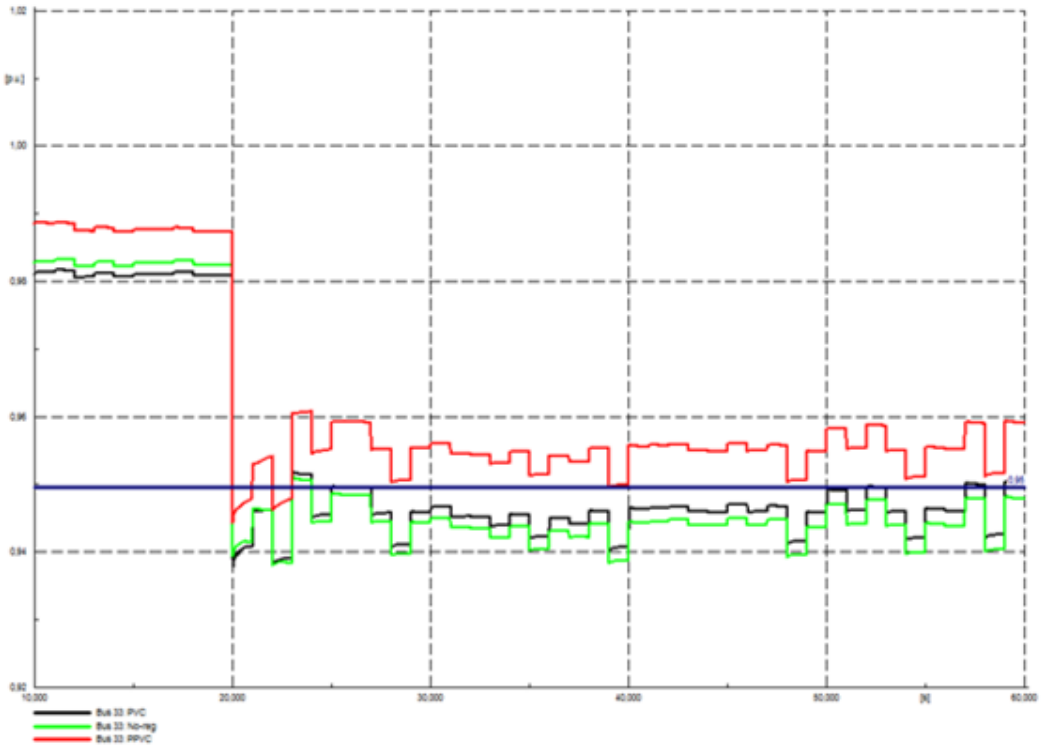

Figure 5.13: Comparison between non-regulated sources, PVC, and PVC and PPVC schemes

It can be observed that the PVC acts automatically to stop the voltage drop in the bus. However, the PVC is not intended to recover the voltages up to the safe band and thus, even the voltage is over the non-regulated case, it is still out of the safe band. The joint action of the PVC and PPVC controllers acts to retrieve the voltages to the safe optimal values in a very short time, that is, within the margins of the current secondary scheme (seconds to a few minutes).

CHIL-based validation achievements

The primary goals of the CHIL-based validation approach from AIT was to apply the above outlined clustering method in order to identify suitable ELECTRA cells from a voltage control point of view (i.e., addressing TCR-PP01) and to evaluate the PPVC algorithm with an emulated inverter-based DER unit (i.e., AIT Smart Grid Converter with real controller board) in a CHIL co-simulation based setup as outlined in Section 3.2 by using the CIGRE European MV test grid addressing test criteria TCR-PP04 and TCR-PP05. In this experiment a comparison of the original CIGRE test grid divided into 2 and 3 cells together with a modified version (details see Section 5.1.2) of this grid also divided into 2 and 3 cells was carried out.

During running the co-simulation, the behaviour of the PPVC approach can be monitored in real-time. This experiment shows that the WoC voltage control approach leads to an improvement which has already been observed by the above described simulations. As presented in Figure 5.14, the network losses can be reduced by defining more cells, including the PPVC controller. Also, the impact of the line length shows a big influence on the normalized electrical distance approach for these cells. As outlined in Figure 5.14 the normalized losses were improved by a maximum change of 3.30 % for the implemented scenarios.

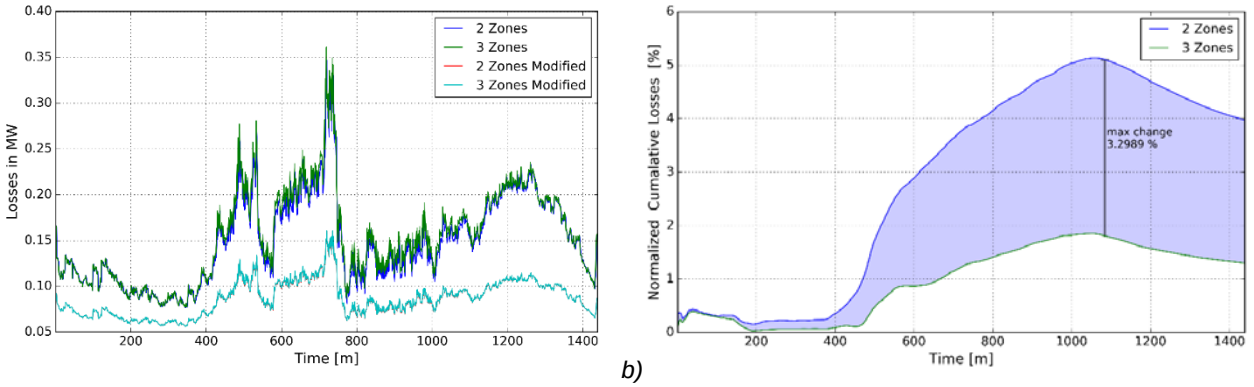

a) *b)*

Figure 5.14: Total network losses for the three scenarios – (a) total losses, (b) normalized losses

A further aim of this experiment was to provide relevant information to the cell operator in a dash-board-based control room visualization showing voltage profiles and DER parameterization errors as outlined in Figure 5.15.

Figure 5.15: Example for control room visualization

PHIL-based validation achievements

The validation of the WoC-based PPVC method in the laboratory of SINTEF is carried out by studying four cases using a PHIL set-up with the CIGRE European MV test grid (see Section 3.2) addressing test criteria TCR-PP04, TCR-PP05, and TCR-PP06:

- Case#1: BAU, with fixed On-Load Tap Changer (OLTC) reference and fixed intercept of droop controllers. In this case, the OLTCs have a fixed reference voltage (U_{set}) which is 1 p.u. and the converter droop controllers have zero intercept values (Q_o). As they normally operate in today's network the OLTCs and the converters adjust themselves automatically following the voltage level at the point of common coupling.
- Case#2: Full PPVC, with optimized OLTC reference and optimized intercept of droop controllers. In this case, the OLTCs reference voltage (U_{set}) and the intercept values (Q_o) of the converter droop controllers are optimally set every 15 minutes for proactive mode and at any time step for restorative mode.
- Case#3: Case#1 with network reconfiguration.
- Case#4: Case#2 with network reconfiguration.

In both Case#3 and Case#4 the normally closed switches in the network are opened after about 19 minutes. Figure 5.16 and Figure 5.17 show voltage profiles for Case#1 and Case#2 for similar 30-minutes loading and generation conditions. While Figure 5.18 and Figure 5.19 present the voltage profiles for Cases #3 and #4. Figure 5.20 shows the total active and reactive power at the swing bus.

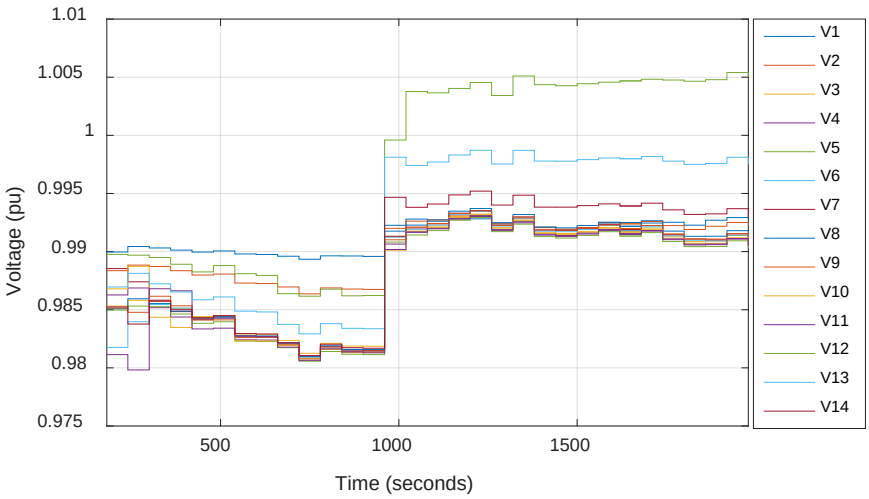

Figure 5.16: BAU case voltage profiles from simulation (Case#1)

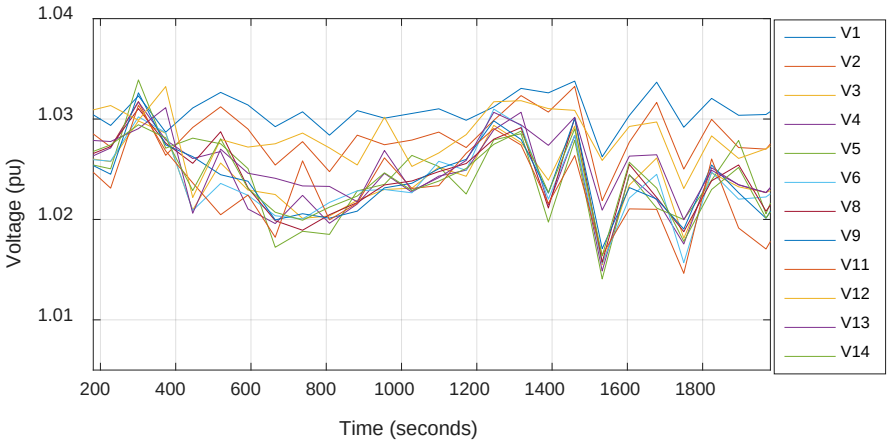

Figure 5.17: The PPVC case voltage profiles from the PHIL test (Case#2)

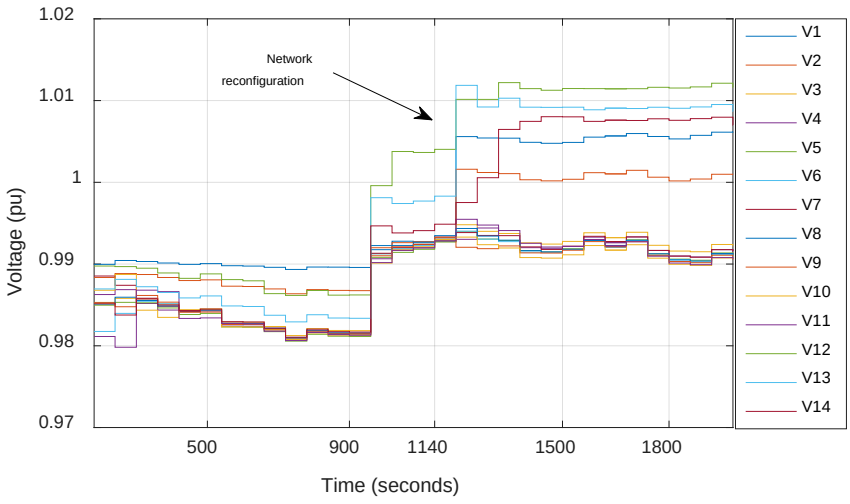

Figure 5.18: BAU case voltage profiles from simulation (Case#3)

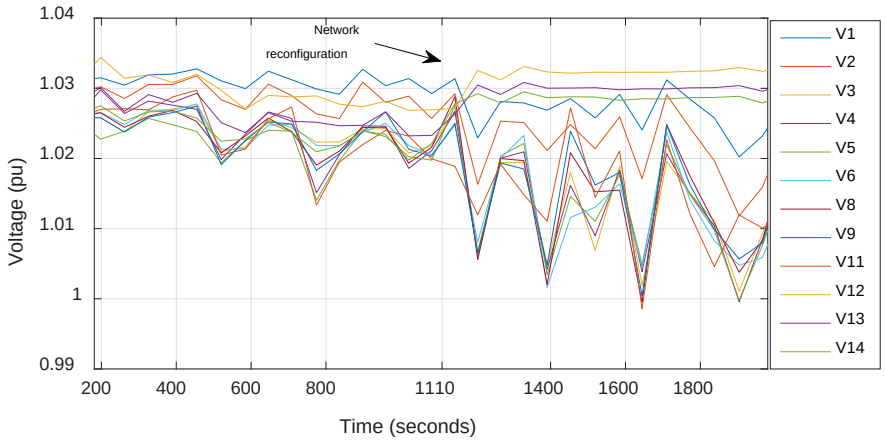

Figure 5.19: The PPVC case voltage profiles from the PHIL test (Case#4)

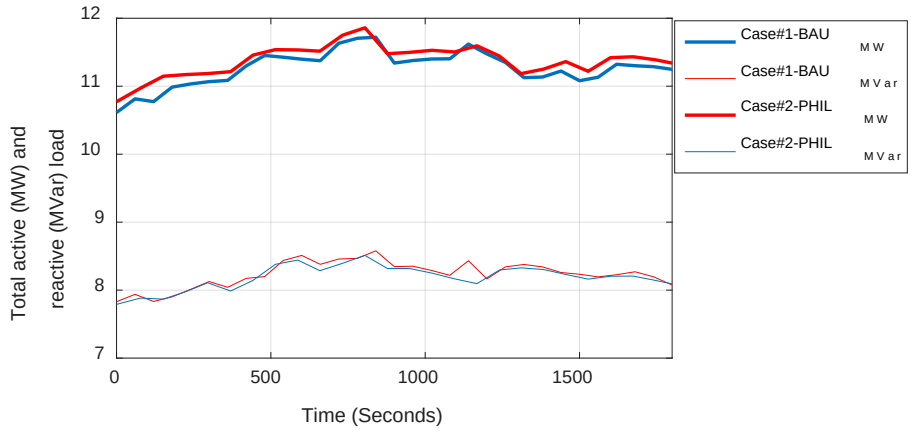

Figure 5.20: Total active and reactive load demand at the slack bus (Case#1 and Case#2)

There has been one tap change during the BAU case in normal situation (Case#1) and two tap changes for BAU case with network reconfiguration (Case#3). However, no tap changes have been experienced with both cases (Cases #2 and #4) of the PPVC implementation in PHIL test. Due to the continuous updating of the reference voltage of the OLTCs, lower intervention of tap changers is observed in case of PPVC than the BAU case.

As shown in Figure 5.16 and Figure 5.17 the voltage profile is more stable in case of PPVC compared to the BAU case. This is essentially due to the pre-adjustment of the PPVC controllers based on the forecasted load and generations. The reference voltage for the OLTC has been updated every 15 minutes avoiding unnecessary involvement of OLTCs tap changes.

The PPVC controllers can adapt to network configuration changes better than the BAU cases. As shown in Figure 5.18 and Figure 5.19, the OLTC reference voltages and the droop controller intercept points were positioned better for incoming loading scenarios and there was no need of OLTC tap change to mitigate the under-voltage problems. The response for network configuration change is fast in case of PPVC as well. The controllers can be re-adjusted if existing settings cannot respond to voltage limit violations in case of PPVC.

As it can be seen in Figure 5.20, the PPVC PHIL implementation in Case#2 demonstrated higher loss in active power and used the reactive power resources in the network more than the BAU Case#1.

5.2.4 Discussions

The realized proof of concept experiments for the combination of the PVC and PPVC control concepts have been accomplished for different cell-configurations using different test grids and in several generation/load scenarios. Some general remarks can be highlighted from the results that are of application to all cases. The implementation of a PVC and PPVC scheme in the WoC is advantageous from the perspective of the power losses reduction if compared with traditional planning schemes as it is based on the use of optimal power flows due to the observability capacities of the WoC. It also shows a faster recovery in case of an unexpected event as the system is able to restore the voltages to the optimal values in very short time frames. Additionally, it is beneficial in terms of a reduction in the number of activations of the PPVC. From the voltage control perspective, there is no real-time coordination between the neighbouring cells but only common agreements in terms of reactive power exchanges in the tie-lines. That means that, while ensuring enough reactive power reserves within the cell to reach an OPF solution in the system, it is going to work properly. However, the possible conflicts between voltage and frequency controllers has not been explored and remains as future work to be accomplished.

6 Conclusions and Outlook

The feasibility of the WoC real-time control approach and its corresponding control schemes have been proven in principle on the basis of selected simulation studies and laboratory experiments. Those experiments have also shown that some of the control schemes and corresponding functions – especially for voltage control – are not only bounded to the WoC concept and can therefore also be applied to existing solutions.

For the identification of suitable testing environments, a KPI/SGAM-based validation approach has been developed which was very helpful for deriving validation KPIs and in the development, implementation, and proof of concept validation of the control concept. This approach has also supported interdisciplinary collaboration across domains (i.e., power system, information and control system) and the operation of distributed teams and laboratories. An important take-away from the exercise was the need of a common understanding of the specific evaluation goals. A more in-depth analysis of the lessons learned in provided in the corresponding Deliverable D7.2 [5].

As planned, the Technology Readiness Level (TRL) of ELECTRA IRP outcomes reaches 3 to 4, with TRL4 representing “Prototype or component validation under laboratory conditions”. TRL5 and beyond are for pre-commercialization and testing of prototypes under real or field conditions, and are clearly beyond the scope of the ELECTRA project. The project took developments of the WoC concept up to laboratory-scale validation, encompassing the flexible (aggregate) resource level, cell level, and inter-cell level. The physical, single device level was not in scope for the research but was involved when setting up the test cases and performing the individual lab-scale experiments.

The validation conducted in the project has been focussed primarily on the containment and restoration from discrete incidents in scenarios of a few cells. The proposed WoC concept’s handling of continuous streams of forecast deviations (i.e., multiple consecutive but relatively minor deviations) has not been analysed due to lack of time. However, due to consultations among the control developers, it can be expected that an increase in size of the system would not affect the ability of the proposed control to handle such deviations. With the increase in penetration of renewable energy resources and various transformations expected in a future (2030+) power system, system operators will be faced with both increased uncertainty and hence continuous streams of deviations, and more regular discrete events for which credible contingencies are required. The focus of the laboratory work has therefore been to validate the ability of the control functions to mitigate such discrete, major incidents. Validation of scalability – involving larger numbers of cells responding in real-time – remains a future research challenge to be addressed. Therefore, with development and wide-scale interest of the community in decentralized and distributed control regimes, novel methods for proving scalability at the laboratory level are under development having started in ELECTRA. Two examples of this are the preliminary development of aggregated measurement-based load models, and the advances made in PHIL appraisal of collaborative virtual and hardware-implemented cells.

For increasing the TRL of the WoC concept and enabling the implementation and application in real networks, further effort at the device level as well as on the actual communication interfaces and protocols is required, in order to ensure the provision of the required flexibility. This includes flexible and adaptive sets of active grid components capable of efficiently delivering the quality of supply specified by grid codes and standards, irrespective of size or position (central or regional). Before applying the WoC in real networks, it is needed to further detail and refine the concepts as well as to analyse and verify them taking into consideration the implementation of the functionalities at device level in particular. Also, system-level validation approaches and benchmark criteria should be developed and refined. Since corresponding proof of concept tests have been carried out with some limitations, further research and development on higher TRL levels is necessary (including more concrete rules for defining cells, corresponding test networks and benchmark criteria).

7 References

[1] "Description of the detailed Functional Architecture of the Frequency and Voltage control solution (functional and information layer)," ELECTRA IRP consortium, Deliverable D4.2, 2017.

[2] "The Web of Cells control architecture for operating future power systems," ELECTRA IRP consortium, Deliverable D5.3, 2018.

[3] "Core functions of Web-of-Cells control scheme," ELECTRA IRP consortium, Deliverable D6.3, 2018.

[4] "Simulation-based Evaluation of ELECTRA Web-of-Cell Solution for Voltage and Balancing Control," ELECTRA IRP consortium, Deliverable D6.4, 2018.

[5] "Lessons learned from the ELECTRA WoC control concept evaluation and recommendations for further testing and validation of 2030 integrated frequency and voltage control approaches", ELECTRA IRP consortium, Deliverable D7.2, 2018.

[6] M.H. Syed, E. Guillo, S.M. Blair, G.M. Burt, T.I. Strasser, H. Brunner, O. Gehrke, J.E. Rodriguez-Seco, "Laboratory infrastructure driven key performance indicator development using the Smart Grid Architecture Model,", in Proceedings of 24th International Conference and Exhibition on Electricity Distribution, Glasgow, United Kingdom, 12-15 June 2017.

[7] Task Force C6.04, "Benchmark Systems for Network Integration of Renewable and Distributed Energy Resources," International Council on Large Electric Systems (CIGRE), Tech. Rep., 2014. [Online] Available: https://e-cigre.org/publication/575-benchmark-systems-for-network-integration-of-renewable-and-distributed-energy-resources

[8] E. Rikos, C. Caerts, M. Cabiati, M. Syed, G. Burt, "Adaptive fuzzy control for power-frequency characteristic regulation in high-RES power systems," Energies, vol. 10, no. 7, 2017.

[9] "P1 – Policy 1: Load-Frequency Control and Performance," European Network of Transmission System Operators for Electricity (ENTSO-E), Tech. Rep. [Online] Available: https://www.entsoe.eu/publications/system-operations-reports/operation-handbook/Pages/default.aspx

[10] "Balancing and Frequency Control," NERC, Tech. Rep., 2011. [Online] Available: http://www.nerc.com/docs/oc/rs/NERC%20Balancing%20and%20Frequency%20Control%20040520111.pdf

[11] "Guide to Ancillary Services in the National Electricity Market", AEMO, Tech. Rep., 2015. [Online] Available: https://www.aemo.com.au/-/media/Files/PDF/Guide-to-Ancillary-Services-in-the-National-Electricity-Market.ashx

[12] "System Operability Framework 2016", National Grid, Tech. Rep., 2016. [Online] Available: http://www2.nationalgrid.com/UK/Industry-information/Future-of-Energy/System-Operability-Framework/

[13] P. Dambrauskas, M. Syed, S. Blair, J. Irvine, I. Abdulhadi, G. Burt, D. Bondy, "Impact of realistic communications for fast-acting demand side management," in 24th International Conference and Exhibition on Electricity Distribution (CIRED), Glasgow, United Kingdom, June 12-15, 2017.

[14] M. H. Syed, E. Guillo-Sansano, S. M. Blair, A. J. Roscoe, G. M. Burt, "A Novel Decentralized Responsibilizing Primary Frequency Control," in IEEE Transactions on Power Systems, vol. PP, no. 99, pp. 1-3, 2018.

[15] A. M. Prostejovsky, M. Marinelli, M. Rezkalla, M. H. Syed, E. Guillo-Sansano, "Tuningless Load Frequency Control Through Active Engagement of Distributed Resources," in IEEE Transactions on Power Systems, vol. PP, no. 99, 2017.

[16] A. Latif, I. Ahmad, P. Palensky, W. Gawlik, "Zone based optimal reactive power dispatch in smart distribution network using distributed generation," in 2017 Workshop on Modeling and Simulation of Cyber-Physical Energy Systems (MSCPES), 2017.

8 Disclaimer

The ELECTRA project is co-funded by the European Commission under the 7th Framework Programme 2013.

The sole responsibility for the content of this publication lies with the authors. It does not necessarily reflect the opinion of the European Commission.

The European Commission is not responsible for any use that may be made of the information contained therein.

ANNEX: Integration and Validation Fact Sheets

“Balancing and Frequency Control”

Integration and Validation of

FCC — Frequency Containment Control

+

BRC — Balance Restoration Control

Scenario

Evaluation of FCC+BRC controls effectiveness to maintain network frequency stability. The objective is to integrate and validate the correct operation of the FCC+BRC approach in presence of a step load increase event and a frequency threshold error of 1Hz. This will be accomplished through implementing in DigSilent simulation environment a modified CIGRE MV grid.

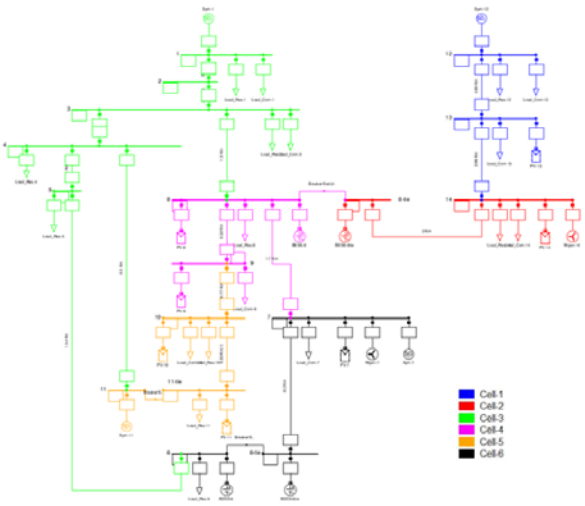

Fig. 1. Web of cell representation

Research Questions

- Are the developed FCC+BRC controls effective to guarantee an adequate network frequency stability?
- How the Secondary Control presence in the cell improves the frequency response to instability events?

Operational Parameters

Software simulation based on DigSILENT Powerfactory:

- 6 cells
- RES (PV)
- Non controllable/controllable loads
- DG (Batteries)

Key Performance Indicators

Technical KPI's	Definition
FCC performance	Maximum frequency deviation after a disturbance

ELECTRA IRP is funded from the European Union Seventh Framework Programme (*FP7/2007-2013*) under *grant agreement* n° 609687

www.electrairp.eu

Simulation

The grid model is based on a modified CIGRÉ EUROPEAN MV DISTRIBUTION NETWORK consisting of six cells. Each cells is composed of several devices such as: load, PV, Synchronous machines, energy storage systems. Based on the ELECTRA procedures, the Merit Order Collection (MOC), Merit Order Decision(MOD) and DDSD (Device droop slope determination) matrices are calculated. For each devices within the cell (load, PV, Synchronous machines, storages), new model is defined to adapt frequency response to the DDSD matrix (Device droop slope). The developed controllers are based on the reference control shown in figure below.

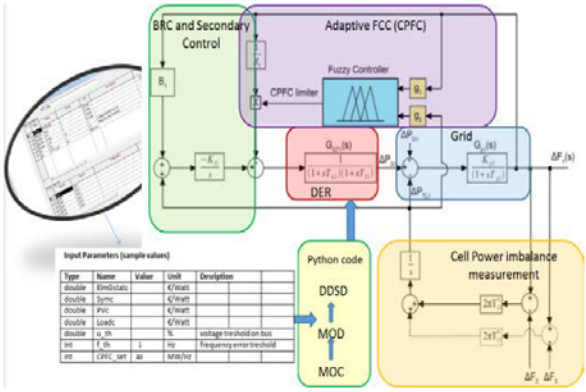

Fig. 2. Reference Control

Some examples of control frames and simulation outcomes are shown in Figures 3-5.

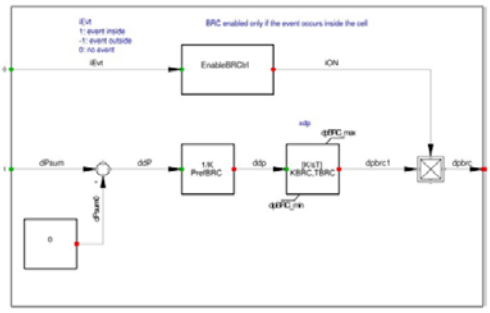

Fig. 3. BRC Control

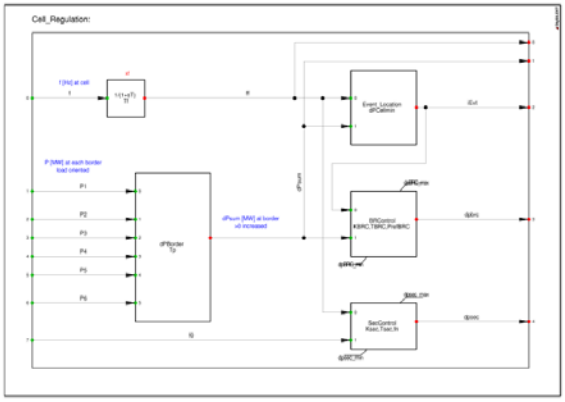

Fig. 4. Cell Control

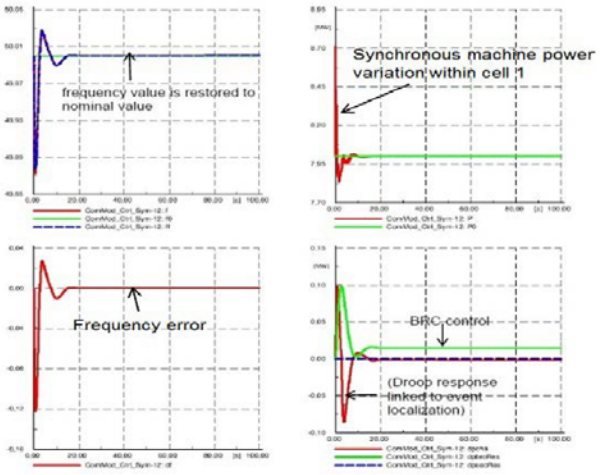

Fig.5. FCC+BRC and resources response after a disturbance

Conclusions

The FCC+BRC controls, together with Secondary Control, are able to restore frequency stability at the cell level using only cell's resources. Therefore the instability within the cell doesn't affect stability of the closer cells. Moreover with the Secondary control presence the system frequency response is better and the frequency is restored to the nominal value very quickly (about 15 seconds).

ELECTRA IRP is funded from the European Union Seventh Framework Programme (*FP7/2007-2013*) under *grant agreement* n° 609687

Integration and Validation of

FCC — Frequency Containment Control

BRC — Balance Restoration Control

Scenario

Validation of the FCC and BRC functions in the Web-of-Cells concept, developed in ELECTRA. In order to evaluate the effectiveness and the advantages that these functions can bring for system operation, they were compared with the traditional functions of the frequency control that are used nowadays. It is simulated a disturbance (increase of load) in all scenarios. The reference model chosen to run the simulations was the MV grid proposed by CIGRE (Fig, 1) and it was implemented in Matlab/Simulink.

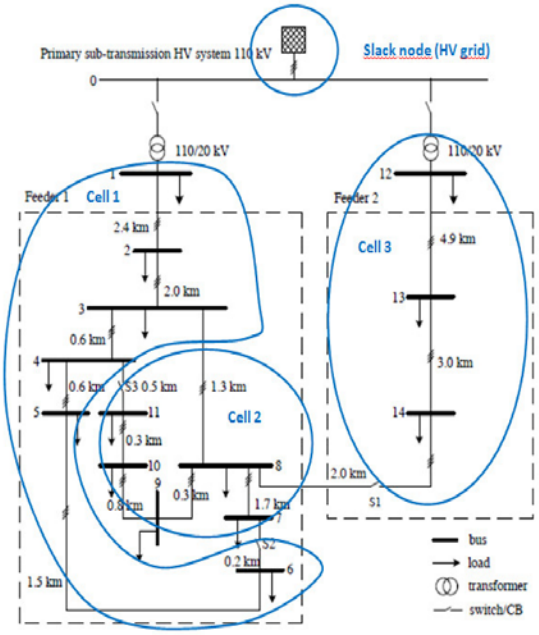

Fig. 1. Test grid (CIGRE MV)

Research Questions

- Are distributed DER capable of providing fast dynamic power injections to improve dynamic frequency behavior?
- How is the interaction between FCC and BRC?
- What is a reasonable dimensioning of the resources for FCC and BRC?
- With fast communication in the future, is BRC fast enough to replace FCC?

Operational Parameters

- 3 cells:
  - Cell 1: PVs, a battery, a wind turbine and loads
  - Cell 2: PVs, FCs, a battery, a CHP plant, a wind turbine and loads
  - Cell 3: loads
- 3 tie-lines

Key Performance Indicators

WoC Integration KPI's	Technical KPI's
Losses reduction	Percentage of reduction in power losses from activated reserves.
Efficiency of FCC	Time required for bringing back freq. dev. to an acceptable level
Efficiency of BRC	Time required for the restoration reserve capacity in the cells

ELECTRA IRP is funded from the European Union Seventh Framework Programme (FP7/2007-2013) under grant agreement n° 609687

www.electrairp.eu

Simulation

The electrical network was implemented using Matlab Simulink. To test the new functions, several scenarios were created in order to compare them with the solutions available nowadays: the primary frequency control (FCR) and the secondary frequency control (AGC). The scenarios created are the following:

- Case 0 (FCR+AGC) – this is the base case with the frequency control functionalities used nowadays. The primary frequency control uses a droop control in each device in order to calculate ts output power considering the frequency variations. The secondary frequency control uses an AGC to reestablish the frequency to the nominal value.
- Case 1 (FCC+AGC) – in this scenario, the FCR is replaced by the FCC, but a common AGC is considered for the secondary frequency control.
- Case 2 (FCC+BRC) – in this scenario, both the FCR and the AGC are replaced by the new functions developed, the FCC and the BRC.

Conclusions

It was possible to conclude that with the BRC installed, the frequency returned to the nominal value much faster than with the traditional approach (Fig. 3). The BRC induced a substantial reduction in the losses of the system (Fig. 4) and had a better primary frequency control performance. The implementation of the FCC induced a better performance in terms of balance restoration effectivity. However, with the traditional FCR, the performance was better in terms of the primary frequency control since all the cells contribute continuously for the disturbance mitigation.

Results

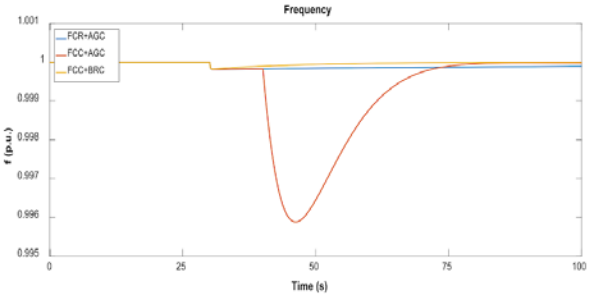

Fig. 2. Frequency of the system (100s)

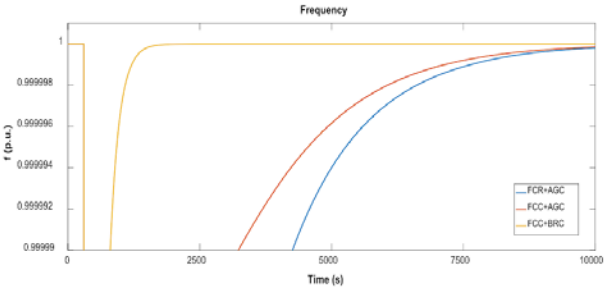

Fig. 3. Frequency of the system (10000s)

Tab. 1. Time necessary to reach nominal value

	TIME (SECONDS)
FCR+AGC	658.7
FCC+AGC	603.3
FCC+BRC	105.6

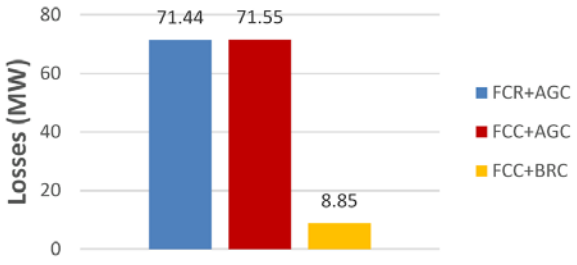

Fig. 4. Total losses

ELECTRA IRP is funded from the European Union Seventh Framework Programme (FP7/2007-2013) under grant agreement n° 609687

Integration and Validation of

FCC — Frequency Containment Control

BRC — Balance Restoration Control

Scenario

The RSE microgrid laboratory *DER Test Facility (DERTF)* is inserted in the urban distribution MV grid. The scenario assumes the presence in each cell of the BRC and FCC control functionalities. For this experiment the DERTF was configured as a islanded power system with three physical LV cells.

The objective of the tests is to assess the BRC and FCC control functionalities effectively:

- Correct inter-cell imbalances
- Manage a loss of 1 cell reserve
- Correct the grid frequency error

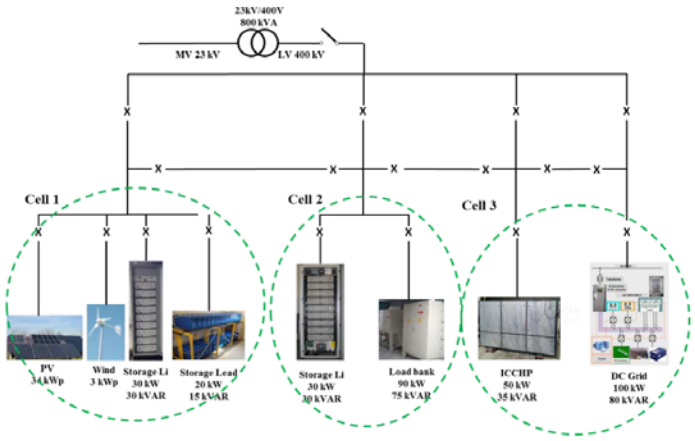

Fig. 1 - RSE DERTF lab

Research Questions

- Evaluate BRC control effectivity without a BSC participation.
- Investigate possible conflict between BRC and Adaptive FCC.

Operational Parameters

- the laboratory infrastructure at RSE allows hardware simulation of multiple interacting cells
- 3 cells
- 3 tie-lines
- >50% converter coupled generation
- 100% flexible demand

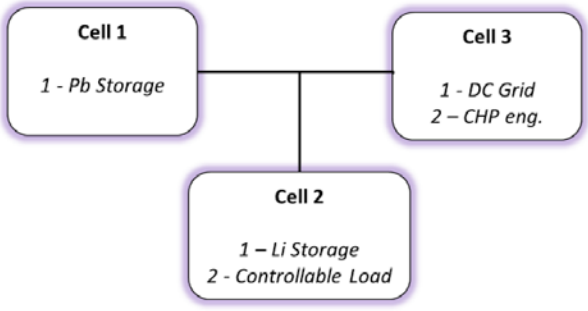

Fig. 2 - WoC implementation in the RSE DERTF

Key Performance Indicators

WoC Integration KPI's	Technical KPI
Efficient use of BRC	Tie lines power errors less than max. acceptable error
System stability	FCC performances and interaction with BRC

ELECTRA IRP is funded from the European Union Seventh Framework Programme (*FP7/2007-2013*) under *grant agreement* n° 609687

www.electrairp.eu

Test setup

RSE DERTF was configured as a WoC of 3 physical cells, each one connected with the others by a tie-line. From starting condition (with nominal frequency and power at tie lines regulated as scheduled) a power disturbance in a cell has been made. According to droop controls (FCC) and BRC cells controls, frequency variation will be compensated and power at tie lines will be restored. FCC control are directly implemented in the inverter firmware (frequency/power droop). Droop curve slope can also be modified in real time, this is needed in order to operate in Adaptive FCC (A-FCC) mode. Different tests with BRC enabled or disabled at different cells were performed.

Results

The test in the figures shows the behavior of the cells with BRC enabled and A-FCC disabled (with 5% constant droop), from 0 to 600 sec. and A-FCC enabled, from 600 sec. Cell 1 was configured with only the Pb storage active.

The BRC tie-line power flow set-points were: cell 1: 0 kW, for cell 2 : -30 kW and for cell 3: +30 kW. The disturbances were a load step of +/-15 kW followed by a CHP power step of +/- 15 kW.

Figure 3 shows the power disturbances and the grid frequency, fine controlled with no steady state error. A-FCC mode contains better the grid frequency.

Figure 4 shows the tie-lines power, well controlled by BRC.

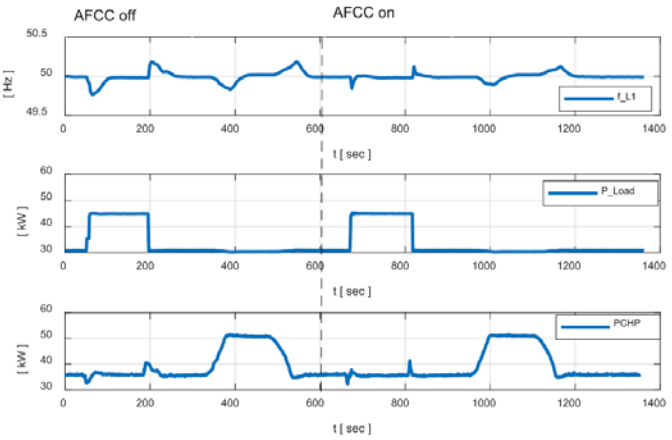

Fig. 3 - *BRC with Adaptive FCC enabled and disabled*
Frequency, load step and CHP generation step.

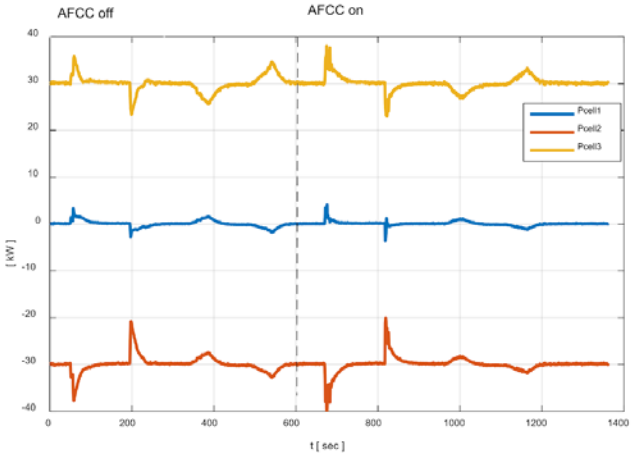

Fig. 4 - BRC with Adaptive FCC enabled and disabled
Tie-lines Power Flows

Conclusions

Against of load and generation power disturbances the grid frequency was recovered to the nominal value with low under or overshoots. The test confirmed the good performances of the A-FCC that better contains the frequency variation.

ELECTRA IRP is funded from the European Union Seventh Framework Programme (*FP7/2007-2013*) under *grant agreement* n° 609687

Integration and Validation of

Technical University of Denmark

FCC — Frequency Containment Control

BRC — Balance Restoration Control

Scenario

The developed BRC called *Direct Load Frequency Control* (DLFC, Fig. 1) is a fast, simple and tuningless secondary control method that effectively harnesses the opportunities provided by the Web-of-Cells (WoC) concept, in particular high observability and active communication between cells [1,2]. In this scenario, the DLFC's theoretical advantages are validated: In simulations for different cell configurations, communication delays, ramp limits, and inertial constants; By experimental testing with off-the-shelf DERs and online topology changes in SYSLAB.

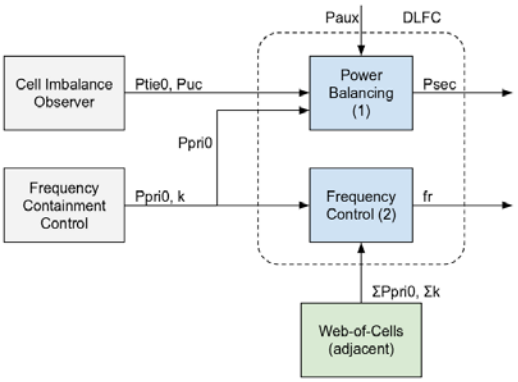

Fig. 1: Signal flow for the BRC/FCC parts of the DLFC.

Research Questions

- How can high observability and active communication be used for designing an adaptive LFC?
- How does performance of the resulting DLFC compare to state-of-the-art Automatic Generation Control (AGC)?
- What are the stability margins of the DLFC for variations of the system's inertia?
- How do non-linear constraints such as generator slew rates impact the DLFC?

Key Performance Indicators

Technical KPI's/ Criterion	Definition
Balance Restoration control effectivity (TCR01)	Trumpet-shaped curves were obtained by monitoring the system frequency over years. When the frequency stays within these curves, the control performance is satisfactory.
Adaptation to topology change (TCR09)	Time until system finds a new steady state after disconnection of a tie-line (assuming enough capacity on the other tie-lines).
Effective negotiation between cells (TCR16)	Lab-based validation of System stability in Distributed LFC in view of uncertain device parameters and delays

Operational Parameters

Software simulations and experimental verification in SYSLAB (Fig. 2, 4) using

- 3 cells (meshed/radial)
- RES (wind, PV)
- Battery
- Diesel generator
- Flexible demand
- Electric vehicles

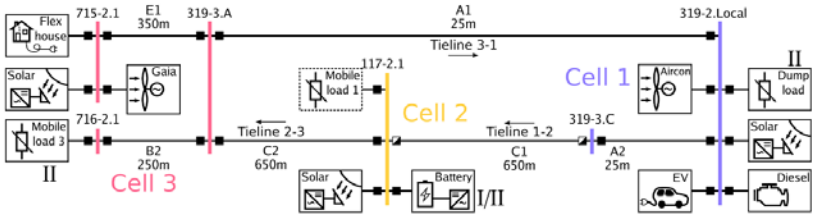

Fig. 2: Simulation and experimental topology.

[1] A. M. Prostejovsky, M. Marinelli, M. Rezkalla, M. H. Syed and E. Guillo-Sansano, "Tuningless Load Frequency Control Through Active Engagement of Distributed Resources," in IEEE Transactions on Power Systems, vol. PP, no. 99, pp. 1-1.
[2] A. M. Prostejovsky and M. Marinelli, "Comparison between AGC and a tuningless LFC approach based on direct observation of DERs," 2017 52nd International Universities Power Engineering Conference (UPEC), HERAKLION, Crete, Greece, 2017, pp. 1-6.

ELECTRA IRP is funded from the European Union Seventh Framework Programme (*FP7/2007-2013*) under *grant agreement* n° 609687

www.electrairp.eu

Integration and Validation of

FCC — Frequency Containment Control

BRC — Balance Restoration Control

Methodology

The DLFC consists of two parts: i) Secondary power balancing through direct observation of generation and consumption; and ii) Frequency Control through systematic adjustments of the primary resources' reference frequency. The approach is Lyapunov-stable for a wide range of parameters, and supports FCC methods.

Simulation

MATLAB/Simulink was used to design a simplified AC model, comprising both the electrical system with various non-linearities (ramp limitations, full line power flow equations), as well as the communication channels subject to package drop and delays. Variations of the cell inertial constants, ramp rates, delays, and disturbances were investigated (see Fig. 3).

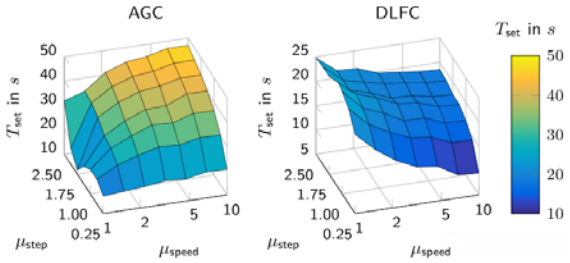

Fig. 3: Performance AGC vs. DLFC (lower is better).

Conclusions

The DLFC performed satisfactorily in all investigated scenarios, with the average frequency remaining exactly at 50 Hz in the investigated period from 150 s onwards, as shown in Fig. 5.

- TCR01 is satisfied as the DLFC's response is exponentially bounded and well within ENTSO-E's requirements [1].
- Only neighbourhood communication is carried out, which renders the solution nearly scale-invariant, satisfying TCR05.
- Lyapunov-stability entails tolerance to topology changes, answering TCR09.

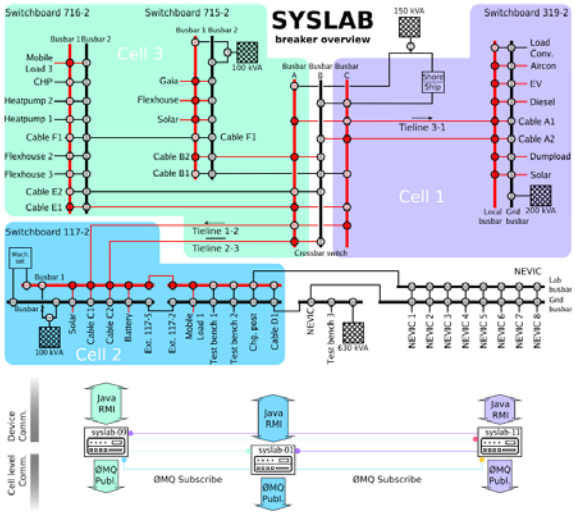

Fig. 4: SYSLAB Laboratory setup – Electric and ICT.

Laboratory Experiments

The practical validation of the DLFC was carried out in SYSLAB, an experimental low-voltage grid consisting of 3 km of cables, a wide range of components in arbitrary layouts with a distributed SCADA system (see Fig. 2, 4). The total realisable production and consumption are 110 kW and 190 kW, respectively. Each cell had its own DLFC controller running on geographically separated computer nodes performing inter-cell and device communication. A 60 kVA Diesel generator provided real inertia to the grid. The system was exposed to various discrete and continuous disturbances and topology changes.

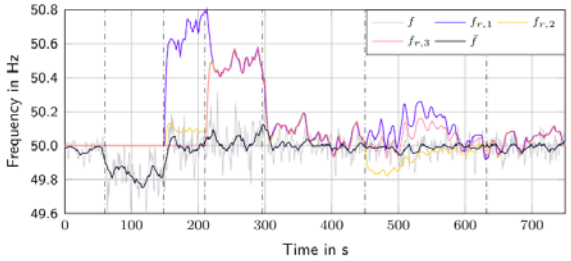

Fig. 5: Resulting system and reference frequencies.

ELECTRA IRP is funded from the European Union Seventh Framework Programme (FP7/2007-2013) under grant agreement n° 609687

www.electrairp.eu

Integration and Validation of

FCC — Frequency Containment Control

BRC — Balance Restoration Control

University of Strathclyde Glasgow

Scenario

There is an emerging need to prioritize remedial frequency control measures closer to the source of an imbalance event, which is referred to by the term "responsibilization". This approach, driven by the Web-of-Cells (WoC) concept within ELECTRA, enables a new paradigm of increased decentralization and distributed control. In the work undertaken by the University of Strathclyde, the performance of the responsibilizing controls developed are evaluated for the GB grid (as shown in Fig. 1). A number of occurrences of ~1GW generation loss have been experienced by the GB grid within the last year, and therefore this has been chosen as the reference event. Controls are validated by simulations, small-signal analysis and laboratory experiments.

Research Questions

- Can the location of an imbalance event be rapidly identified based on local measurements?
- Can responsibilization be introduced within the operating timescale of primary frequency control?
- Can responsibilization within secondary frequency control be further improved to support faster restoration?
- Can BRC activate fast enough (utilizing local flexibility) to limit global activations by FCC?
- Can BRC ensure stable operation at increased response speeds?

Key Performance Indicators

Technical KPI's/ Criteria	Definition
Enhanced responsibilization	Reduced remote boundary flow changes and increased local reserve activation in response to event (compared to BAU).
Balance restoration control effectivity	When the frequency stays within the trumpet curve, as defined by ENTSO-E, the control performance is satisfactory.
Time to frequency restoration	Time it takes for frequency to restore to its nominal value after occurrence of an event.
Maximum frequency deviation	Maximum deviation of frequency after an event.

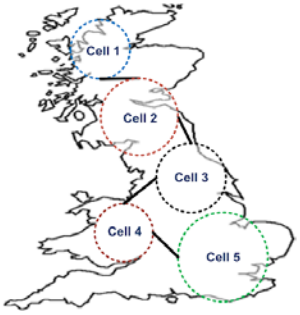

Fig. 1. WoC representation of GB grid

Responsibilizing FCC

ELECTRA proposes a novel decentralized FCC, where responsibilization is achieved by means of measuring the transient phase offset (TPO) within each of the Cells [1]. The proposed approach is fully decentralized as it relies on local measurement only and requires no form of communication.

Upon occurrence of an event, the TPO is larger when measured geographically closer to the event than further away as shown in Fig. 2 (a) and (b). A TPO-based droop curve designed to achieve responsibilization in FCC is presented in Fig. 2 (c).

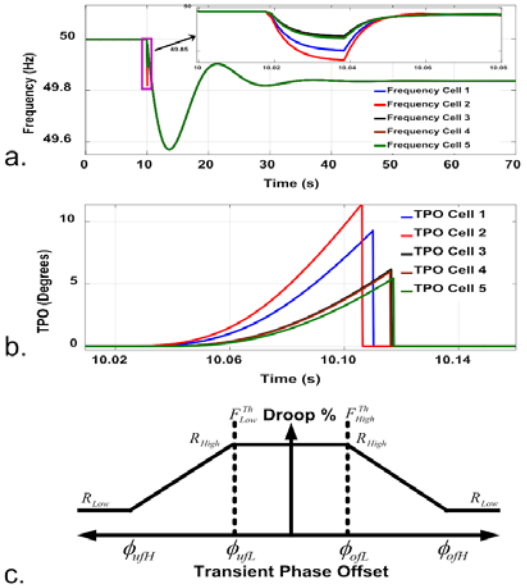

Fig. 2. Reference event in cell 2: (a) frequency (b) TPO and (c) Proposed TPO-based droop curve

ELECTRA IRP is funded from the European Union Seventh Framework Programme (FP7/2007-2013) under grant agreement n° 609687

www.electrairp.eu

Simulation Results

For a 1 GW loss of generation, the system frequency response is shown in Fig. 3 (a) to be stable and between fixed droop response of R_{Low} and R_{High}. The FCC power contribution of each cell is presented in Fig. 3 (b). The solid line represents the system response with fixed droop and the dotted line represents system response with the proposed control. Cell 2 increases its contribution to the event, demonstrating greater responsibilization.

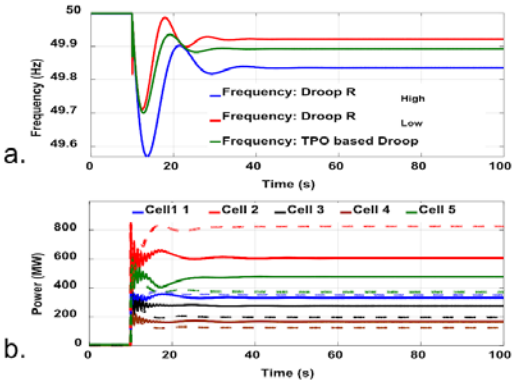

Fig. 3. Reference event in cell 2: (a) frequency response and (b) cells power output.

Balance Restoration Control

The developed BRC called *Enhanced Load Frequency Control* (ELFC) framework is presented in Fig. 4. The framework incorporates a fast acting balance control loop (BCL), in addition to the primary and secondary control loop. The key features are:

- Fast and autonomous identification of disturbance location, ensuring unilateral activation of reserves allowing for faster response speeds.
- Use of cell power imbalance over conventionally utilized area control error (ACE) as control input.
- Employs only fast acting demand side resources, eliminating any restriction on speed of response due to ramp-rate constraints.

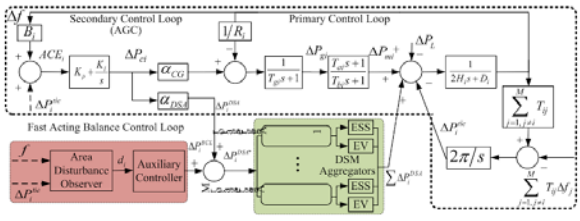

Fig. 4. BRC- Enhanced Load Frequency Control

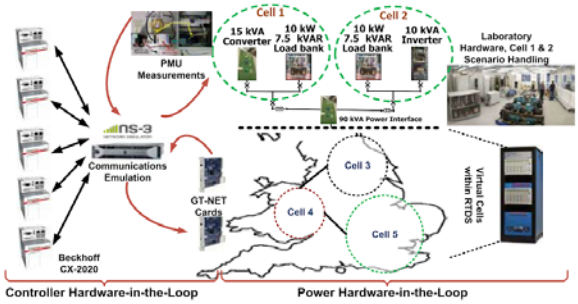

Fig. 5. C-HiL and P-HiL validation setup

Experimental Validation

The validation setup presented in Fig. 5 has been used to answer the key research questions as follows:

- The location of an imbalance event can be determined within 200 ms, enabling effective responsibilization.
- Location enables the fast-acting operation of restoration control at the timescale of containment control, allowing BRC to:
  - contribute to objective of containment
  - restore frequency faster (as shown in Fig. 6).

Validation is enabled by the state-of-the-art Dynamic Power Systems Lab at the University of Strathclyde [2].

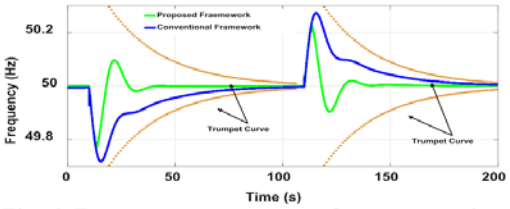

Fig. 6. Frequency response to reference event in cell 2

Conclusions

To deliver the Web-of Cells concept and the promise of decentralised future power systems, a new responsibilizing frequency control approach – i.e. targeting responses closer to the source of imbalance – has been proven at Technology Readiness Level (TRL) 5. This advance enables faster-acting ancillary services to assist in addressing the problematic decline in system inertia and to leverage the wealth of flexible resources in future low-carbon grids.

[1] Syed, MH, Guillo-Sansano, E, Blair, SM, Roscoe, AJ & Burt, GM 2018, 'A novel decentralized responsibilizing primary frequency control' *IEEE Transactions on Power Systems*. DOI: 10.1109/TPWRS.2018.2799483

[2] Dynamic Power Systems Laboratory, University of Strathclyde: https://www.ulabequipment.com/facility/dynamicpowersystems

ELECTRA IRP is funded from the European Union Seventh Framework Programme (*FP7/2007-2013*) under *grant agreement* n° 609687

Modelling and Simulation of

FCC — Frequency Containment Control

BRC — Balance Restoration Control

BSC — Balance Steering Control

University of Strathclyde Glasgow

Test Description

The ELECTRA Web-of-Cells concept provides a radical new approach to frequency and voltage control for future power system operation. There are exciting opportunities for advanced, decentralised control in a power system dominated by very large numbers of small, fast-acting renewable energy sources, including energy storage. The ELECTRA project introduces Frequency Containment Control (FCC), Balance Restoration Control (BRC) and Balance Steering Control (BSC) as novel methods to replace the traditional Primary, Secondary and Tertiary frequency control of the present day. The FCC and BRC controllers are tested together in a 5-cell system under imbalance scenarios, and their successful implementation is tested under a BSC (imbalance netting) scenario.

Test System

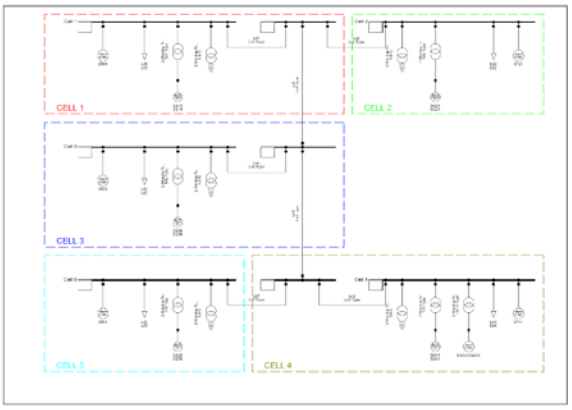

Fig. 1. 5-cell GB test system.

Each cell in the test system contains transmission-level load and generation and a radial LV distribution system. Each cell also has autonomous responsibility for control of primary and secondary active power reserve activation through FCC and BRC respectively. The cell controllers integrate FCC and BRC, and one cell controller is allocated to each of the cells in the system. As well as the transmission-level generation and load, each of the five cells also contains an LV network based on the University of Strathclyde Power Networks Demonstration Centre (PNDC) in order to show the successful use of the cell controllers at differing voltage levels within the same network and prove the ELECTRA operational requirement that a single cell may contain these different voltage levels.

Research Questions

- Can the location of an imbalance event be rapidly identified based on local measurements?
- Does the use of FCC and BRC successfully reduce non-local activation of active power reserves?
- Does the use of fast-acting BRC reserves reduce the strain on generator primary response (FCC)?

Key Performance Indicators

Technical KPI's/ Criteria	Definition
Enhanced responsibilization	Reduced remote boundary flow changes and increased local reserve activation in response to event (compared to BAU).
Balance restoration control effectivity	When the frequency stays within the trumpet curve, as defined by ENTSO-E, the control performance is satisfactory.
Time to frequency restoration	Time it takes for frequency to restore to its nominal value after occurrence of an event.
Maximum frequency deviation	Maximum deviation of frequency after an event.

FCC and BRC

The key innovation is the ability to "solve local problems locally", by providing maximum balancing power from the "cell" with the imbalance, reducing distant reserve actions. In **FCC** this is done by tailoring the droop response depending on whether the cell in question is the problem cell. Droop response is increased in the problem cell and reduced otherwise.

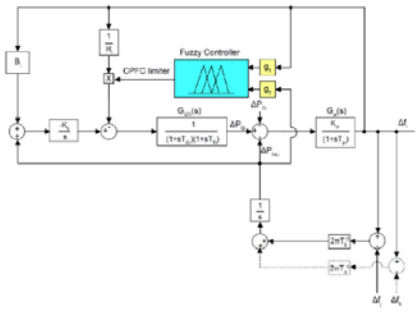

Fig. 2. Frequency Containment Control.

ELECTRA IRP is funded from the European Union Seventh Framework Programme (*FP7/2007-2013*) under *grant agreement* n° 609687

www.electrairp.eu

In **BRC**, the controller uses the cell power imbalance and network frequency measurements to decide whether the cell in question is responsible for the imbalance. If so, fast-acting secondary frequency reserves will only be activated in that cell and not in others. This approach achieves the ELECTRA objective to "solve local problems locally".

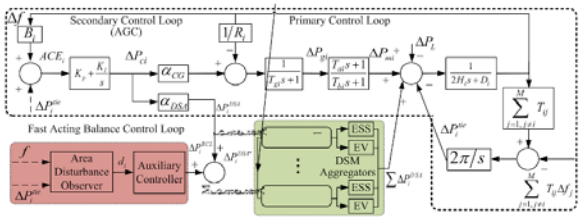

Fig. 3. BRC- Enhanced Load Frequency Control.

Simulation Results

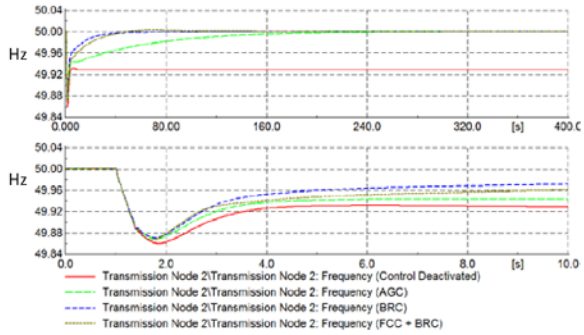

Fig. 4. FCC/BRC impact on frequency response.

Fig. 4 shows the long- and short-term frequency response to an imbalance event in Cell 2. It can be seen that the replacement of traditional AGC with BRC allows a much quicker recovery to nominal frequency.

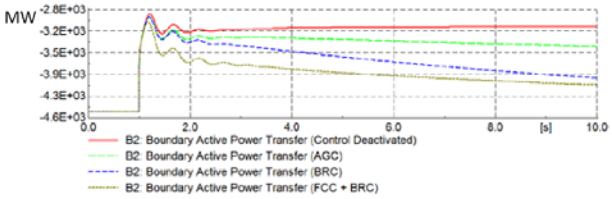

Fig. 5. Controller impact on boundary flows.

Fig. 5 shows the immediate boundary power flow of Cell 2, showing successful localisation of reserves as a result of implementing FCC and BRC controllers.

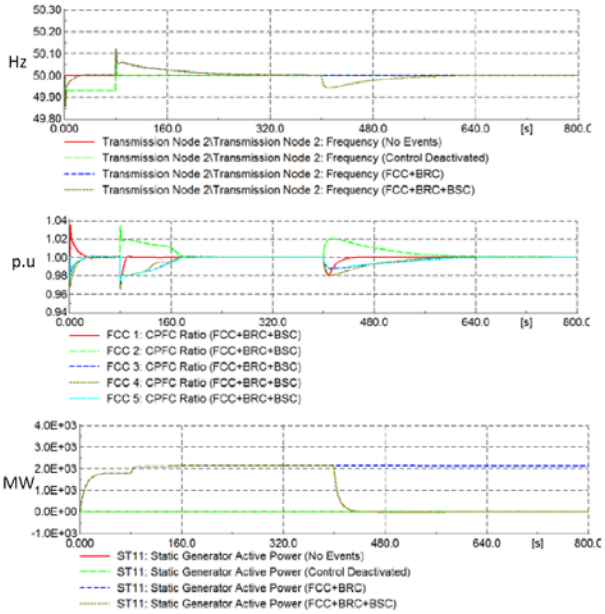

Fig. 6. FCC and BRC are stable for BSC scenario.

The stable performance of the FCC and BRC controllers throughout a BSC scenario are shown in the traces in Fig. 6. Two equal-but-opposite imbalance events occur in neighbouring cells, and BSC (imbalance netting) occurs at 400 seconds. The frequency of the system returns to nominal and remains stable. The FCC output response remains stable, and the BRC reserves are returned to their pre-event levels, as expected. This shows that there is no control conflict between FCC, BRC and BSC action.

Conclusions

The Web-of-Cells concept and associated control systems are shown to successfully localise the reserve response by identifying whether the imbalance originates in a given cell, and if so tailoring droop settings (FCC) and activating fast-acting reserves (BRC) in that cell only. These actions result in fewer and smaller reserve activation in non-problem cells and lower transmission boundary flows immediately following an event. The FCC and BRC operation are not impeded by, nor do they impede the operation of, imbalance netting through BSC control.

ELECTRA IRP is funded from the European Union Seventh Framework Programme (*FP7/2007-2013*) under *grant agreement* n° 609687

Integration and Validation of

FCC — Frequency Containment Control

BRC — Balance Restoration Control

BSC — Balance Steering Control

Scenario

Implementation of corrective BSC control in a system of 4 (simulation) or 2 (experiment) cells taking advantage of imbalance netting. The scenario presumes the presence of a BRC and an Adaptive FCC control loop for each cell. The objective of the tests is to show that the corrective mode of BSC is capable of handling on-going imbalances and, efficiently adjust the tie-line set points in order to deactivate BRC reserves .

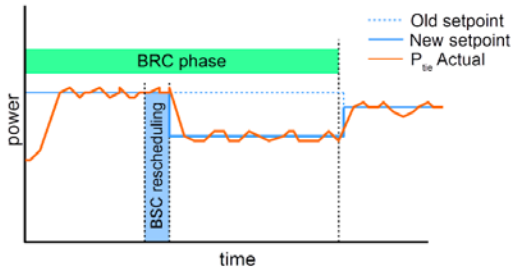

Fig. 1. Corrective tie-line setpoint adjustment

Research Questions

- Is the BSC functions able to negotiate an acceptable (correct) amount of scheduled power adjustment?
- Is the short-term use of BRC reserves reduced benefiting from imbalance netting?
- Is stability always ensured in terms of steady-state and dynamic frequency deviations?
- Is the set-point adjustment always within the tie-line operating limits?

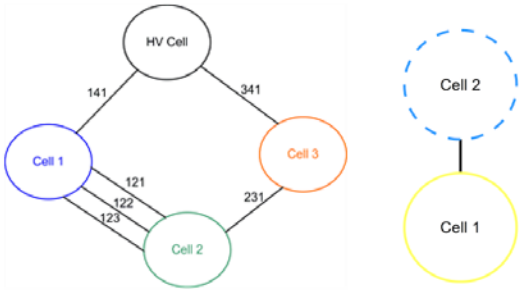

Fig. 2. web of cells representation on the CRES' lab: a) simulation and b) experiment

Operational Parameters

- 4 (sim.) or 2 (exp.) cells
- 6 (sim.) or 1 (exp.) tie-lines
- Photovoltaics (sim. and exp.), Wind (sim.)
- 3 (sim.) or 2 (exp.) storage units
- FCC flexibility in simulation is provided by various resources (RES, storage etc.)
- BRC flexibility by storage units

Key Performance Indicators

Technical KPIs	Target metrics
Effective negotiation between cells	Cell Setpoint Adjusting output signals
Imbalance netting exploitation	Active power of BRC providing units
System stability	Frequency
Tie-lines operating limits	Active power of tie-lines

ELECTRA IRP is funded from the European Union Seventh Framework Programme (FP7/2007-2013) under grant agreement n° 609687

www.electrairp.eu

Validation Setup

Simulation: Modified CIGRE MV grid in a meshed topology modelled using MATLAB/Simulink. Cells 1-3 are equipped with the complete set of controllers. Scenarios implemented include equal or unequal imbalances in two cells, violation of one tie-lines capacity and communication delay.

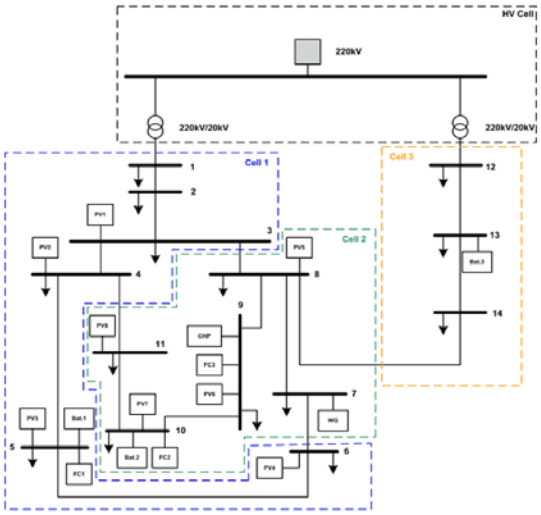

Fig. 3. Simulation setup consisting of 4 cells

Experiment: CRES Microgrid consisting of two cells. Scenario implemented includes unequal imbalances

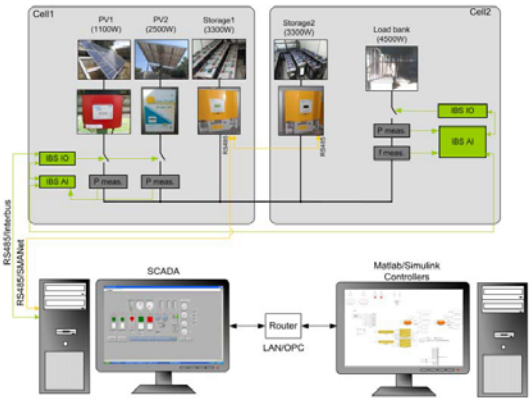

Fig. 4. Experimental setup consisting of 2 cells

Achieved Results

Both in the simulation and experimental validation the controllers achieve the deactivation BRC reserves while frequency stability is always maintained.

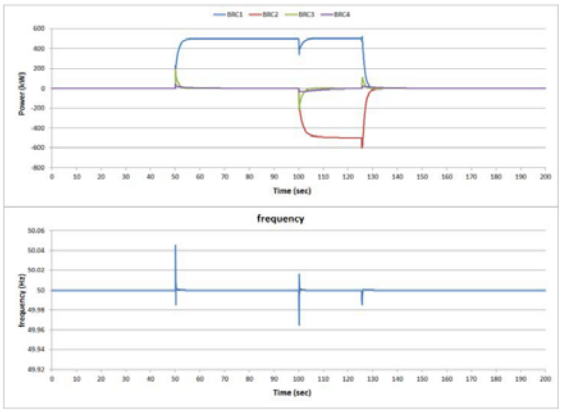

Fig. 5. Simulation results

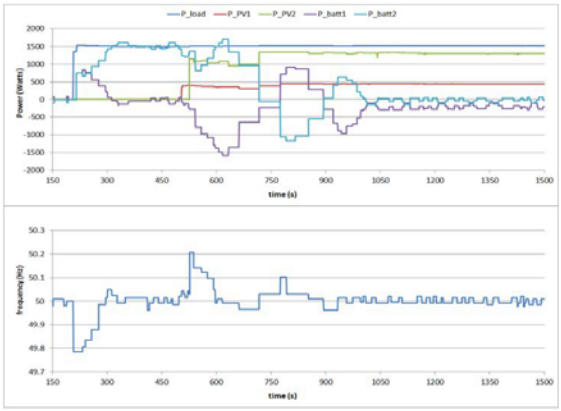

Fig. 6. Experimental results

Conclusions

BSC achieves the exploitation of imbalance netting towards minimising the use of BRC reserves. The whole process ensures the system stability in terms of frequency and tie-line power flow deviations.

ELECTRA IRP is funded from the European Union Seventh Framework Programme (*FP7/2007-2013*) under *grant agreement* n° 609687

Integration and Validation of

IRPC — Inertial Response Power Controller

FCC — Frequency Containment Control

Scenario

Implementation of IRPC and FCC in real time Hardware-in-the-Loop testing environment. The cells will be simulated in RT on OPAL RT, the frequency controller will be modelled on a Triphase rapid prototyping inverter platform. An imbalance will be simulated on one of the cells and the controller response will be monitored. The system will be based on IEEE 9 Bus system for reference.

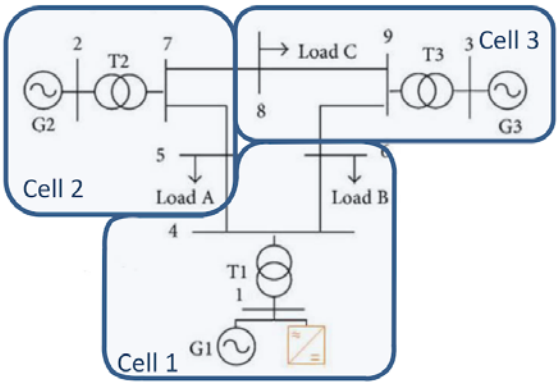

Fig. 1. IEEE 9-Bus system and cells

Research Questions

- How to define a criteria for analysing the controller response?
- How to evaluate the interaction between the WoC frequency control and other automated frequency controllers present in the cells?
- Will IRPC and FCC interact or conflict with each other since high inertia values slow down the power system?
- How to determine the maximum inertia set point in order to size IRPC and FCC reserves?

Fig. 2. PHIL-Set-up

Operational Parameters

- 3 cells representation on RTDS
- Flexible demand
- RES penetration>50%
- Opal RT
- Triphase RPT
- IEEE 9 Bus Reference System

Key Performance Indicators

WoC Integration KPI's	Technical KPI's
Overall system stability: frequency, voltage	voltage, ROCOF, frequency nadir
Available resources limitations impact on system behaviour	Controller response
Conflicting behaviour of FCC and IRPC	

ELECTRA IRP is funded from the European Union Seventh Framework Programme (FP7/2007-2013) under grant agreement n° 609687

www.electrairp.eu

Validation Setup

The Cigre MV network served as the reference network:

- Divided into three interconnected cells
- Additional controllers at all decentralised energy resources for FCC, adaptive FCC
- Additional IRPC controllers for storages and wind turbine
- Load step as disturbance

Following Scenarios:

- Combinations of control functions
- Reserves limitation due to operating point
- Different inertia constants

Achieved Results

- IRPC controllers improve the overall system stability, see Fig.3.
- Adaptive FCC causes the activation of local resources and herewith an insignificant frequency deterioration compared to the use of conventional FCC.
- Also, the voltage variations due to the controllers are relatively small.
- IRPC and FCC are not conflicting if implemented in a common device since the time of peak activation is different.
- The amount of inertia which needs to be provided must be determined under consideration of storage capacity, aging effects of batteries and mechanical load of wind turbines, see Fig. 4.

Conclusion

The combination of IRPC and FCC ensures system's stability, improves the local activation of FCC reserves and has small influence on the grid's voltage.

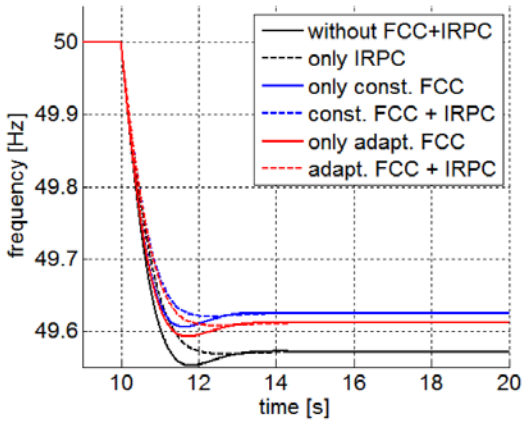

Fig. 3. Rate of change of frequency (RoCoF) is reduced by IRPC devices, small frequency deterioration due to A-FCC.

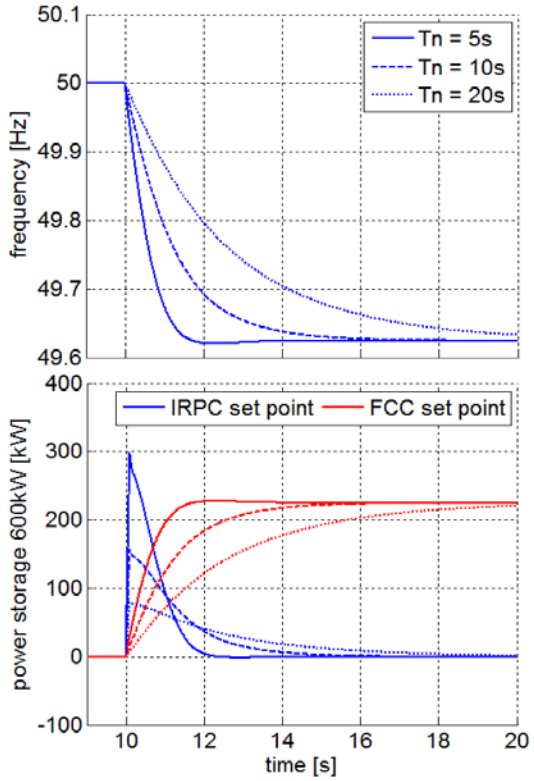

Fig. 4. The bigger the inertia time constant, the less the IRPC power peak and the less the overall energy from IRPC and FCC to balance the disturbance.

ELECTRA IRP is funded from the European Union Seventh Framework Programme (FP7/2007-2013) under grant agreement n° 609687

Integration and Validation of

IRPC — Inertial Response Power Controller

FCC — Frequency Containment Control

Scenario

Implementation of IRPC in combination with two FCC versions: fixed-droop and Adaptive-FCC. The tests are in a simulation environment on a test grid consisting of 3 MV and 1 HV cells. The objective of the tests is to evaluate the system stability as well as to assess the impact of the controllers on the voltage variations and conflicting use of output power.

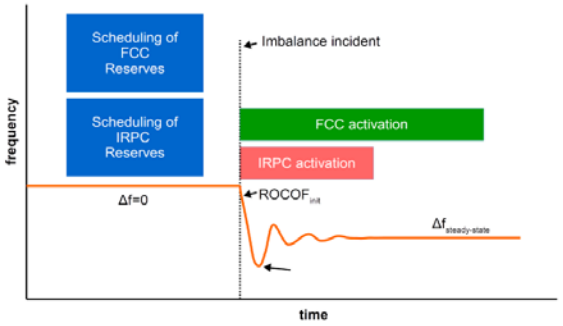

Fig. 1. Combined IRPC and FCC response

Research Questions

- Is the frequency stability of the system ensured?
- What are the values of specific frequency metrics such as the initial ROCOF maximum frequency deviation as well as steady-state frequency?
- What is the influence on voltage?
- Does the control lead to conflicts of power use?

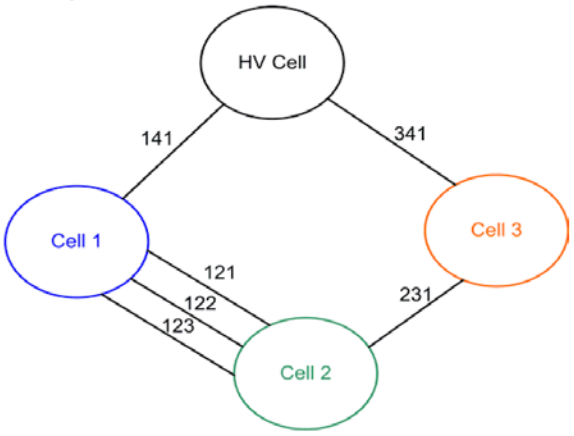

Fig. 2. web of cells representation

Operational Parameters

- 3 MV and 1 HV cells
- Use of detailed grid models for the 3 MV cells.
- One synchronous generator in the HV cell
- 100% flexibility of generation
- Load disturbances are step-changes of power

Key Performance Indicators

Technical KPIs	Target metrics
Overall frequency stability	steady state frequency deviation, frequency nadir, ROCOF
Conflicting use of reserves	Active power of IRPC/FCC reserves
Impact on voltage	RMS voltage at each DER's connection point
Maximum ROCOF/frequency deviation	ROCOF and frequency nadir

ELECTRA IRP is funded from the European Union Seventh Framework Programme (FP7/2007-2013) under grant agreement n° 609687

www.electrairp.eu

Validation Setup

The setup involves the modified CIGRE MV grid in a meshed topology modelled using MATLAB/Simulink. Cells 1-3 are equipped with the complete set of controllers. Scenarios implemented include various combinations of IRPC with fixed-droop FCC as well as IRPC together with A-FCC. The disturbances include abrupt (step) increase/decrease of loads.

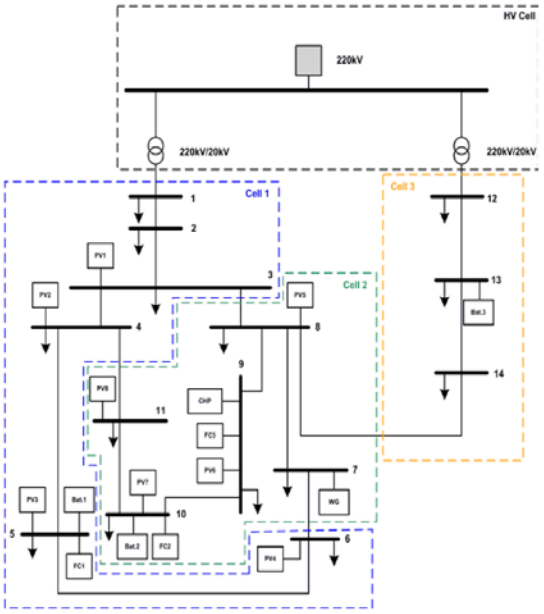

Fig. 3. Simulation setup consisting of 4 cells

Achieved Results

Simulation tests of the above system under different disturbances showed that the system stability is improves with the introduction of IRPC. Furthermore, the presence of A-FCC causes an insignificant frequency deterioration. In this case, the Cell Power-Frequency Characteristic (CPFC) changes based on the correct location identification of the imbalance. This way, mainly local activation of FCC reserves is achieved with rather insignificant frequency deterioration. Also, the voltage variations due to the controllers are relatively small. Last but not least, potential output power conflicts shown by the tests can be dealt with by proper controller design.

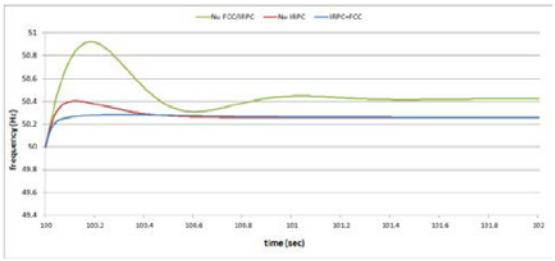

Fig. 4. Frequency for various IRPC combinations

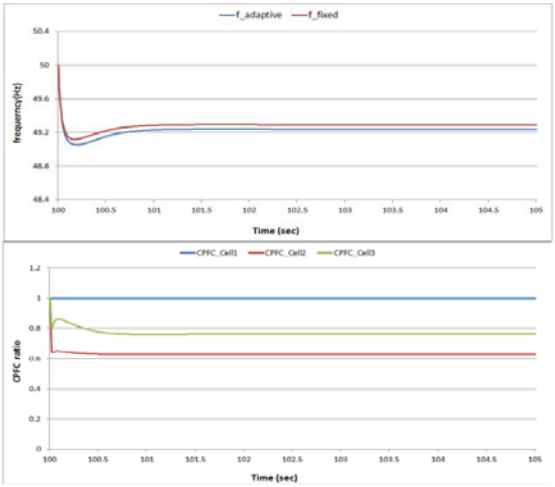

Fig. 5. Frequency and CPFC response for A-FCC

Conclusions

The combination of IRPC and FCC ensures system's stability, improves the local activation of FCC reserves and has small influence on the grid's voltage.

ELECTRA IRP is funded from the European Union Seventh Framework Programme (*FP7/2007-2013*) under *grant agreement* n° 609687

Integration and Validation of

IRPC — Inertial Response Power Controller

FCC — Frequency Containment Control

Scenario

Implementation of IRPC and FCC in a system composed by 2 cells in a synchronised area. The scenario aims at presenting a comparative analysis between FCC and IRPC capability in limiting RoCoF and nadir. Following a power imbalance, one of the two services is activated. The experiment is executed firstly employing IRPC and then employing FCC.

The two controllers employs as reserves the electrical vehicles' flexibility acting on the unidirectional charging.

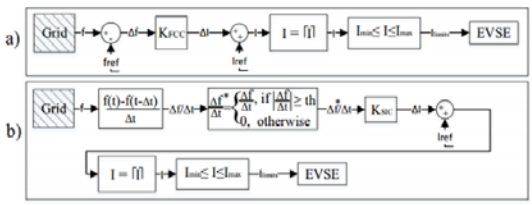

Fig. 1. (a) FCC control diagram, (b) IRPC control diagram

Research Questions

- Can IRPC mitigate the RoCoF and improve the frequency performance in terms of nadir and steady state?
- Can FCC mitigate the RoCoF and improve the frequency performance in terms of nadir and steady state?
- What are the capabilities and limitations of each controller?
- How can the Web of Cells (WoC) concept deliver effective coordination of IRPC/FCC across neighbouring cells?

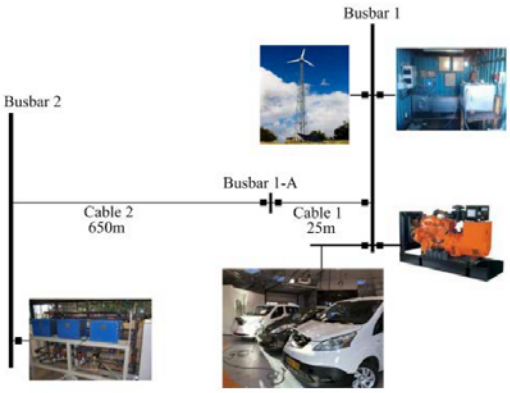

Fig. 2. Web of Cells representation

Operational Parameters

- 2 cells
- RES (1 wind turbines, 2 PVs)
- Battery
- Diesel gen
- Flexible demand
- Electric vehicles

Key Performance Indicators

WoC Integration KPI's	Technical KPI's
Maintaining a given inertia set-point on the WoC level	Respect the Max RoCoF (predefined value)
Maintain a given frequency deviation on the WoC level	Respect the Max frequency deviation (predefined value)

ELECTRA IRP is funded from the European Union Seventh Framework Programme (*FP7/2007-2013*) under *grant agreement* n° 609687

www.electrairp.eu

Experiment

The experiments are executed in the experimental infrastructure SYSLAB. The experimental setup is composed by Vanadium battery, Aircon wind turbine, resistive load, diesel generator and three EVs as shown in Fig.1. The experiments are executed in an islanded configuration where the diesel generator-set acts as the grid forming unit and is the only synchronous inertia device. The VRB, the Aircon and the Dump load are controlled through a Matlab/Java interface, while the EVs are controlled through a Python interface.

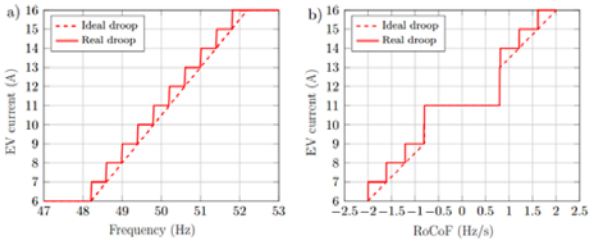

Fig. 3. (a) FCC droop characteristic, (b) SIC droop characteristic

Results

The experimental validation presented the capabilities and limitations of the two controllers under two different circumstances: following load events in both directions and exogenous wind generation profiles. the experiments showed the ability of FCC in limiting the maximum frequency deviation, both following a series of load events or considering a wind power generation. On the other hand, due to the EVs 1 A granularity, the EV absorbed current was oscillating between two consecutive set points, worsening the calculated RoCoF. However, this effect can be limited by employing an hysteresis-based algorithm. Applying the IRPC, the experiments showed that in terms of frequency, the IRPC effects were negligible. In the case of only load events, even if the EVs were able to follow the desired set points, the IRPC did not show a noticeable improvement in terms of RoCoF. On the other hand, considering wind power generation, the IRPC had a very remarkable negative effect. It should be noted that this effect might have been limited by employing less steep droop parameters but limiting the EVs flexibility. The full study is present in [1].

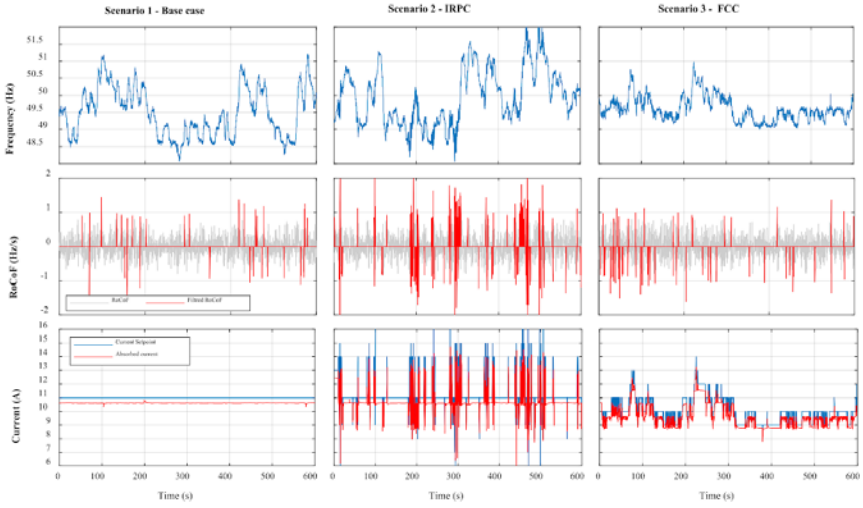

Fig. 4. Achieved results for Scenarios 1-3

[1] M. Rezkalla, A. Zecchino, S. Martinenas, A. M. Prostejovsky, and M. Marinelli, "Comparison between synthetic inertia and fast frequency containment control based on single phase EVs in a microgrid," Appl. Energy, vol. 210, pp. 764–775, 2017.

ELECTRA IRP is funded from the European Union Seventh Framework Programme (*FP7/2007-2013*) under *grant agreement* n° 609687

Fact Sheets “Voltage Control”

Development of DER Models for

PVC — Primary Voltage Control

PPVC — Post Primary Voltage Control

Scenario

Supporting the Validation of the voltage control strategy designed in ELECTRA for the WoC.

The objective is to develop Distributed Energy Resources (DER) models in PowerFactory software in order to support and accelarete the validation studies of PVC and PPVC. Interpretation of the effectiveness of the proactive mode and the corrective mode of PPVC, comprehensive modeling of DERs are needed such as PVs and Wind sources.

Research Questions

- How to visualize the Cp-Lambda-Curve of a wind turbine?
- How to analyze a micro-grid with PV and a Battery System using Quasi-Dynamic Simulation
- How to model PV generator with battery storage?
- How to create a co-generation of a PV system and a diesel engine for Quasi-Dynamic Simulation
- How to create a a photovoltaic generator feeding in parallel with a synchronous machine for dynamic simulations
- How to utilize a PV system model?
- How to develop and utilize a unbalanced/unsymmetrical distribution system model?
- Development of Wind Turbine driving an async machine
- How to model a synchronous generator wind turbine with full converter in detail?

Operational Parameters

Model Developments are created on PowerFactory sofware in consideration of all the parameters of DERs such as PV and Wind as much as possible:

- The aerodynamic efficiency Cp of the wind turbineTie-lines between cells
- The behavior of a microgrid containing PV systems and a battery system
- PWM Converter, Battery/storage Element
- Synchronous Generator, Diesel Engine, PV system, Quasi-Dynamic Simulation
- Static Generator, Loads and the Load Flow
- Unbalanced Power System Models, Distribution System Models
- Induction generator and dynmaic models for Wind Turbines

Key Performance Indicators

(Supported studies, not validated)

Technical KPIs	Metrics
Minimum power losses in the cells (TCR28)	Comparison of power losses in the grid between the PPVC and the BaU voltage control in the planning phase, based on conventional power flows.
Safe and robust voltages for all nodes (TCR30)	Comparison of the voltages setpoints between a situation with PPVC versus no PPVC
Time for voltage restoration (TCR31)	Voltage restauration time will be compared with and without PPVC

ELECTRA IRP is funded from the European Union Seventh Framework Programme (*FP7/2007-2013*) under *grant agreement* n° 609687

www.electrairp.eu

Developed DER Models & Achievements

i. Cp lambda Curve of Wind Turbines: The function cp=f(beta,lambda) is realised using a spline approximation of a series of cp-lambda characteristics. The DSL command sapprox2 is used for this purpose. The developed model contains only multiple modified common models to show the curve for different pitch angles (beta). For demonstration purpose an integrator is added, which increases the tip speed ratio (lambda). All values are displayed together in one plot, sharing the same x-axis (the tip speed ratio)

ii. Quasi-Dynamic Simulation the behaviour of a microgrid containing PV systems and a battery system: The two study cases are developed: typical setup where the micro-grid has no battery system active, setup where only the battery is balancing the network while the diesel generator is disconnected

iii. Detailed parametric model for PV with battery storage: The PV generator consists of a DC current source, connected to the AC system by a PWM converter; The battery storage system consists of a DC voltage source using as well a PWM converter

iv. Small medium voltage network with four loads of different behaviour including DERs: This setup provides a possible way to model a co-generation of PV and a diesel engine, where the feed in of the diesel does not fall under its limit and the PV is curtailed if the solar radiation exceeds the networks demand

v. Photovoltaic (PV) system running in parallel with a synchronous generator: The PV generator (Static Generator) is feeding the load. The grid also contains a synchronous machine. The static generator is feeding the available generated power independent of the load. The reactive power of the PV generator is controlled to zero. Thus the synchronous generator has to control the voltage and the active power balance (frequency) in the grid.

vi. Dynamic simulation of a PV system consisting of parametric PV panels: Solar PV generation is modeled with some detailed parameters such as: PV panel type, tilt angle, number, GPS and so on in order to create a custom PV generator with desired features.

vii. Versality of unbalanced power system models: All kinds of unbalanced power system models can be utilized:

- 3phase, 3 wire (loads in Delta, can be unbalanced, lines can be unbalanced)
- 3phase, 4 wire (neutral is modelled explicitly)
- 2phase, 2 wire, 3 wire
- bi-phase (180deg phase shift), 2 wire, 3wire
- single phase, earth return, neutral return
- loads (1P, 2P, 3P),
- transformers (1P, 2P, 3P),
- lines (1P, 2P, 3P)
- PV-System (1P)
- Switch gears (1P, 3P))

viii. Induction generator with the necessary dynamic models: The reactive power is balanced using a switched capacitor. The dynamic models are a shaft model and a turbine model. The shaft model represents a two mass oscillator where one mass is represented in the DSL model and the other in the generator model. The turbine model contains equations for the aerodynamic part, which has some influence during dynamic speed changes.

ix. Synchronous generator with wind turbine model and the necessary controllers: modeling of an synchronous generator with wind turbine model and the necessary controllers. The PWM converter models with DC voltage circuits are modeled in detail including controllers as well as a chopper to limit the DC voltage. The synchronous generator represents a permanent magnet generator since this is not available as build in element there is a controller used which maintains the excitation current through the excitation voltage constant. Overall, the model represents an aggregated model of 30 wind turbines each having a rated power of 1.5MW.

Conclusions

A comprehensive set of DER models consisting of 9 different types and topologies are developed in detail in order to be used for PPVC validation analyses that supports and accelerates the studies.

By the help of the models and the PPVC analysis study, it is validated with success that the PPVC minimizes the active and reactive power losses and is able to restore the voltages to the safe-band in a very short time also the proactive PPVC also reduces the number of corrective activations.

ELECTRA IRP is funded from the European Union Seventh Framework Programme (FP7/2007-2013) under grant agreement n° 609687

Integration and Validation of

PVC + PPVC

Primary Voltage Control

Post Primary Voltage Control

Scenario

Demonstration of the impact of varying the number of cells in a defined network topology. The focus will be on the voltage control and on the resulting power flows between and within the cells. This scenario will be only simulated in MATLAB/Simulink.

Fig. 1. Operation of PVC and PPVC

Research Questions

- What is the impact of the of cell division on the operation of a determined network? In terms of:
  - Reaction time
  - Losses
  - OPF calculation speed
- Cell control concept in faults?
- Effect of ZIP load to optimal power flow in general?

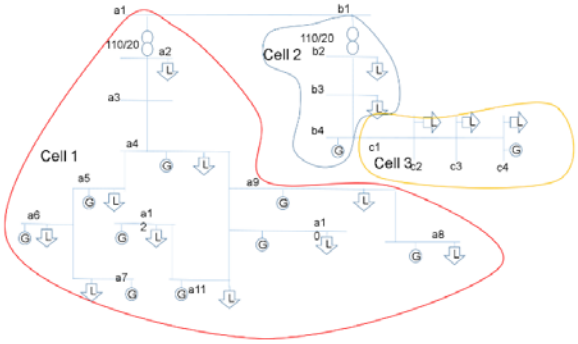

Fig. 2. Web of cells representation

Operational Parameters

Simulation based on the CIGRÉ MV and LV benchmarks with:

- 1/3 cells
- Tie-lines between cells
- PV and wind penetration
- Flexible demand
- Energy storages

Key Performance Indicators

WoC Integration KPI's	Technical KPI's
Power losses due to reserves activation	Time for voltage restoration
Cost of voltage restauration	Depth of the voltage dip or swell

ELECTRA IRP is funded from the European Union Seventh Framework Programme (FP7/2007-2013) under grant agreement n° 609687

www.electrairp.eu

Simulation

Simulation consist of evaluating performance of loss optimized reactive power injection with optimum power flow tool Matpower using cell division and single cell(not cell division) Result of the OPF tool is fed also to Simulink transient model to see interaction with tap changer dynamics.

In addition, ZIP load effect is also analysed on loss optimization and how should it be taken into account. If there is permanent impedance style response of load to increased voltage, savings in transmission losses can be erased by increased load.

Combined simulation with fault location was also done with PPVC method in WP6

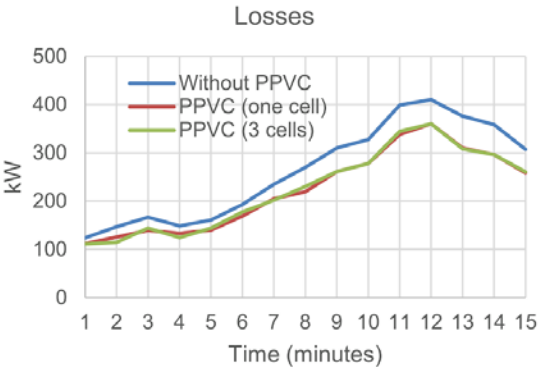

Fig. 3: Differences between one and three cell grids in losses

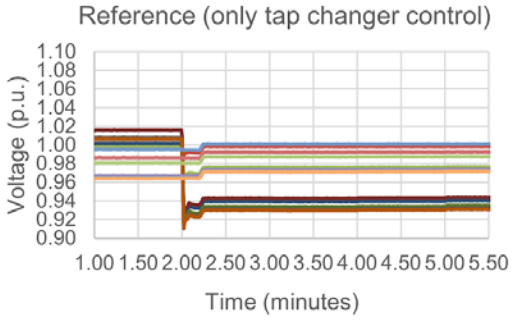

Fig. 4: Reference case with only tap changer reacting

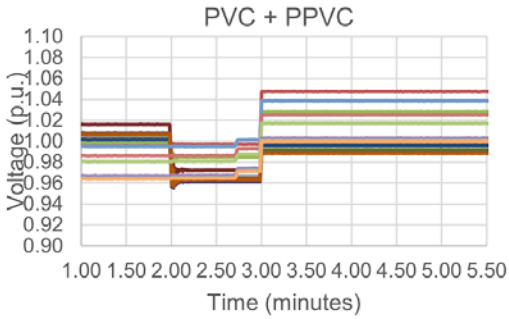

Fig. 5: Selected node voltage before voltage drop, corrective method reacting and proactive activating again when voltage is stabilized

Conclusions

- Cell calculation method has significant speed benefit and almost non existent calculation error if cells are selected properly("electrically distant").
- Post primary voltage control is a good way to proactively control the grid. Optimal response curve settings of primary voltage control droops need more research so that we get also good results if forecast fails bad and PVC needs to activate
- ZIP loads are a real part of power systems and create interesting dynamic of conflicted interest: impedance load can increase load much more than savings of power losses by using higher voltage. Is more holistic approach better for future grid control or are lower losses the only goal?
- For fault clearance and disconnection of cells, there would be higher than necessary losses in OPF if grid model in the algorithm is no updated after some cell drops out in faults
- Voltage restoration time was shorter with PPVC activation and sag lower than without it. The cost of activation depends on how reactive power injection is valued in DSO service model

ELECTRA IRP is funded from the European Union Seventh Framework Programme (FP7/2007-2013) under grant agreement n° 609687

Integration and Validation of

PVC — Primary Voltage Control

PPVC — Post Primary Voltage Control

Scenario

Validation of the voltage control strategy designed in ELECTRA for the Web-of-Cells. The objective is to show that the correct operation of the PPVC can reduce the number of PVC activations by predicting future voltage safe-band violations (proactive mode), as well as to restore the voltage levels in the nodes to the optimal values in case of unexpected events, while minimizing the total losses in the system (corrective mode).

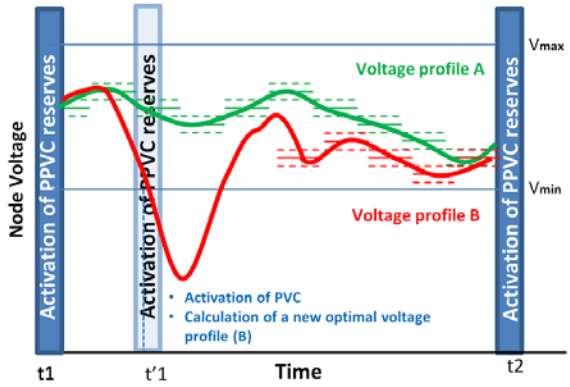

t1: activation of PPVC reserves if future out-of-bands events are expected between t1 and t2 (based on generation/load short-term forecasts): PPVC proactive mode
t1':activation of PPVC reserves after PVC operation: PPVC corrective mode

Fig. 1. Operation of the PVC/PPVC strategy (proactive/corrective)

Research Questions

- Can the PPVC proactive avoid the trip of the corrective mechanisms compared with the business as usual (BaU) case?
- Is the PPVC able to restore the optimal voltage values in the node in the current secondary voltage control timeframes?
- What is the advantage in terms of power losses of using the PPVC?

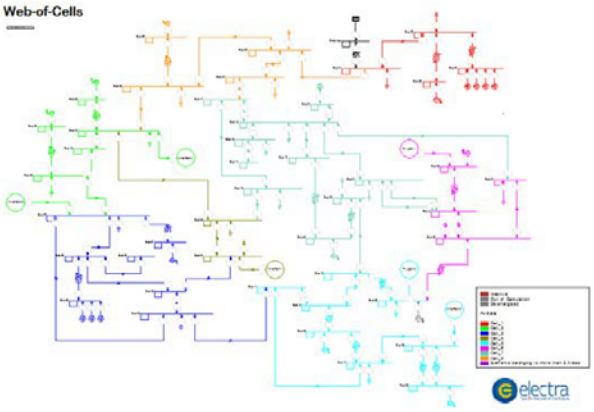

Fig. 2. Web of Cells representation

Operational Parameters

Simulations tested on a flexible grid model (FLEXTEC) designed within ELECTRA:

- 1-9 cells (the number of cells can be variable for the same network)
- RES (PV, Wind, Hydro)
- DG (Synchronous generators, batteries)
- Flexible demand

Key Performance Indicators

Technical KPIs	Metrics
Minimum power losses in the cells	Comparison of power losses in the grid between the PPVC and the BaU voltage control in the planning phase, based on conventional power flows.
Safe and robust voltages for all nodes	Comparison of the voltages setpoints betw. a situation with PPVC versus no PPVC
Time for voltage restoration	Voltage restauration time will be compared with and without PPVC

ELECTRA IRP is funded from the European Union Seventh Framework Programme (FP7/2007-2013) under grant agreement n° 609687

www.electrairp.eu

Validation setup

The validation of the PVC+PPVC Use Case combination has been accomplished over the FLEXTEC grid model previously shown in Figure 2 implemented in Powerfactory, where the dynamic controls of the conventional and non-conventional distributed resources have also been included. FLEXTEX is a flexible grid that allows several WoC configurations with a variable number of cells, and different RES penetration scenarios. The 1-cell, 3-cell and 9-cell cases have been tested. Results corresponding to the 3-cell case are shown in this factsheet.

Achieved results

1. Reduction of PPVC activations

Comparison between the voltage profiles in representative nodes are shown in Fig. 3 for the current voltage control strategy (dashed lines) and the PPVC (solid lines). It can be seen that the implementation of the proactive PPVC avoids the PVC/PPVC corrective trip due to an undervoltage in a node for the ongoing operation window.

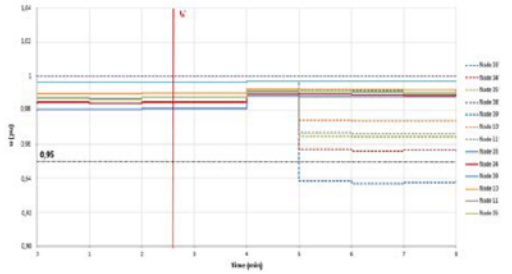

Fig. 3. Voltage profiles for BaU and proactive PPVC

2. Reduction of power losses

Comparison between the active and reactive power losses in BaU (green) and PPVC (blue) are shown in Fig. 4a (active) and 4b (reactive). For the grid state shown, a reduction of 21% and 31% in active and reactive losses is achieved by using the PPVC strategy.

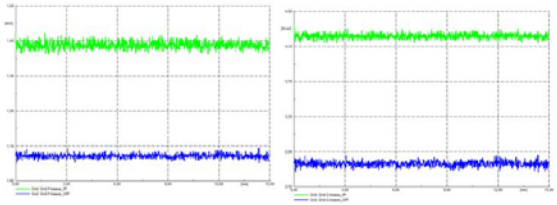

Fig. 4. a) Active power and b) Reactive power losses

3. Voltage restoration

Voltage profiles in representative nodes for a load event are shown in Fig. 5. Voltage in bus 33 trips the corrective PPVC. Fig. 6 shows the comparison of the voltage evolution for the bus in case of no voltage control (green line), PVC control, that stops the voltage drop (black line) and PPVC (red line), that is able to restore the voltage in a very short time (in around 5 s).

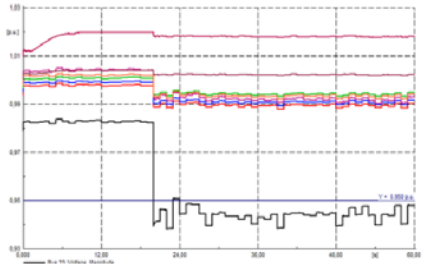

Fig. 5. Voltage profiles in case of a load event

Conclusions

The combination of PVC+PPVC shows the system is stable and secure. The PPVC minimizes the active and reactive power losses and is able to restore the voltages to the safe-band in a very short time. The proactive PPVC also reduces the number of corrective activations.

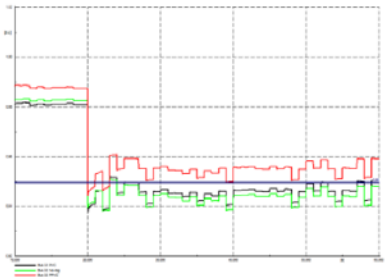

Fig. 6. Comparison on uncontrolled, PVC/PPVC for voltage restoration

ELECTRA IRP is funded from the European Union Seventh Framework Programme (*FP7/2007-2013*) under *grant agreement* n° 609687

Integration and Validation of

PVC — Primary Voltage Control

PPVC — Post Primary Voltage Control

Scenario

This validation scenario addresses the proof-of-concept evaluation of the ELECTRA IRP voltage control schemes (PVC + PPVC) of the distributed, real-time Web-of-Cell (WoC) control concept.

The objective is to test the correct operation of the voltage control algorithm's for MV/LV distribution grids in rural areas with a high amount of renewable generation by using components from the AIT SmartEST lab.

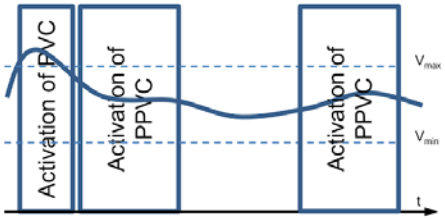

Fig. 1. Operation of the PVC/PPVC

Research Questions

- How can ELECTRA cells be identified? What are optimal configurations for them?
- What is the impact of the of cell division on the operation of a determined network?
- How can parameterization errors (e.g., droop control settings) of inverter-based Distributed Energy Resources (DER) be identified and represented in future control room scenarios?

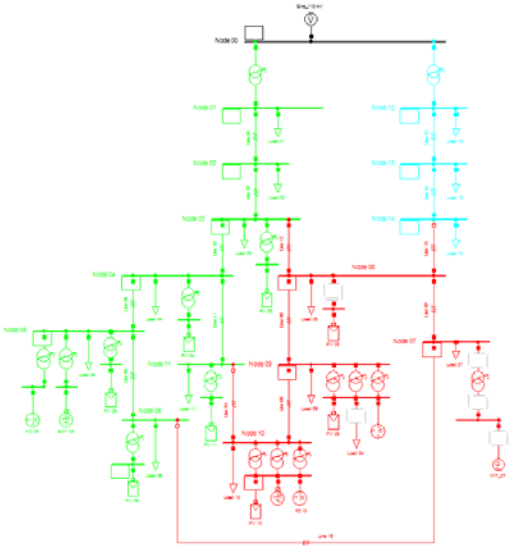

Fig. 2. CIGRE MV test grid represented in the WoC framework (3 cells)

Operational Parameters

Software simulations, real-time hardware- in-the-loop co-simulations based on:

- Involvement of 2-3 cells (i.e., single cells; based on CIGRE MV test grid)
- High-penetration of distributed, renewable generation (i.e., inverter-based DER – mainly wind and PV)
- Loads, tie-lines, tap-changing transformers

Key Performance Indicators (KPI)

Criterion	Definition
Optimal cell division for voltage control	Optimal configuration of a cell for voltage control taking local resources (generators and loads) into account
Safe and robust voltage for all nodes	The voltage setpoints are within deadbands with additional margins in order to avoid undesirable (excessive) OPF calculations
Minimum power losses in the cell	Network losses [kWh]: sum of all real power generated in a cell and/or imported from other cells minus all real power consumed by cell loads in the evaluated period

ELECTRA IRP is funded from the European Union Seventh Framework Programme (FP7/2007-2013) under grant agreement n° 609687

www.electrairp.eu

Identification of Cells

- Identification of potential cells using the normalized electrical distance approach
- Clustering and selection of suitable cells (with sufficient flexibility)

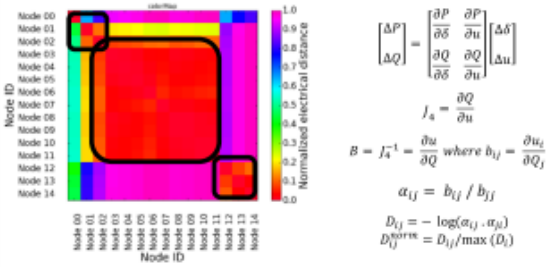

Fig. 3. Colour plot of the normalized electrical distance matrix for the CIGRE MV test grid

Hardware-in-the-Loop (HIL) Test

- Integration of emulated inverter-based DER (i.e., AIT Smart Grid Converter - ASGC)
  - Full four quadrant operation
  - Immediate and frequency control services
- Realization of a real-time co-simulation/ HIL experiment using
  - Grid simulation and control algorithm execution in PowerFactory (with Python API)
  - ASGC emulation in Tyhoon-HIL (power electronics, grid connection) and real controller board (PVC)
  - Coupling of tools via AIT LabLink framework

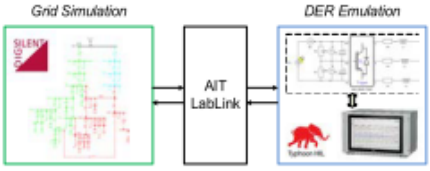

Fig. 5. Coupling via AIT LabLink

- Dashboard-based control room visualization (e.g., voltages, DER parameterization errors)

Fig. 6. Control room visualization

Simulation-based Validation

- Implementation of CIGRE MV test grid (different versions with modifications resulting in 2 and 3 cells configuration) in DIgSILENT PowerFactory
- Voltage control algorithms and optimization implemented in PowerFactory and Python
- Comparison of ELECTRA with centralized voltage control approach (base case)

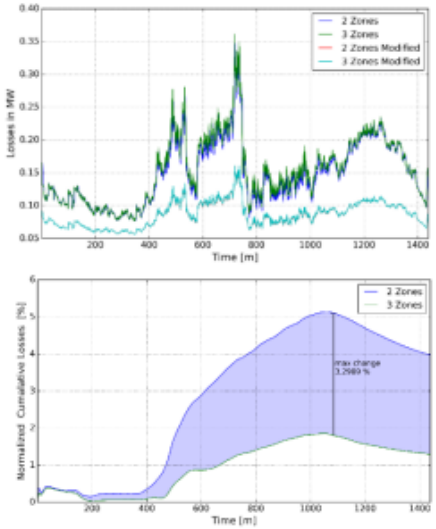

Fig. 4. CIGRE MV test grid simulation results with 2 and 3 cells

Conclusions & Lessons Learned

- Clustering approach using the normalized electrical distance provides a suitable tool for the identification of ELECTRA cells
- Simulation and HIL experiments show the successful operation of the ELECTRA voltage control in context of the WoC
- Around 6% decrease in loses can be observed for the used testing scenario compared to the base case
- The ELECTRA voltage control approach is also suitable to be used for traditional distribution grid optimization
- Real-time co-simulation was very helpful for carrying out the validation experiments

ELECTRA IRP is funded from the European Union Seventh Framework Programme (FP7/2007-2013) under grant agreement n° 609687

www.electrairp.eu

Integration and Validation of SINTEF

PVC — Primary Voltage Control

PPVC — Post Primary Voltage Control

Scenario

Validation of the distributed, real-time Web- of-Cell (WoC) control approach for MV/LV grids in a rural area with renewable generation and difficult operating conditions (weak grid). The objective is to integrate and validate the correct operation of the PVC/PPVC approach during various grid events such as loss of a line, loss of a generator, etc. This will be accomplished through implementing a cell-based control architecture in the SINTEF Smart Grid laboratory.

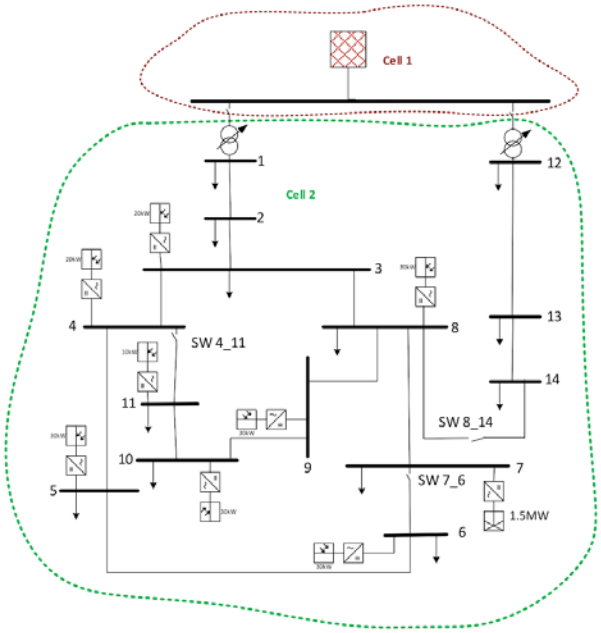

Fig. 1. Web of Cells representation

Research Questions

- Can PPVC replace the present secondary (local) and tertiary voltage control (global) schemes existing in power grids by a decentralized control located at a cell level?
- How would PPVC interact with PVC and balancing control?
- How would PPVC respond to different network conditions?

Operational Parameters

Software simulations and hardware with software in the loop testing based on.

- 2 cells (basically single cell)
- Converter interfaced wind and PV
- Loads, tie-lines and breakers

Key Performance Indicators

Technical KPI's/ Criterion	Definition
Minimum power losses in the cell	Network losses [kWh]: sum of all the real power generated in the cell and/or imported from other cells and then subtracting all real power consumed by the cell loads in the evaluated period.
Safe and robust voltage for all nodes	The voltage setpoints are within deadbands with additional margins in order to avoid undesirable (excessive) OPF calculations
Time for voltage restauration	Time between the instant the fault occurs (voltage crossed the threshold of 90%/110% of its nominal value) and the instant the voltage is back within 10% of its desired value.

ELECTRA IRP is funded from the European Union Seventh Framework Programme (*FP7/2007-2013*) under *grant agreement* n° 609687

www.electrairp.eu

Simulation

The electrical network is implemented using Matlab Simulink and the OPF is written using the General Algebraic Modeling System (GAMS). The objective in the OPF formulation is loss minimization and the OLTC and converter droop controller parameters are included in the constraint. As the tap setting is integer variable, the loss minimizing OPF is Mixed Integer Nonlinear Programing (MINLP) problem. As shown in Fig. 2, the PPVC process starts as the Simulink based network start running.

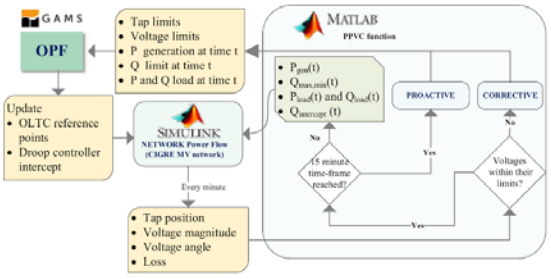

Fig. 2. Workflow for the proactive and the corrective (restorative) schemes of the PPVC

Conclusions

The experiments (especially the real-time simulation experiments) have helped to draw the following conclusions:

1. The PPVC method has demonstrated better capability than the BAU case in keeping the voltage profiles more stable and within limits. This is because of the optimal orientation of the OLTC reference voltage and the Converter droop controller characteristics intercept base on forecasted load and generation scenarios.
2. Generally, the PPVC case reduces losses within cells. This is essentially due to the optimal utilization of local reactive power resources in the network.
3. The tap changes needed in case of PPVC significantly lower than the BAU case. This is because of the optimal orientation of the reference voltage of the OLTC avoiding the tracking of it to keep the voltage around a fixed reference, as it is in BAU case.

Laboratory experiment

Details of the PHIL experimental setup is outlined in Fig. 3. The main components in the experiment are: OPAL-RT platform (OP5600 5 cores activated), 200 kW high-bandwidth (20 kHz) power converter operating as a grid emulator (EGSTON-COMPISO), Two 60 kW converter units (one is used as a DC source), Windows based interface computer, RT-LAB, Matlab and GAMS programs and softwares.

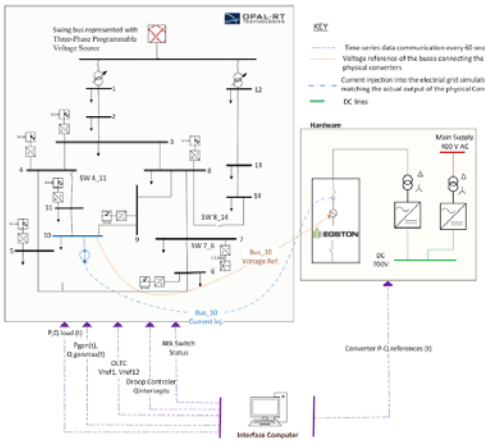

Fig. 3. The electrical connectivity of the grid emulator and the two converters in the laboratory

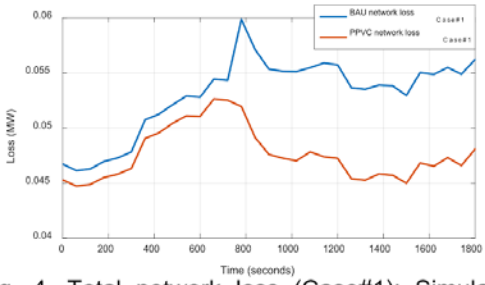

Fig. 4. Total network loss (Case#1): Simulation results

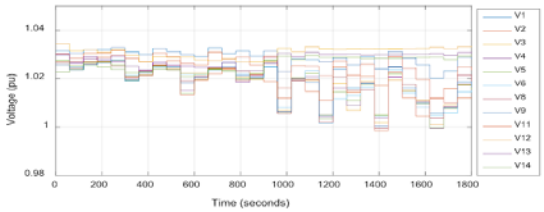

Fig. 5. Voltage profiles for the PPVC PHIL implementation (Case#2_PHIL)

ELECTRA IRP is funded from the European Union Seventh Framework Programme (FP7/2007-2013) under grant agreement n° 609687